INVOLVEMENT OF LYSOSOMAL SIALIDASE IN TAY-SACHS DISEASE

TAY-SACHS DISEASE: MECHANISMS OF NEUROPATHOLOGY AND POTENTIAL THERAPEUTIC STRATEGIES UTILIZING HUMAN LYSOSOMAL SIALIDASE

By
DAVID A. EGIER, B.SC.

A Thesis

Submitted to the School of Graduate Studies

In Partial Fulfillment of the Requirements

for the Degree

Master of Science

McMaster University

MASTER OF SCIENCE (2011) McMaster University
(Biology) Hamilton, Ontario

TITLE: Tay-Sachs Disease: Mechanisms of Neuropathology and Potential Therapeutic Strategies Utilizing Human Lysosomal Sialidase

AUTHOR: David A. Egier, B.Sc. (McMaster University)

SUPERVISOR: Dr. Suleiman Igdoura

NUMBER OF PAGES: x, 108

Abstract

GM2 gangliosidoses encompass a group of chronic neurodegenerative disorders characterized by metabolic defects in ganglioside catabolism and marked intralysosomal accumulation of GM2 in central nervous system (CNS)-resident neurons. Included in this group are Tay-Sachs and Sandhoff disease. Human cases of Tay-Sachs and Sandhoff disease present with devastating neurological deterioration; however, murine models display drastically divergent phenotypes. Tay-Sachs mice avoid pathology via a sialidase-mediated bypass of β-hexosaminidase A (HEXA) deficiency, though the precise mechanism of avoidance is not fully elucidated. The following work aimed to: i) determine if the murine sialidase-mediated bypass could be potentiated in human cells, and ii) help clarify the mechanism of disease avoidance in Tay-Sachs animals.

Adenoviral overexpression of truncated CCAAT displacement protein ($CDP^{831-1505}$) in human Tay-Sachs neuroglia augmented neuraminidase 1/lysosomal sialidase (NEU1) protein levels, which reduced intralysosomal GM2 accumulations. Chromatin immunoprecipitation revealed binding of $CDP^{831-1505}$ to the human *NEU1* promoter in Tay-Sachs neuroglia. These results provide mechanistic and functional evidence supporting therapeutic exploitation of *NEU1* for Tay-Sachs disease.

Comparison of immunological responses of bone marrow-derived macrophages (BMDMs) to pathogen associated molecular patterns (PAMPs) or GM2 demonstrated that Sandhoff macrophages secrete increased TNF and reduced IL-10 following lipopolysaccharide stimulation. GM2 treatment failed to stimulate an immune response. Such behaviour occurred in the absence of clearly observable intralysosomal ganglioside accumulations. Altered LAMP2 protein size, potentially due to aberrant glycosylation, is hypothesized to disrupt autophagosomal/lysosomal fusion. Subsequent autophagosomal accumulation could result in inherent macrophage hypersensitivity and immunologic irritability. Downstream interleukin-10 (IL-10)/signal transducer and activator of transcription 3 (Stat3) axis, mitogen activated protein kinase (MAPK), and glycogen synthase kinase 3-beta (GSK3β) signaling pathways were affected in Sandhoff BMDMs. These data indicate inherent differences in immunological responses of BMDMs from Sandhoff mice, presumably related to their β-hexosaminidase B (HEXB) deficiency.

Data presented here provides evidence to suggest a paradigm shift in the neurodegenerative model of Tay-Sachs and Sandhoff Diseases towards one that places immune cells as an initiating factor for widespread neuroinflammation.

Acknowledgements

I would like to primarily thank my supervisor, Dr. Suleiman Igdoura, for providing me with the opportunity to become a member of his laboratory. This experience has allowed me to grow not just intellectually, but also professionally, and the skills I have acquired over the past several years will undoubtedly assist me in my future endeavors. His enthusiasm, leadership, academic contribution, and humour were integral components in my success as a graduate student. I will never forget the sense of belonging that I felt while working in his laboratory.

A special thank you to my second family - Liz (Doctor), Abe (Abraham!), Rose (agaRose), Gabe (Gab-a-roo), and Alex (*a…Lex!*), with whom I likely spent more time with than my biological relatives. More specifically, I commend Liz and Gabe for dealing with my ruthless onslaught of ridiculous questions and for their technical assistance, Abe for his wealth of conceptual knowledge, Rose for her frequent and unmistakable laughter, and Alex for the random after-hours laboratory hangouts and liters of borrowed Western buffers.

A special thank you to my mother, Ro, and father, Brian, whose own actions have taught me that anything is achievable if you want it badly enough - I could not have asked for better role models. I would also like to thank them for continuously being there for me, even while dealing with struggles of their own. Furthermore, I'd like to voice my appreciation for my mother's unyielding support, which fueled my drive to carry on during difficult times, and my father's uncanny ability to set me back on course whenever I would become distracted. I love you both.

Lastly, I thank Sara, who provided relentless encouragement and reassurance that my efforts would eventually pay off.

Table of Contents

List of Figures and Tables

Abbreviations List

Ad	adenovirus
AKT	(PKB; protein kinase B)
AP1	(activator protein 1)
bp	base pair
BMDM	bone marrow derived macrophage
CDP	CCAAT displacement protein
Cer	ceramide
CREB	(cAMP response element-binding)
HD	cut homeodomain
CNS	central nervous system
CR3	cut repeat 3
ddH_2O	distilled water
DEAE	diethylaminoethyl
DMEM	Dulbecco's Modified Eagle's Medium
DNA	deoxyribonucleic acid
DUSP1	dual specificity protein phosphatase 1
EGF	epidermal growth factor
EGFR	epidermal growth factor receptor
ELISA	enzyme-linked immunosorbent assay
ERT	enzyme replacement therapy
FBS	fetal bovine serum
GAPDH	glyceraldehyde 3-phosphate dehydrogenase
GFAP	glial fibrillary acidic protein
GlcCer	glucosylceramide
GPCR	G-protein coupled receptor
Gpnmb	glycoprotein (transmembrane) nmb
GSK3β	glycogen synthase kinase 3-beta
GSL	glycosphingolipid
HEXA	β-hexosaminidase A
HEXB	β-hexosaminidase B
HEPES	4-(2-hydroxyethyl)-1-piperazineethanesulfonic acid
IFN-γ	interferon-gamma
IL	interleukin
kDa	kilodalton
LacCer	lactosylceramide
LAMP2	lysosomal-associated membrane protein 2
LPS	lipopolysaccharide
MALDI-TOF	matrix-assisted laser desorption/ionization-time of flight

MAP1-LC3	microtubule-associated protein 1 light chain 3
MAP	2-amino-2-methyl-1-propanol
MAPK	mitogen activated protein kinase
M-CSF	macrophage colony stimulating factor
MOI	multiplicity of infection
Mpg1	macrophage expressed gene 1
mRNA	messenger ribonucleic acid
4-Mu-NANA	4-methylumbelliferyl-n-acetyl-α-D-neuramide
NEU1	neuraminidase 1/lysosomal sialidase
PAGE	polyacrylamide gel electrophoresis
PAMP	pathogen-associated molecular pattern
PBS	phosphate-buffered saline
PCR	polymerase chain reaction
Poly I:C	polyinosinic:polycytidylic acid
PPCA	protective protein/cathepsin A
qPCR	quantitative polymerase chain reaction
RIPA	radioimmunoprecipitation assay
RPMI	Roswell Park Memorial Institute
SDS	sodium dodecyl sulfate
Stat3	signal transducer and activator of transcription 3
TBST	tris-buffered saline with Tween-20
TGFβ	transforming growth factor beta
TLC	thin layer chromatography
TLR	toll-like receptor
TNF	tumour necrosis factor

CHAPTER 1

INTRODUCTION

1.1 Glycosphingolipids

Glycosphingolipids (GSLs) are a type of glycolipid that contain sphingosine and include gangliosides, cerebrosides and globosides[1]. Glycolipids consist of a carbohydrate component and a lipid chain and play a crucial role in supplying energy to cells. Additional functions include roles in cellular recognition, eukaryotic cell membrane stability, processes of cell-matrix and cell-cell adhesion, metabolism, and immune response[1, 2, 3]. The composition of the sugar and lipid moieties attached to the sphingosine in GSLs can vary greatly in size and complexity[1, 4].

Gangliosides are modified GSLs that contain at least one N-acetylneuraminic acid (sialic acid) residue linked to the oligosaccharide chain. Like GSLs, gangliosides are found in the plasma membrane in a similar orientation and participate in cell-cell signaling and cellular recognition events[3,4]. There is much variation in the spatial, temporal and type of ganglioside expression between tissues and species. Gangliosides are usually concentrated in lipid rafts and are highly prevalent in the nervous system where they account for approximately 10-12% of all lipids and 20-25% of the outer layer of neuronal membranes. The synthesis of gangliosides occurs in a stepwise fashion in the Golgi from lactosylceramide (LacCer) and involves the activity of both sialyltransferases and glycosyltransferases[5]. GM3, the simplest ganglioside, is synthesized in the *cis*-region of the Golgi by the sialyltransferase, GM3 synthase. Conversely, those enzymes that catalyze the latter steps of ganglioside synthesis are located in the *trans*-Golgi compartment[1, 5]. The importance of gangliosides in brain formation and development is well documented[6]. Furthermore, during brain development, the quantity and the degree of sialylation of gangliosides increases[7]. Studies have shown that mature mouse brains contain approximately 8 times more gangliosides than embryos and that the complexity of these lipids increases with age[7]. Treatment of cells *in vitro* and *in vivo* with injections of gangliosides results in rapid internalization of these molecules by cells and tissues[6, 8, 9].

Proper breakdown of intralysosomal lipids is necessary for normal cellular function[10]. Catalysis of complex membrane associated glycoconjugates occurs via the "endosomal-lysosomal system" or "vascular apparatus" and involves plasma membrane-derived, clathrin-containing, endosomal compartments that subsequently develop into mature, digestion-competent lysosomes. These lysosomal vesicles are involved in the degradation of cellular components and utilize acid hydrolases contained within their highly acidic (pH≈ 4.5-5) lumen. Once in the lysosome, the internalized membrane-associated macromolecules are degraded in a step-wise fashion by lysosome-resident enzymes[10, 11]. It is by this pathway that the cell breaks down the sphingolipids found to accumulate in lysosomal storage disorders.

GSLs and ganglioside catabolism has been thoroughly studied over the past few decades. Investigation has revealed that faults at any step in the catabolic pathway lead to the development of one or more lysosomal storage disorders (LSDs) (Figure 1)[10]. More specifically, mutations associated with improper or reduced activity in catabolic enzymes or cofactors lead to defects in the acid hydrolysis of endogenous intralysosomal molecules, resulting in the storage of certain liposaccharides[12].

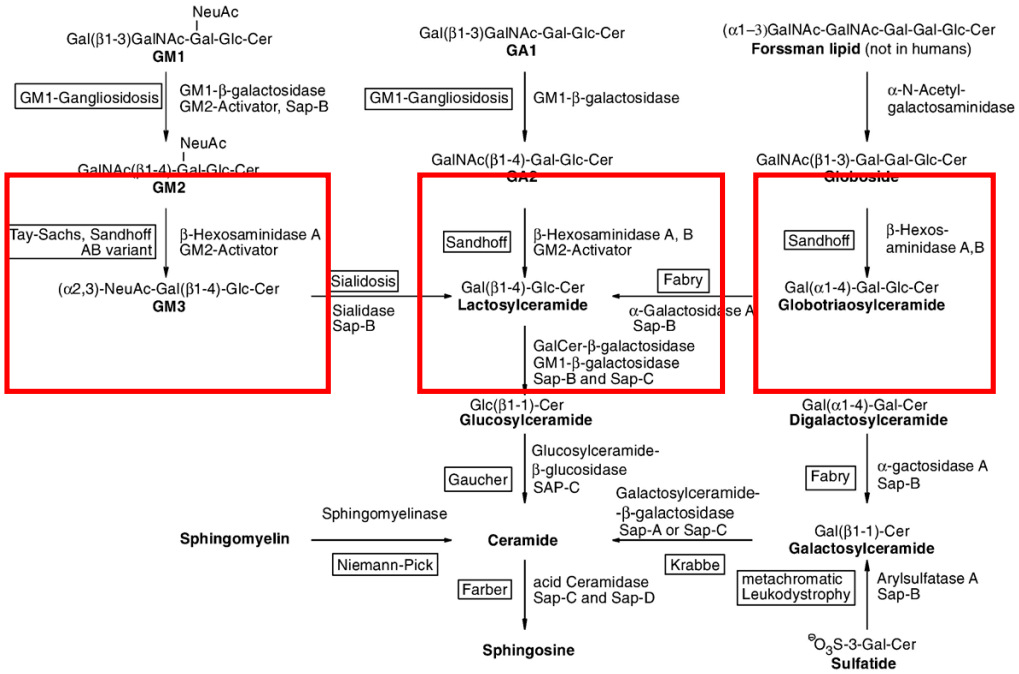

Figure 1. ***Sphingolipid Metabolism.*** Deficiencies in enzymatic activity at any step of the catabolic pathway results in accumulation of the corresponding substrate. The red boxes designate portions of the pathway that are of direct relevance. Modified from Kolter, et al. (2006)[10].

Lysosomal deposits and accumulations often result in a disturbance of normal cellular function once they reach a certain threshold. The resultant pathological events/symptoms are classified as LSDs. Lysosomal storage diseases are a group of more than forty rare and inherited metabolic disorders, each stemming from a different genetic mutation in a gene encoding a different lysosomal enzyme and are further classified either by the material that is primarily stored or by the deficient enzyme[13, 14, 15]. Most LSDs follow an autosomal recessive pattern of inheritance, however, several disorders (Mucopolysaccharidosis type II, Fabry disease and Danon disease) are X-linked[16]. The severity of the resulting illness stems from the nature of the defect and is directly related to how much residual enzymatic activity remains and thus the extent of macromolecule accumulation[13, 16, 17]. Total eradication of activity results in an infantile or early-onset of disease, more severe symptoms, poorer prognosis and often death during childhood. Conversely, adult-onset, which is associated with milder symptoms and a more optimistic prognosis, is typically observed in cases with supportive residual enzyme activity.

LSDs have been a topic of intensive study over the past several decades. Although the prevalence of such diseases amongst the general population is not considered high (cumulatively estimated to affect ~1/7,700), amid several sub-populations, termed "carrier populations", disease alleles are much more prevalent[14, 18, 19, 20].

Currently, no cure exists for lysosomal storage diseases, however, over the past two decades treatment options have drastically improved[13, 16]. In more recent years, several promising methods such as bone marrow transplantation and enzyme replacement therapy (ERT) have been explored with some success[21, 22, 23, 24]. Gene therapy has also gained credence as an emerging therapeutic alternative over the last several years[24, 25]. The rationale behind each of these potential therapies is to reestablish/restore the deficient enzymatic activity to aid in clearance of accumulated intralysosomal metabolic intermediates. Treatments based on other principles include substrate reduction therapy whereby the production of the deficient enzyme's substrate is reduced to a level manageable by the residual enzyme activity, and the utilization of chemical chaperones that act to stabilize the mutated enzyme[16, 22, 26, 27, 28, 29, 30, 31, 32, 33]. While these methods have been successfully implemented in the treatment of several LSDs, the expense of clinical implementation of such treatments is enormous and is currently one of their major drawbacks[13]. One potential, yet relatively unexplored therapeutic avenue is the development of alternate gene therapy. Such therapeutic options aim to circumvent the primary defect by shunting the accumulated substance through a metabolic bypass. Ideally, this bypass would be achieved through manipulation of an endogenous pathway; however, the specific mechanism to be utilized would be compound/disease-specific.

Analogous to the catabolic pathway, defects in sphingolipid biosynthesis also lead to devastating and often lethal outcomes. Given the essential role of sphingolipids during embryogenesis and development, many symptoms of

systemic knockout mutations are masked by an embryonic lethal phenotype[34]. However, evidence provided from other studies suggests not all defects in sphingolipid biosynthesis will result in lethality. For example, decreased C18-ceramide synthesis has been linked to non-lethal events such as head and neck squamous cell carcinomas[35].

1.2 GM2 Gangliosidoses

The designation GM2 gangliosidoses encompasses a group of diseases whose pathological outcomes and similar clinical phenotypes result from distinct molecular defects, all of which cause the intralysosomal accumulation of GM2 gangliosides. There are three inherited (autosomal recessive) disorders grouped into this class of neurodegenerative diseases: Tay-Sachs, Sandhoff and GM2 Activator deficiency[36]. Mutations affecting each of the subunits or the cofactor of the enzyme β-hexosaminidase, which is involved in the catabolic breakdown of these lipids, leads to the toxic buildup of GM2 ganglioside[36]. It is this toxic buildup that indirectly initiates the biological cascade towards progressive neuronal apoptosis, eventually leading to nervous system dysfunction and patient death[10, 12, 37, 38].

Deposits of undigested intermediate lipids in neurons are contained within membranous cytoplasmic bodies (MBCs). These MCBs are composed of endosomal membranes with plasma membrane (PM) lipids rafts enroute to the lysosome for degradation[10, 39]. Storage of these lipid components causes increased levels of endoplasmic reticulum (ER) and golgi body stress[40]. Pro-apoptotic pathways have been shown to encourage cell death in cells experiencing significant ER stress[41]. These changes are also accompanied by alterations in neuronal morphology, neuronal signal transmission and neuronal cell receptor signaling, which lead to astrogliosis and immune cell (specifically microglial/macrophage) activation[41, 42]. This extensive immune response, augmented by positive feedback signaling between immune cells of the central nervous system (CNS) and CNS-resident damaged/apoptotic neuronal cells, leads to considerable neuroinflammation and subsequent neurodegeneration including denervation of the spinal cord, brain stem and cerebellum, basal ganglia and cerebral cortex[41, 42].

1.3 β-Hexosaminidase

β-hexosaminidase A (HEXA) is an essential enzyme responsible for partial catabolism of negatively charged ganglioside species such as GM2 ganglioside in the lysosomes of cells in the central and peripheral nervous system[43]. Its ability to cleave N-acetylgalactosamine from GM2 is dependent

upon proper function of its two subunits (α and β) – each of which is encoded by a separate gene (*HEXA* and *HEXB*, respectively) and its cofactor, GM2 activator protein[43]. The activator protein functions by hoisting the substrate (GM2) into the enzyme's active site for catalysis. Defects in any of these three critical pieces leads to an accumulation of GM2 in the lysosomes of neurons and development of neurodegenerative disorders[20, 43]. As mentioned previously, these disorders constitute the class, "GM2 gangliosidoses". Successful catabolism of GM2 ganglioside within the lysosome yields the product, GM3, and does not result in the lysosomal buildup of catabolic intermediates.

β-hexosaminidase B (HEXB) is also involved in the breakdown of lipids in the lysosome. More specifically, HEXB cleaves uncharged substrates and is responsible for the conversion of GA2 to lactosylceramide, and globoside to globotriacylceramide[44]. In contrast to HEXA, HEXB is composed of two β subunits, both encoded by the *HEXB* gene. Homozygous defects in the gene encoding the β subunit lead to a deficiency of both enzymes (HEXA and HEXB), resulting in a type of GM2 gangliosidosis called Sandhoff Disease[45].

Biosynthesis of hexosaminidase in the ER results in a pro-hexosaminidase isozyme, which undergoes proteolytic and glycosidic post-translational processing in the late endosome or the lysosome before reaching maturity[20]. Genetic mapping initiatives have localized *HEXA* (gene encoding the pro-α subunit) to 15q23-24 and *HEXB* (gene encoding the pro-β subunit) to 5q13[44].

1.4 Tay-Sachs disease

Tay-Sachs disease (TSD) is a chronic, autosomal recessive lysosomal storage disorder that is characterized by profound neurodegeneration and for which no cure is currently available. TSD is caused by a deficiency in the HEXA enzyme due to mutations in the gene encoding its alpha subunit[46, 47]. Over 100 mutations in *HEXA* have been identified, each of which lead to the inhibition of the function of HEXA. As a result of this enzymatic deficiency, neuronal cells accumulate harmful levels of GM2 ganglioside in their lysosomes leading to their premature death[36, 37, 38, 41]. Consequently, motor malfunctions, seizures, ataxia, tremors, muscular atrophy and in many cases death of the individual follow[46]. TSD can be classified into three sub-types (infantile, juvenile and adult) by its age of onset and coinciding severity of neurological symptoms, and is diagnosable by a characteristic cherry red spot on the macula[46]. The frequency of *HEXA* mutant alleles is approximately 1/300, however, several "carrier populations" have been recognized in which this frequency is drastically elevated. Ashkenazi (Eastern European) Jews, French Canadians of southeastern Quebec, and Cajuns of southern Louisiana are all considered to have *HEXA* mutations at frequencies significantly more prevalent than the general population

(e.g. Ashkenazi Jews ~ 1/27 – 1/30)[18, 19, 48]. The Ashkenazi Jew and Cajun populations both share the same most prevalent mutation – an insertion of four base pairs (bp) (TATC) in exon 11 of *HEXA* at position 1278, which creates an altered reading frame, and a premature stop codon nine base pairs downstream of the insertion[18, 19, 20]. However, French Canadians most commonly possess a long sequence deletion in the *HEXA* gene, which renders its product non-functional[48].

Symptom severity in Tay-Sachs disease is inversely proportional to the age of onset. For example, subjects with the infantile form of TSD suffer from rapid neurological deterioration in their second year of life and fail to maintain visually evoked cortical responses after 16 months of age[49]. Conversely, patients with late-onset Tay-Sachs (LOTS) disease present saccadic eye movement but have otherwise unaffected afferent visual pathways[50]. LOTS patients experience dampened neurological symptoms (in comparison to infantile and juvenile onset cases) such as general clumsiness in early childhood, which often worsens into ataxia and general weakness in the second and third decade of life with subsequent denervation atrophy in middle-aged and elderly individuals[51]. Additionally, LOTS patients often suffer from adulthood neuropsychiatric illness such as catatonic schizophrenia, hallucinations, anxiety and depression but most still maintain cognitive capacity[52, 53]. Furthermore, symptom nature and temporal presentation can vary in a case-dependent manner even within a single class of onset. This phenomenon is typically observed in late-onset cases of the disease[51]. Given this outstanding clinical heterogeneity, it is expected that studies would show weak correlation between neurological decline and the severity of disease phenotype.

Sandhoff Disease (SD), like TSD is an autosomal recessive, lysosomal storage disorder. SD is a specific type of GM2 gangliosidosis caused by a deficiency of both the HEXA and HEXB enzymes, and results in the toxic buildup of GM2 gangliosides in a variety of cell types[45, 54]. These deficiencies arise from mutation(s) in the gene encoding the β subunit of β-hexosaminidase, *HEXB*[45]. In a similar fashion to that described previously, elevated stores of GM2 ganglioside in the CNS causes progressive neurodegeneration, ultimately resulting in death[45]. SD, too, is classified by its age of onset and corresponding neurological symptoms into categories identical to those established for TSD. In humans, SD and TSD follow a similar pathological course and share the same symptoms[10, 45]. Thus, they cannot be clinically distinguished from one another.

1.5 Sialidase and regulation of the human sialidase promoter

Sialic acid is a nine-carbon hexose terminal monosaccharide derivative of neuraminic acid, which possess N- or O- substituted domains. It is found bound to glycoproteins and glycolipids in both animal tissue and bacteria[55]. Both sialidase and sialyltransferase activity determines the extent of sialylation on cell

surface glycoproteins and thus, the magnitude of negative cell surface charge[56]. Additionally, the degree of sialylation functions to regulate cell identification, cell adhesion, cell-cell interactions, cell proliferation and to maintain conformational stability[57]. For example, cell surface expression of molecules such as sialylated Lewis X (sLe^x)/CD15, which binds to selectin, can be regulated by post-Golgi membrane sialidase activity[58].

Sialidase enzymatically removes sialic acid whereas sialyltransferases catalyze the addition of sialic acid to nascent oligosaccharides[56]. Neuraminidase 1 is the lysosomal form of the sialidase enzyme, which hydrolytically cleaves terminal alpha-2,3 and alpha-2,6 linked sialic acid residues[59]. Most important to this project is the 46 kDa enzymatic glycoprotein, neuraminidase 1/lysosomal sialidase (NEU1)[60]. It associates with protective protein/cathepsin A (PPCA) prior to segregation to the lysosome and forms a heterotrimeric complex with beta-galactosidase. Studies have demonstrated that optimal activity of lysosomal sialidase occurs at an acidic pH of 4.5[60, 61]. The human NEU1 gene has been mapped to chromosome 6p21 within the major histocompatibility complex (MHC) and the mouse gene to chromosome 17 near the H-2D end of its MHC[61]. Structural mutations in the neuraminidase 1 gene lead to a condition called Sialidosis, whereas defects in PPCA cause galactosialidosis[60]. Sequencing of the sialidase promoter has uncovered a CCAAT box that is responsive to several proteins such as C/EBP (CCAAT enhancer-binding protein) and CCAAT displacement protein (CDP)[62]. The full form of CDP is associated with transcriptional repression[63]. However, in its N-terminally truncated form has been shown to cause augmented expression of *NEU1* (Figure 2)[64]. It has been hypothesized that truncated CDP can no longer effectively suppress transcription via competitive concealment of the upstream activator domain of the sialidase gene. Thus, regardless of CDP attachment to its DNA binding domain, activators of the sialidase gene can still be recruited for the initiation of transcription. An alternate hypothesis concerning the ability for CDP to actively increase transcription has also been put forth; however, a putative mechanism has yet to be elucidated, and until falsified, this possibility cannot be ignored.

Sialidases have been the topic of much study due to their extensive impact on many cellular and physiological processes. By acting on molecules such as glycoproteins and glycolipids, sialidase plays a direct role in normal cellular behaviours and thus, altered activity may play a role in disease and pathology. As discussed in previous sections, lysosomal sialidase is intimately involved in the catabolism of lipids in lysosomes where it acts to desialylate these sialoglycoconjugates[65]. Deficiency of lysosomal sialidase (NEU1) results in the lysosomal storage disease, Sialidosis (Mucolipidosis type I)[65]. This fatal disease is characterized by an accumulation of mucopolysaccharides in cells such as neurons, bone marrow and other immune cells. Individuals suffering from this illness often show symptoms of hepatosplenomegaly, skeletal malformations, myoclonus, ataxia, tremors, and impaired vision[66, 67, 68]. Additionally, patients show signs of mental retardation and normally die before 1 year of age[66]. Recent

work has described sialidase as being intimately associated with toll-like receptor (TLR) 2, 3, and 4 activation and signaling. Specifically, activation of NEU1 is induced by the interaction of TLR receptors and their ligands. Activated NEU1 (lysosomal sialidase) has been shown to desialylate sugar N-glycan moieties on complexes such as MyD88/TLR4 leading to subsequent activation of NFκB, a potent transcription factor in the regulation of immune responses and cytokine production[69]. Amith et al. (2009) demonstrated that NFκB activation in macrophage and dendritic cells is dependent upon the removal of α-2,3-sialyl residues linked to β-galactoside on TLR4[69, 70]. Together, these findings present strong evidence for the involvement of sialidase in the neuroinflammatory process.

1.7 The connection between neuroinflammation and neurodegeneration

In the CNS, the process of inflammation changes dramatically from that of peripheral tissue. Since the brain and the spinal cord are isolated from the rest of the body by the blood brain barrier, very few pathogen-recognizing antibodies are able to enter and circulate in the CNS. Innate immune responses in the CNS are ignited by systemic invasion of pathogens and the development of an adaptive immune response occurs afterward. Thus, the central nervous system must possess and utilize its own antigen-presenting cells, which recognize and phagocytose foreign particles and subsequently activate the T-cells of the immune system; microglial cells perform this function[71]. Production of immuno-modulatory molecules secreted by these cell types is elevated in many neurological disorders, linking the complex progression of neurodegeneration with the inflammatory process[71, 72, 73]. Two types of neuroinflammation exist: acute and chronic. In the prior type, acute neuronal injury triggers microglial activation and subsequent phagocytosis of deceased cells and debris material[73]. The definitive aspect of an acute response is inflammation that subsides once "cleanup" is complete. Conversely, chronic neuroinflammatory responses involve sustained microglial activation and consequently, continual production of microglial inflammatory mediators such as proinflammatory cytokines, chemokines, proteases and amyloid precursor protein (APP)[71, 72]. Persistent production of these molecules facilitates neuronal death. As a consequence of chronic activation, microglia may lose some of their trophic functions, once again contributing to the induction of neurodegeneration via neuroinflammation[72].

The role of the inflammatory process in neurodegeneration has been well documented in Alzheimer's, amyotrophic lateral sclerosis (ALS) and prion-related diseases[74, 75, 76]. Prior work has temporally studied the events leading to neurodegeneration and has found that microglial activation precedes large events of neuronal cell death in Sandhoff disease mice[77]. Furthermore, cDNA

microarray analysis revealed an upregulation of genes related to a microglia-dominated inflammatory process prior to acute neurodegeneration[77].

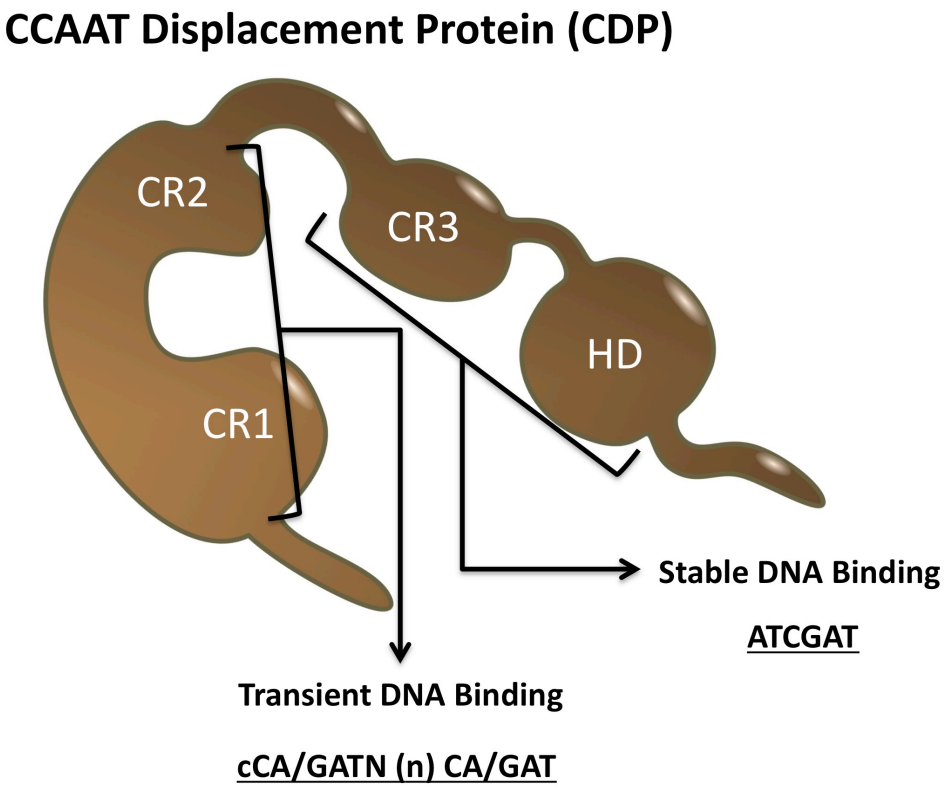

Figure 2. ***CCAAT displacement protein binding activity.*** Depicted above is the full-length CDP protein. CDP contains four domains: CR1-3 and a cut homeodomain (HD), which are utilized in combination to carry out its promoter binding activities. The CR1 and CR2 domains take place in transient binding and CCAAT box displacing activity. Conversely, the CR3 and HD components are responsible for stable interaction with DNA at the consensus sequence ATCGAT. Modeled after Nepveu, et al. (2001)[63]. HD (cut homeodomain), CR (cut repeat).

1.8 The role of immune cells in the propagation of neuroinflammation

Microglia are glial cells that act as the isolated macrophage population in the CNS. Therefore, microglia serve as the primary mechanism of CNS defense. Studies stimulating their toll-like receptors have found that these cells are an important component of both the innate and active immune response, and active immunity in the brain and the spinal cord is linked to the regulation of neuroinflammation[78, 79]. Microglia are derived from $CD45^+$ bone marrow cells in the fetal brain and subsequently differentiate from $CD14^+$ monocytes to make up approximately 20% of the brain's total glial cell population[71]. Expression of cell surface proteins changes with their state of differentiation and activation[80, 81]. For example, differentiation from monocyte to microglia results in subsequent loss of CD14 and other myeloid-lineage markers[80]. However, many of these proteins may reappear upon injury in activated microglial cells; reexpression of CD14 was found in the CNS following stroke and HIVE[82]. Work utilizing the mouse model for Alzheimer's disease describes CD14's response to amyloid peptide and shows that mice with a genetic deficiency for CD14 show reduced microglial activation and subsequent neuronal death[83]. These findings strongly suggest that CD14 contributes to the neuroinflammatory response that is associated with neurodegenerative disorders. In contrast to the low levels expressed by undifferentiated microglia, active-phagocytic microglia express high levels of MHC class II proteins that they use to act as antigen-presenting cells, which activate T-cells to further the immune response[71, 84]. To prevent damage to critical neurons of the CNS, microglia must act quickly and to even minute pathological changes. In addition to dealing with harmful and infectious pathogens, microglial cells also take part in the scavenger cell processes such as cleaning up damaged and dying neurons[71, 81].

Like macrophages, microglia display a great degree of phenotypic and genotypic plasticity[71, 81]. Their state depends upon several factors including their present responsibility and relative location and similar to macrophages, they require appropriate stimulation in order to undergo their stepwise transformation/activation processes[84]. Under normal conditions, most microglial cells are found in their resting/ramified or quiescent state[71, 81]. In this form, a microglia's cell body is reduced in size while its branches or projections, which are constantly surveying its proximity, are large and branched. Ramified microglia serve as a constant "surveillance team", whose duty is to detect and react readily to minute pathological changes[81]. Glutamate receptor agonists, proinflammatory cytokines, cell necrosis factors (i.e. TNF-α), lipopolysaccharide (LPS) and extracellular potassium can trigger an activation response. Each of these compounds interact with cell surface receptors on microglia[85, 86, 87]. For example, LPS binds to LPS-binding protein (LBP) in the serum and interacts with its binding partner CD14[80]. CD14 then networks with TLR4 to create a

heteromeric receptor complex with myeloid differentiation protein-2 (MD-2) and induces the step-wise process of immunoactivation and cytokine production[80]. Additional cell surface receptors have been implicated in microglial response to LPS. For example, the CD11b (MAC1) integrin receptor serves as a TLR4-independent receptor for LPS and work using MAC1 -/- microglia demonstrates that these cells do not produce superoxide and other cytokines and reactive oxygen species (ROS) in response to LPS treatment[88]. During the process of immunoactivation, microglia can take on an activated but non-phagocytic form. Transformation from the quiescent to the non-phagocytic activated stage involves the retraction of peripheral branches, changes in protein expression and the secretion of signals involved in the proinflammatory cascade (i.e. cytokines, recruitment and proinflammatory molecules). In addition to these changes, it is during this stage that the microglia will begin to rapidly expand in preparation for an impending immune response. Furthermore, microglia in their most mature active form can become phagocytic and take on an amoeboid-like morphology[81]. Activated phagocytic microglia also possess the ability to migrate to the site of infection, engulf foreign bodies (e.g. viruses, bacteria, etc.) and display phagocytosed particles for T-cell activation[71, 81]. As the "housekeeping" cells of the CNS, microglia (in their amoeboid and resting forms) constantly monitor their surroundings for foreign material, apoptotic/damaged cells, extracellular/foreign DNA or neural tangles. In addition to their ability to sense and phagocytose the above material, microglia can take up extracellular lipids and other cellular waste. In neurodegenerative diseases, apoptotic cells and/or cellular debris are abundant and in the CNS, microglia serve as the primary mechanism aiding in their breakdown and disposal[71, 81]. Once an activated phagocytic microglia becomes completely engorged with phagocytic material, it is referred to as a granular corpuscle, which is unable to take up additional infectious material, and appears grainy in comparison to their non-engorged counterparts.

Microglia also aid in regional homeostatic maintenance by controlling the secretion of proinflammatory cytokines and immune cell chemo-attractants[84]. Studies have confirmed that microglial-produced TNF induces inflammation and neuronal cell apoptosis[84]. Prior work has shown that microglia are responsive, become activated, and secrete further IFN-γ in response to IFN-γ treatment[87]. This positive feedback pathway results in a cascade of microglial activation. Furthermore, activation of microglia stimulates NFκB, MAPK and MyD88-independent pathways that result in inflammatory mediator production[78, 85]. Also, measurable amounts of MDC, IL-8, and MIP-3β, involved in dendritic and T-cell recruitment, are produced by microglia[81]. In addition to the secretion of proinflammatory factors in response to LPS, microglia also activate NADPH oxidase, allowing for the production of extracellular superoxide and intracellular ROS. Elevated intracellular ROS concentrations are crucial for proinflammatory signaling. Interestingly and in support of this, NADPH deficient mice show a 50% reduction in TNF mRNA levels in response to LPS[85]. Superoxide

production in response to LPS stimulation has been recognized as independent of TLR4 activity; however, ROS species generated from this superoxide have been implicated in the production of TNF (through a TLR4 independent pathway)[85]. Furthermore, LPS exposure has been shown to induce nitric oxide (NO) production, which significantly up-regulated CD11b, a signal of microglia activation. Other known activators of NO production, such as IFN-γ, polyinosinic:polycytidylic acid (Poly I:C), IL-1β and HIV type1 gp120, all induced CD11b expression through the NO pathway[89]. Additionally, it has been shown that NO induces CD11b expression through the GC-cGMP-PKG-CREB pathway and that this pathway may be linked to neurodegenerative pathogenesis[89].

While the primary function of microglial cyto- and chemokine production is to protect the central nervous system, persistent and excessive activation contributes to neurotoxicity and neuropathology[84]. In response to homeostatic abnormalities in the CNS, microglia respond with the release of molecules that can regulate innate defenses, initiate adaptive processes, recruit additional support, and aid in tissue restoration[84]. These immunoregulatory signals act in an auto- and paracrine fashion, allowing microglia to communicate with other CNS-resident cell types (e.g. neurons, infiltrating leukocytes, astrocytes, etc.)[84]. Neuronal tissue is sensitive to the inflammatory process, and thus, microglial defense responses are tightly regulated. As a result, microglia are hesitant to initiate immune responses and cause CNS inflammation that may potentially lead to CNS damage[84]. Therefore, in the context of neurodegenerative disease, one can compare this mechanism to a double-edged sword, whereby immune responses and cytokine production is intended to act in a protective manner, however, aberrant control/overactivation results in pathological consequences.

Macrophages, like microglia, are vital in the initiation and propagation of both immune and inflammatory responses[90]. Monocytes and differentiated macrophages secrete both pro- and anti-inflammatory cytokines such as TNF, MIP-1α, IL-10 and MCP-1[91]. As such their proinflammatory functions have been implicated in many chronic diseases such as atherosclerosis and those of neurodegenerative nature such as multiple sclerosis, ALS, Tay-Sachs, Sandhoff and Alzheimer's disease[71, 75, 79, 90, 92]. Thus, a proposed therapeutic strategy to combat the effects of macrophage damage in the CNS has suggested the use of antibodies to interfere with monocyte recruitment and passage across the blood-brain barrier[93].

The profound similarities in the behaviour and origin of macrophages and microglia provide rationale for comparing inter-genotype bone marrow-derived macrophage (BMDM) behaviour and cytokine secretion in mouse models of neurodegeneration.

1.9 The roll of Toll-like receptors in inflammatory signaling

Toll-like receptors are single membrane-spanning pattern recognition receptors (PRRs) that are involved in the initiation of immune responses. TLRs recognize molecules that fall under the pathogen-associated molecular patterns (PAMPs) classification[94]. Material such as bacterial DNA, flagellin, lipopolysaccharide, peptidoglycans, and lipopeptides are all classified as PAMPs[94]. The expression of TLRs has been identified on macrophages as well as on both microglial and astrocytes in the CNS[95]. Activated TLRs interact with cytoplasmic adapter molecules (MyD88, MAL/TIRAP, TRIF and TRAM) to trigger/propagate two distinct downstream signaling pathways; the MyD88-dependent pathway and the TRAM and TRIF cascade (also known as the MyD88-independent pathway)[94]. Protein kinase pathways such as those involving PI3K, IKKs and MAP3Ks are involved in the signaling cascade responsible for the activation of transcription factors, which ultimately result in altered expression of genes involved in the immune response[94]. More specifically, TLR4 signaling in microglia leads to activation of NFκB and the downstream production of cytokines (e.g. IL-1, TNF and IL-6) or chemokines (e.g. IL-8/CXCL8) through the MyD88-dependent pathways (Figure 3)[94]. TRAM and TRIF-mediated signaling activates IFN regulatory factor-3 (IRF-3) and several IFN-β dependent genes[94, 96].

Crystallography studies of the human TLR3 ectodomain have indicated that TLRs share a highly glycosylated horseshoe-shaped structure with fifteen sites for potential N-linked glycosylation[97]. These N-linked glycosylation sites are found within the inner concave surface, are sialylated in the TLRs inactive state, and can be acted upon by sialidase to invoke TLR activation[97]. Sequence analysis suggests that the ectodomain of TLR4 contains nine N-glycosylation sites, each of which can be acted upon by NEU1 and thus, play a role in TLR activation and successive signaling[69, 70].

Microglial cells express mRNA for TLRs 1-9, including TLR4, and the stimulation of this receptor plays a pivotal role in their activation, which can lead to autoregulatory microglial apoptosis and neuronal cell death[78, 98]. Typically, TLR4 is considered to be the primary receptor for LPS[94]. It has been demonstrated that stimulation with LPS (TLR4 ligand) resulted in macrophage and microglial activation, ROS production, and caused brain microglia to undergo apoptosis[85]. Recent work by Fernandez-Lizarbe et al. (2009) has supported TLR4's role in microglial activation and neuronal cell death[99]. Their work showed evidence confirming TLR4-mediated microglial activation, cytokine production, and subsequent neuron death. Additionally, TLR4 -/- mice were devoid of ethanol-induced microglial activation, further supporting their hypothesis[99]. Furthermore, work by Jung et al. (2005) demonstrated that TLR4 is associated with microglial apoptosis through the action of autocrine/paracrine IFN-β production[100]. Other work has revealed that many external stimuli induce

microglial activation through TLR-mediated pathways. For example, Poly I:C responses utilize TLR3 and reaction to CpG DNA is mediated by TLR9[78, 101].

The presence of gangliosides indisputably leads to the activation of microglia[86, 102, 103]. Gangliosides cause the activation of NFκB, leading to the production of IL-1β, TNF and inducible nitric oxide synthase (iNOS). The JAK-STAT inflammatory signaling pathway has been implicated in ganglioside-stimulated microglial activation. Gangliosides were shown to activate JAK1 and JAK2 as well as cause Stat1 and signal transducer and activator of transcription 3 (Stat3) phosphorylation, leading to increased ICAM-1 and MCP-1 transcription[103]. Furthermore, neuraminidase treatment has been shown to have a dose-dependent inhibitory effect on the phosphorylation of STAT1, indicating that the sialic acid component of the gangliosides may play a crucial role in JAK-STAT-mediated microglial activation[103]. Additionally, asialo derivatives of GM1 were not able to induce STAT phosphorylation and transcription of iNOS, ICAM-1 and MCP-1[103]. More recently, Min et al. (2004) showed that the microglial ganglioside response occurs via the protein kinase C (PKC) and NADPH oxidase pathways[102]. Moreover, protein kinase A (PKA) has also been implicated in ganglioside-mediated microglial production of proinflammatory cytokines[86].

Microglia also respond to Poly I:C via TLR3. Wild-type primary culture microglia upregulate TLR3 and IFN-β mRNA in response to synthetic dsRNA Poly I:C and secrete TNF and IL-6 in a dose-dependent manner. In support of these findings, TLR3 -/- mice were found to have reduced microglial activation following infection with West Nile virus[101]. Furthermore, wild-type mice displayed clear microgliosis following Poly I:C injection, whereas this phenotype was virtually nonexistent in TLR3 -/- animals[104]. CpG-induced microglia activation has also been shown to cause upregulation of cytokine and chemokine production at both the transcription and protein level[78]. Cells react to CpG-containing oligonucleotide motifs via TLR9.

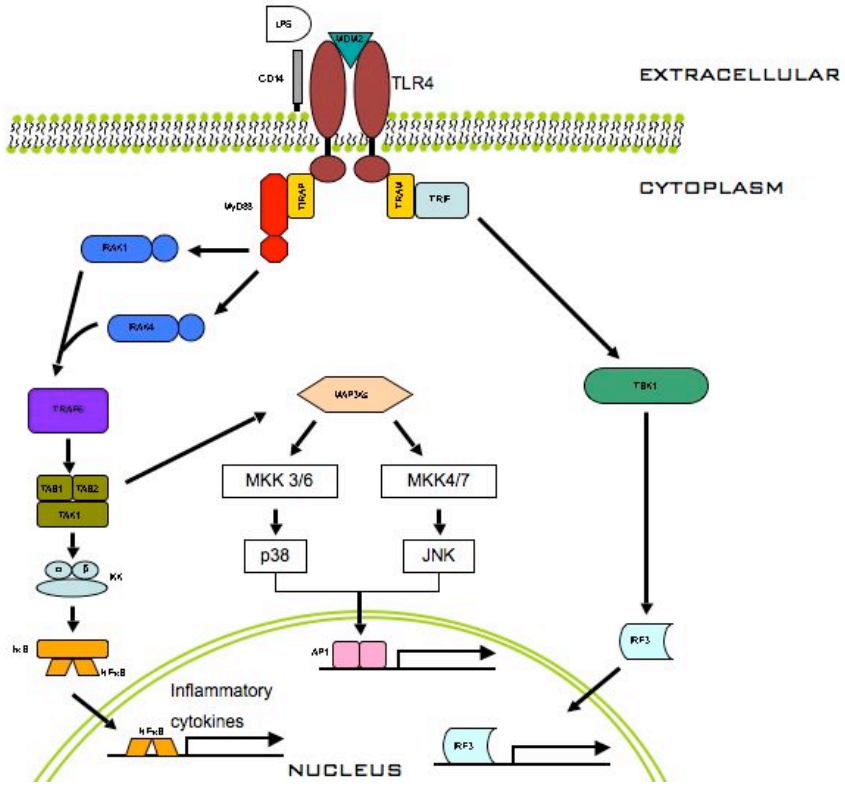

Figure 3. ***TLR4 signaling pathway.*** Toll-like receptors mediate transmembrane intracellular responses to extracellular stimuli. This figure depicts TLR4 signaling during LPS stimulation. Binding of LPS to the extracellular domain of TLR4 initiates intracellular signaling via the MyD-88 dependent and/or MyD-88 independent pathway(s). The MyD-88 dependent kinase cascade culminates in NFκB and/or AP1 translocation into the nucleus and corresponding gene transcription. TLR signaling is intimately linked with inflammatory processes such as cytokine secretion.

1.10 Recent work on LSDs in transgenic animal models

Recent advancements in transgenic, cloning and knockout/knock-in technologies have allowed comprehensive study of lysosomal storage diseases. Such strategies have been used to produce murine models possessing defects in the genes, *HEXA* and *HEXB*. These mice, like their human counterparts have deficiencies in the enzyme β-hexosaminidase, however, their corresponding phenotypes differ drastically from those seen in humans[105, 106]. As outlined previously, human GM2 gangliosidoses all present with clinically indistinguishable phenotypes. Conversely, *hexa* -/- (TSD) and *hexb* -/- (Sandhoff) mice display drastically different disease progression. At 3-4 months of age, *hexb* KO mice develop neurological symptoms and die of profound neurodegeneration approximately 4-6 weeks later. In contrast, the disease course experienced by *hexa* KO mice is greatly delayed; these mice remain virtually asymptomatic into their 2nd year of life[105, 106]. Tay-Sachs mice avoid disease for a significant proportion of their lifespan by utilizing a sialidase-mediated bypass of HEXA deficiency in the catabolism of intralysosomal gangliosides[64]. In HEXA deficient patients, a significant accumulation of GM2 gangliosides occurs in the lysosomes as a result of an inability to break GM2 down to GM3. However, in *hexa* -/- mice, GM2 can be metabolized through an alternative pathway where it is desialylated by murine lysosomal sialidase (human NEU1 homolog) to the asialo derivative, GA2, and then further broken down to lactosylceramide by the HEXB isozyme (Figure 4)[64]. Sandhoff mice are unable to utilize this bypass to cope with accumulated GM2 ganglioside because they are also deficient in HEXB activity. As a result, Sandhoff mice show significant intralysosomal accumulations of GM2 and GA2 gangliosides[45, 105]. Investigation into the mechanism responsible for the pathophysiology seen in the *hexb* -/- mice has revealed significant neuronal apoptosis and subsequent denervation in areas of the spinal cord, cerebellum and brain stem[105]. Furthermore, neuronal GM2 accumulation has been shown to occur in these regions as well as other parts of the brain[105]. These findings are consistent with those observed in human subjects. As such, the Sandhoff (*hexb* -/-) mouse is an important animal model that closely mimics human neuropathology and can be used to study disease progression.

Wada et al. have demonstrated that the process of neuronal death in these mice was preceded by increased transcription of genes involved in microglia-mediated inflammation[77]. Furthermore, Wu and Proia (2004) show evidence for peripheral microglial invasion into the CNS and heightened astrocyte MIP-1α expression. Decreased invasion and immune-cell-mediated neuronal death could be observed following abolishment of MIP-1α expression[92]. Thus, evidence supports cytokine-induced, macrophage/microglial-mediated neuronal apoptosis as the prevailing mechanism responsible for neurodegeneration in Sandhoff disease.

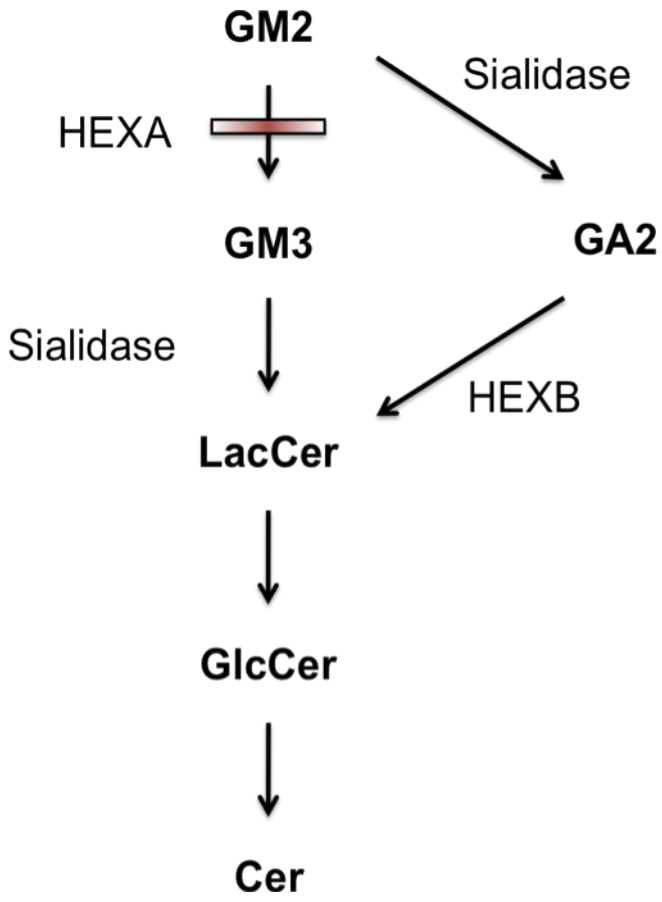

Figure 4. ***Sialidase mediated bypass utilized by hexa -/- (Tay-Sachs) mice.*** HEXA deficiency in *hexa* knockout mice renders them unable to catabolize GM2 via the typical pathway. However, Tay-Sachs animals avoid intralysosomal accumulation of GM2 through the utilization of a lysosomal sialidase-mediated bypass. This circumventive mechanism converts GM2 to its asialo-derivative, GA2, before further processing to lactosylceramide by residual HEXB activity. In Sandhoff (*hexb* -/-) mice, no residual HEXB activity remains, resulting in a blockage of both the normal catabolic and bypass pathways. Figure adapted from Igdoura et al (1999)[64]. Cer (ceramide), GlcCer (glucosylceramide), LacCer (lactosylceramide), HEXA (β-hexosaminidase A), HEXB (β-hexosaminidase B).

1.11 Research Objectives

Part I

As discussed above, previous work has illustrated that *hexa* -/- mice avoid classical pathological symptom development by lessening intralysosomal ganglioside accumulation via a sialidase-mediated bypass. However, whether humans naturally utilize this mechanism of disease avoidance has not been well studied. The recent creation of a truncated protein able to increase sialidase transcription ($CDP^{831-1505}$), its packaging into a suitable delivery vector, and infection of human neuroglia cells has suggested that this bypass may be possible in human cells. Immunohistochemical analysis has shown decreased GM2 ganglioside in TSD neuroglia with increased sialidase activity. Furthermore, overexpression of sialidase via adenoviral infection with exogenous *NEU1* showed a marked reduction in GM2 accumulation in human Tay-Sachs fibroblasts. Recent work by Matthew Johnson has shown that overexpression of a truncated repressor protein, CCAAT displacement protein, is able to increase sialidase activity in human TSD neuroglia. These observations lend credence to the pursuit of compounds capable of transcriptionally regulating lysosomal sialidase, for the treatment of human Tay-Sachs disease. However, there is a lack of *in vitro* empirical evidence linking the overexpression of truncated CDP to increased protein levels of lysosomal sialidase and lessening of intralysosomal GM2 accumulation. As such, the goals of this aspect of my research were to: i) observe the effects of CDP overexpression on sialidase protein expression in human TSD neuroglia, ii) examine the effects of CDP overexpression on the ganglioside profile of TSD neuroglia, and iii) investigate the potential mechanism(s) of action of CDP on the lysosomal sialidase promoter.

The pinnacle objective of this aim is to uncover pharmacological compounds capable of regulating sialidase for the eventual treatment of Tay-Sachs disease via the sialidase-mediated bypass.

Part II

Previous work has demonstrated that Tay-Sachs (*hexa* -/-) mice escape neurodegeneration and are asymptomatic until approximately 2 years of age. This differs significantly from the progression of Tay-Sachs disease in humans as well as the mouse model of Sandhoff disease that begin to present neurodegenerative symptoms at about 3-4 months of age. Furthermore, prior work has uncovered a sialidase-mediated bypass pathway utilized by Tay-Sachs mice in which accumulated GM2 is indirectly converted to lactosylceramide via sialidase and HEXB though the asialo intermediate, GA2. The current hypothesis states that the bypass pathway sufficiently alleviates intralysosomal ganglioside

accumulation in *hexa* -/- animals to levels below the threshold required for imminent and profound pathology; however the downstream events through which disease is avoided in *hexa* -/- mice and presumably mediated in *hexb* -/- animals is currently unexplored. Given this drastic difference in disease progression between these two closely related lysosomal storage disorder mouse models, we further hypothesize that the subsequent lack of pathology can be explained via differences in immunoregulation and resultant CNS pathology. Moreover, it is predicted that given similar stimulation, the immune response of bone marrow derived macrophages from Tay-Sachs mice will be dampened compared to that of the Sandhoff (*hexb* -/-) mouse. Extrapolated *in vivo*, this could explain their retarded progression of disease (i.e. complex neuropathology). The aims of this objective were to: i) investigate physiological characteristics of *hexa* -/- and *hexb* -/- bone marrow-derived macrophages, ii) assess the extent of ganglioside accumulation in immune cells, and iii) study the response of bone marrow-derived macrophages to various types of stimuli and examine downstream signaling.

CHAPTER 2

MATERIALS AND METHODS

2.1 Cell Culture

Normal (CRB/Nor) and Tay-Sachs (CRB/TSD) neuroglia cells were provided by Dr. Brooks at the Kingsbrook Jewish Medical Center (New York, NY). Cells were maintained in Dulbecco's Modified Eagle's Medium (DMEM) supplemented with 15% fetal bovine serum (FBS), 1% penicillin and streptomycin, and 0.1% fungizone. Bone Marrow Derived Macrophages were cultured in Roswell Park Memorial Institute (RPMI) media supplemented with 10% FBS, 1% penicillin and streptomycin, 0.1% fungizone and 2% 1M 4-(2-hydroxyethyl)-1-piperazineethanesulfonic acid (HEPES).

2.2 Use of Recombinant Adenovirus (Ad)

Construction of the AdCDP$^{831\text{-}1505}$ adenoviral vector was performed by Matthew Johnson and is thoroughly described in his Master's thesis. Infection of CRB/TSD neuroglia with AdCDP$^{831\text{-}1505}$, AdSialidase, AdCathepsin A, Adβ-gal, or AdPFG140 was performed for 30 minutes in a minimal volume of phosphate-buffered saline (PBS)++ at 37°C. Culture dishes were rocked every 5 minutes to ensure even distribution of virus. Following infection, cells were replenished with fresh DMEM supplemented as outlined in 2.1. Infection duration was 72 hours unless otherwise indicated.

2.3 Western Blotting

Cells were harvested in 100μL radioimmunoprecipitation assay (RIPA) buffer (50mM Tris, 150mM NaCl, 1% NP-40, 0.5% deoxycholic acid, 0.1% sodium dodecyl sulfate (SDS), pH 7.4) and frozen at -80°C. Protein determination was performed using the Lowry Assay (BioRad). Lysates were combined with 6x loading buffer and boiled at ~95°C for 5 minutes. Prepared samples were loaded (in equal protein quantity) into a 10% Tris-glycine SDS-polyacrylamide gel electrophoresis (PAGE) resolving gel with a 5% stacking gel, and run for 2.5 hours at 90V. Run gels were blotted onto nitrocellulose membranes for 70 minutes at 90V. Membranes were blocked for ≥ 1 hour at room temperature with 5% non-fat powdered milk in tris-buffered saline with Tween-20 (TBST) (10mM Tris-HCl, 150mM NaCl, 0.05% Tween-20). Blocked membranes were then incubated on a tilting rocker with the indicated primary antibody at the specified concentration (see section 2.12) overnight at 4°C. Following overnight incubation with the primary antibody, blots were washed with TBST before begin incubated with the appropriate horseradish peroxidase

conjugated secondary antibody at a dilution of 1:10,000 for 1-2 hours. Membranes were washed again with TBST before being incubated with ECL reagent (GE Healthcare) for 2 minutes. Luminescent membranes were exposed to Amersham Hyperfilm ECL high chemiluminescence imaging film (GE Healthcare).

Blots subjected to additional probing were first stripped by washing with harsh strip buffer (10mL 0.5M Tris pH 6.8, 70mM SDS, 0.7% β-ME) twice for 15 minutes at 55°C. Stripped blots were then blocked, probed and developed as described above.

2.4 Ganglioside Extraction, Thin Layer Chromatography (TLC) and Mass Spectroscopy

CRB/Nor and CRB/TSD cells were infected as described in 2.2 with 20MOI AdCDP$^{831\text{-}1505}$, AdSialidase, AdCathepsin A, or Adβ-gal. 96 hours post-infection, cells were trypsinized and pelleted via centrifugation (10 minutes at 2050rcf). Media was removed from the tubes and pellets were frozen at -80°C. Thawed pellets were resuspended in 200μL ddH_2O and sonicated using a pulsing probe sonicator (40% output for ~10 seconds). Aliquots of lysed cells were collected to determine protein concentration via the Lowry assay (BioRad) and for western blot analysis. The remaining 160μL of lysate was then added to 3.2mL of chloroform:methanol (1:1). The following steps were subsequently performed: i) water bath sonication for 30 minutes, ii) centrifugation for 15 minutes (at 2050rcf), iii) collection of supernatant, and iv) addition of 4mL of chloroform:methanol:ddH2O (10:10:1). Steps i-iii were repeated and following removal of the second supernatant (step iii), the pellet was resuspended in chloroform:methanol:sodium acetate (0.8M) (30:60:8). Steps i-iii were repeated a final time and supernatants (pooled for each sample) were evaporated under an airstream overnight at room temperature. Dried lipids were resuspended in chloroform:methanol:ddH2O (30:60:8) and kept at pH 11, using KOH, for 4 hours at 50°C. Samples were subsequently cooled and brought to pH 7 using glacial acetic acid. Saponified debris was pelleted via centrifugation (at 2050rcf) and washed once with chloroform:methanol:ddH2O (10:10:1). Supernatants were collected and evaporated overnight as described above. Dried lipids were dissolved in chloroform:methanol:ddH2O (10:10:1), run through a Sephadex G-50 quick spin column (Roche), and then passed through a diethylaminoethyl (DEAE) sepharose column (GE Healthcare). The collected solutions were evaporated overnight and the dried samples subsequently dissolved in chloroform:methanol:potassium chloride (0.1M) (3:48:47). Each sample was then passed through a Sep-PAK C18 reverse phase column (Waters), eluted, and evaporated overnight. Extracted gangliosides were dissolved in 100μL of chloroform:methanol:ddH2O (10:10:1).

Dissolved samples were spotted on a silica gel TLC plate in 1.5cm lanes, 0.5cm apart. Loading volume was normalized to the initial protein concentration of pre-extraction lysates. TLC plates were run in a pure acetone phase, dried, then run in a chloroform:methanol:calcium chloride (0.2%) (60:35:8) phase. Run plates were allowed to dry before being spray with resorcinol (Sigma) in 10.6% H2SO4. Stained plates were baked in a 110-120°C oven between 2 pieces of clean glass for 60 minutes and visualized using incandescent backlighting. Photos were captured using a Canon DSLR and quantified using ImageJ software.

Samples to be sent for analysis by mass spectroscopy were isolated from unstained silica gel TLC plates. Samples were run in duplicate to allow for the determination of band location. Subsequent to running of the second phase, the TLC plate was cut in half using a glass-cutting tool. One half of the plate was stained with resorcinol as previously described. The location of the band to be scraped was determined by overlaying the unstained half onto the stained half. Gangliosides were eluted from the scraped silica in 200µL of methanol with gentle vortexing. Samples were subsequently spun at 1000rpm for 5 minutes to pellet the silica. Supernatants were transferred and pooled in a fresh tube, evaporated under nitrogen gas, and resuspended in 100µL of chloroform. Extracted samples were then analyzed by Matrix-assisted laser desorption/ionization-Time of flight (MALDI-TOF) mass spectroscopy at the McMaster Regional Centre for Mass Spectroscopy. M/Z results were screened using the mass spectroscopy search tool on the Human Metabolome Database.

2.5 Primary Cell Isolation from Murine Bone Marrow and Macrophage lineage differentiation

Male mice of the indicated age and genotype were anesthetized with 5% tribromoethanol (Avertin; Sigma) at a dose of 0.25mL/20g body weight. Femurs, tibiae and humeri were isolated from anesthetized mice, cleaned of muscle tissue and marrow was flushed with 1mL of RPMI culture media supplemented as described in 2.1. Cells were pelleted at 4°C in a microfuge at 1000rcf for 10 minutes, media was removed, and the pellet was resuspended in supplemented RPMI media with 5ng/mL macrophage colony stimulating factor (M-CSF) (Invitrogen). Resuspended cells were plated in 6- or 24-well tissue culture plates (unless otherwise indicated), washed every 48 hours with PBS, and differentiated to macrophages in culture for 10 or 12 days. Fresh M-CSF-supplemented RPMI culture media was added following each PBS wash. Differentiated macrophages were treated with PAMPs at the indicated concentration for the specified duration prior to media collection and cell harvest.

2.6 Detection of Inflammatory Mediators via Enzyme-linked Immunosorbent Assay (ELISA)

Cell media samples collected from bone marrow derived macrophage cultures following PAMP stimulation were assayed for TNF, IL-6, IL-10, MCP-1, and/or IL-1β using Opt-EIA ELISA reagents, standards and antibodies (BD Biosciences). Culture media samples were pre-plated and diluted accordingly in an uncoated 96-well plate before being transferred to the coated ELISA plate; this prevented intra-plate time course variation. Measurements obtained from ELISAs were normalized to total protein concentration as determined by the Lowry assay (BioRad).

2.7 Specific Sialidase Activity Assay

Media was removed and cultured cells were washed twice with ice-cold PBS. 100µL of ice-cold ddH_2O was added directly to each well. Repetitive pipetting was used to ensure cell lysis. 50µL of cell lysate was transferred to its corresponding reaction mixture containing 100mg/mL BSA, sodium acetate buffer (0.8M) and 4-methylumbelliferyl-n-acetyl-α-D-neuramide (4-Mu-NANA) as a substrate for sialidase. Reaction mixtures were incubated for 1 hour at 37°C, after which the reactions were stopped with 2mL of 0.1M 2-amino-2-methyl-1-propanol (MAP), pH 10.5. 200µL of the stopped reaction mixture was plated in a black 96-well plate and fluorescence was measured using an LS Reader Plate Fluorometer (Perkin Elmer). Specific sialidase activity was normalized to cell lysate protein concentration as determined by the Lowry Assay (BioRad).

Note: This assay was performed in the dark.

2.8 Immunocytochemistry

Bone marrow-derived macrophages were cultured and differentiated to macrophages as described in 2.5. Differentiated macrophages were washed twice with ice-cold PBS and subsequently fixed with 3.7% formaldehyde for 30 minutes at room temperature. Fixed cells were permeabilized for 30 minutes at room temperature with 0.5% Triton-X 100 in PBS. Blocking was performed with 10% goat serum in PBS for 1 hour at room temperature. Primary antibodies (α-CD11b and α-SAP-A) were incubated overnight at 4°C in PBS with 1% goat serum. Cells were washed with PBS-T (PBS + 0.1% Tween 20) prior to addition of the fluorescent secondary antibodies (in PBS + 1% goat serum). Secondary antibodies (Texas Red - Alexa 594 and Bodipy-F - Alexa 488) were incubated in the dark for 1.5 hours. Cells were washed again and Hoechst nuclear stain was

added at 1:1000 in PBS for 10 minutes. Excess Hoechst stain was rinsed away with PBS and glass cover slides were mounted using ProLong Gold Antifade Reagent (Invitrogen). Images were captured using a Zeiss Axiovert 200 microscope (with a Zeiss HBO 100 mercury lamp) and Zeiss Axiovision software. CD11b, SAP-A and Hoechst images were taken through the Cy3, FITC and DAPI filters, respectively. Image exposures were held constant for each channel.

2.9 Chromatin Immunoprecipitation (ChIP)

ChIP was performed using the ChIP-IT™ Express Enzymatic kit (Active Motif) in combination with the ChIP-IT™ Human Control Kit (Active Motif). CRB/TSD neuroglia were grown in 150cm dishes with DMEM culture media as described in 2.1. When dishes reached ~75% confluency, cultures were either left untreated or infected with PFG140 (mock virus) or AdCDP$^{831\text{-}1505}$ at 20MOI as described in 2.2. 72 hours post infection, cells were fixed with 3.7% formaldehyde containing 1% methyl alcohol (Sigma) in minimal DMEM culture media for 8 minutes. Washed cells were subsequently harvested by scraping with a rubber policeman, pelleted via centrifugation and frozen at -80°C. Frozen cell pellets were thawed on ice before being resuspended in lysis buffer. Samples were incubated on ice for 30 minutes, transferred to a dounce homogenizer and dounced on ice with ~125-150 strokes to aid in nuclei release (monitored via phase contrast microscopy). Released nuclei were spun down, resuspended in digestion buffer and warmed to 37°C for 5 minutes. Warmed chromatin was sheared using the supplied enzymatic shearing cocktail (200U/mL) for 10 minutes at 37°C with gentle vortexing every 2.5 minutes. ChIP reactions were set up using 21µg of sheared chromatin. RNA Polymerase II and mouse IgG control antibodies were purchased from Active Motif and the α-HA tag antibody was acquired from Santa Cruz Biotechnology. 2µg of each antibody was utilized for each ChIP reaction. Protein G magnetic beads were preincubated with rabbit α mouse bridging antibody (Jackson Immuno Research) before being added directly to the ChIP reaction mixture. Briefly, 25µL of protein G beads were mixed with 5µL of bridge antibody (per reaction) and incubated for 1 hour at 4°C on an end-over-end rotator. Protein G beads were then washed to remove residual unbound bridge antibody before being utilized for ChIP. ChIP reactions were set up as follows:

Treatment	ChIP Antibody	Reaction Number
Uninfected	RNA polymerase II	1
	Mouse IgG	2
	Anti-hemagglutinin	3
AdCDP$^{831\text{-}1505}$	RNA polymerase II	4
	Mouse IgG	5
	Anti-hemagglutinin	6
PFG140 (mock)	RNA polymerase II	7
	Mouse IgG	8
	Anti-hemagglutinin	9

ChIP reactions were incubated overnight (~20 hours) at 4°C on an end-over-end rotator. Samples were then washed a total of three times before eluting the chromatin from the protein G magnetic beads, and reversing the cross-linking between the eluted chromatin and associated transcription factors. Supernatants were then transferred to fresh 200µL polymerase chain reaction (PCR) tubes, heated to 95°C for 15 minutes in a thermocycler, and incubated with proteinase K for 1 hour at 37°C. The resultant DNA was then used immediately for PCR. 5µL of template was used in each reaction and input controls were diluted 1 in 10 prior to use. Expected product sizes for the CR3-HD and intergenic primer sets were 144bp and 101bp, respectively.

PCR conditions:

PCR program: 94°C for 4 minutes
[94°C for 30 seconds
59°C for 30 seconds
72°C for 30 seconds]
72°C for 4 minutes

Note: Bracketed steps were repeated for 36 cycles.

CR3-HD primer sequences: Fwd 5'-ATT CTC TCC ACG ACG ACA GG-3'
Rev 5'-ACT GGC TGG GGT GAA GAA G-3'

Intergenic primer sequences: Fwd 5'-CTA GAA GGC CAA AGG CAT CA-3'
Rev 5'-GTA TCC AGG CTC CCT TCC TT-3'

2.10 Antibodies

Western Blotting: Western blots performed on cell lysates (CRB/TSD neuroglia or *hexa* -/-, *hexb* -/-, *glb1* -/-, or wild type BMDMs) were probed using the following primary antibodies: α-75 sialidase (generated by the Igdoura lab; 1:4000; rabbit α human), α-HA tag (Santa Cruz Biotechnology; 1:1000; mouse), α-phosphorylated-p38 (Santa Cruz Biotechnology; 1:500; rabbit), α-total-p38 (Santa Cruz Biotechnology; 1:500; rabbit), α-phosphorylated-Stat3 (Cell Signaling Technology; 1:1000; rabbit), α-total-Stat3 (Cell Signaling Technology; 1:1000; rabbit), α-Mpg-1 (Cell Sciences; 1:2000; rabbit), α-Gpnmb (Novus Biologicals; 1:1000; rabbit), α-β actin (Cell Signaling Technology; 1:1000; mouse), α-phosphorylated GSK3α/β (Cell Signaling; 1:1000; rabbit), α-total GSK3β (Cell Signaling; 1:1000; rabbit), α-Grp78 (BD Biosciences; 1:1000; mouse), α-LAMP2 (Developmental Studies Hybridoma Bank; 1:1000; rat), and/or α-GAPDH (R&D Systems; 1:2000; goat).

Immunocytochemistry: Immunocytochemical analysis of *hexa* -/-, *hexb* -/-, *glb1* -/- and/or wild type BMDMs utilized the following primary anybodies: α-CD11b (BD Biosciences; 1:250; rat), α-Gpnmb (Novus Biologicals; 1:200; rabbit), α-Mpg-1 (Cell Sciences; 1:200; rabbit), α-Mac3 (BD Biosciences; 1:200; rat), α-Grp78 (BD Biosciences; 1:400; mouse), and α-SAP-A (1:500; rabbit). Corresponding secondary antibodies: Texas Red (Invitrogen; Alexa 594; 1:400; goat α rat), Texas Red (Invitrogen, Alexa 594; 1:400; goat α mouse), and Bodipy-F (Invitrogen; Alexa 488; 1:400; goat α rabbit).

Chromatin Immunoprecipitation: ChIP analysis of CRB/TSD AdCDP$^{831\text{-}1505}$ infected neuroglia utilized the following antibodies: α-RNA Polymerase II (Active Motif; 2μg/rxn; mouse), Mouse IgG (Active Motif; 2μg/rxn; mouse) and α-HA tag (Santa Cruz Biotechnology; 2μg/rxn; mouse). Bridge antibody used between primary and protein G magnetic beads: rabbit α mouse IgG (Jackson Immuno Research; 9μg/rxn).

2.11 Statistical Methods

One-way analyses of variance (ANOVA), Tukey's Post Hoc testing and all other statistical analyses were conducted using GraphPad Prism 5.0 Software (GraphPad Software Inc., La Jolla, California). Significance was defined as $P < 0.05$. Graphs are shown with standard errors unless otherwise indicated.

CHAPTER 3

RESULTS

SECTION I

3.1 Lysosomal sialidase levels in CRB/TSD neuroglia following AdCDP$^{831-1505}$ infection.

The normal and Tay-Sachs neuroglia primary cell lines (CRB/Nor and CRB/TSD, respectively) were gifted from Dr. Brooks at the Kingsbrook Jewish Medical Centre (New York). Prior work in our lab has been conducted on the human lysosomal sialidase promoter and has established CCAAT displacement protein as a repressor capable of influencing lysosomal sialidase expression. Moreover, endogenous CDP expression has been confirmed using RNA extracted from CRB/Nor and CRB/TSD neuroglia. Furthermore, previous studies in our lab have demonstrated a marked increase in sialidase promoter (~50-fold) and specific sialidase activity (~5-8-fold) in CRB/TSD cells following transient transfection with a construct expressing the truncated CDP$^{831-1505}$ protein. However, prior attempts to provide sound evidence to support these findings at the protein level have been unsuccessful.

To assess sialidase protein expression following infection with truncated CDP$^{831-1505}$ protein, infection of these cells was performed with AdCDP$^{831-1505}$ at 100 and 400MOI, followed by the addition of proteasomal and lysosomal inhibitors of protein degradation (Mg132 and E64, respectively) 24 hours later. Cells were harvested 72 hours post infection and subjected to SDS-PAGE. Western blotting for lysosomal sialidase revealed an MOI-dependent increase in sialidase protein levels in infected lysates versus uninfected controls (Figure 5). Further probing with an α-HA antibody revealed a direct correlation between MOI and levels of HA-tag-bound CDP$^{831-1505}$ protein. No differences in sialidase protein expression were observed between groups receiving no post-infection treatment, Mg132 or E64. Thus, infection with the CDP$^{831-1505}$ truncation was correlated with a subsequent increase in lysosomal sialidase protein expression. This was consistent with previous findings that transfection with the CDP$^{831-1505}$ construct stimulates lysosomal sialidase promoter activity as well as specific sialidase activity with 4-Mu-NANA as a substrate.

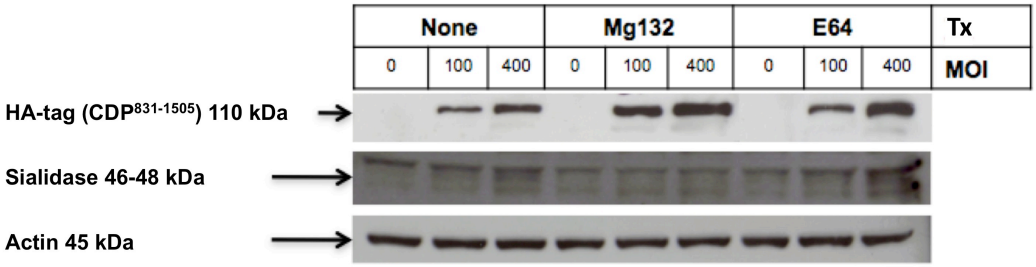

Figure 5. ***Sialidase protein expression in Tay-Sachs neuroglia infected with adenovirus expressing truncated CDP$^{831-1505}$.*** Tay-Sachs neuroglia were infected with 100 or 400MOI of AdCDP$^{831-1505}$ and subsequently treated with inhibitors of protein degradation (0.6μM Mg132 or 10μM E64) 24 hours post infection. Cells were harvested 48 hours after inhibitor addition. 50μg of cell lysate was loaded and run on SDS-PAGE. Membranes were probed for hemagglutinin (HA) to assess infection efficacy, and sialidase to evaluate resultant protein expression. Neuroglia cultures infected with AdCDP$^{831-1505}$ displayed an MOI-related increase in sialidase protein level. MOI (multiplicity of infection), Tx (treatment).

3.2 GM2 ganglioside accumulation in CRB/TSD neuroglia following sialidase augmentation via AdCDP$^{831\text{-}1505}$.

Tay-Sachs disease, resulting from a biochemical deficiency in HEXA, is hallmarked by intralysosomal accumulation of GM2 ganglioside. Such accumulations may then lead to increased ER stress and eventual cellular apoptosis. Widespread neuronal apoptosis in the CNS triggers neuroinflammation and propagates the positive feedback neurodegenerative pathway. Previous work has demonstrated that Tay-Sachs mice, while genetically identical to the human condition, are biochemically distinct regarding their disease progression and [lack of] symptom presentation. Studies by Igdoura et al. (1998) have revealed a bypass mechanism whereby *hexa* -/- mice utilize sialidase (rather than the deficient HEXA enzyme) in the sequential degradation of GM2 ganglioside, thereby lessening intralysosomal lipid accumulation and avoiding disease pathology. Previous hypotheses have implicated that an insufficient quantity of human lysosomal sialidase is responsible for the absence of an operational sialidase-mediated bypass in human tissue. Further (and previously published) work showed that infection with an adenoviral vector expressing human lysosomal sialidase (AdSialidase) lessened intralysosomal GM2 ganglioside accumulation in human neuroglia, lending credence to the previous hypothesis. Moreover, prior work has also provided evidence that truncations of the CCAAT displacement protein can act as an *in vitro* enhancer for the human neuraminidase 1 gene and data presented in 3.1 confirmed that endogenous lysosomal sialidase protein could be unregulated using adenoviral delivery of CDP$^{831\text{-}1505}$.

To assess whether modulation of the endogenous human lysosomal sialidase promoter could result in lessened intralysosomal ganglioside accumulation, TSD neuroglia cultures were grown to ~70% confluency and infected with 20MOI of Adβ-gal, AdCDP$^{831\text{-}1505}$ or AdSialidase + AdCathepsinA (AdCA). 96 hours post-infection, cells were harvested and gangliosides extracted. Isolated gangliosides were then separated using silica gel thin layer chromatography; loading was normalized to the protein concentration of the cell lysates used as input material for the ganglioside extraction. GM2 (top band of doublet quantified) was quantified relative to levels of GM1 starting material using densitometry following resorcinol staining. TSD neuroglia treated with AdCDP$^{831\text{-}1505}$ or AdSialidase + AdCA exhibited significantly reduced GM2 relative to uninfected and mock infected controls (Figure 6 and 7). This data was generated from 5 independent experiments. Final GM2/GM1 quantification ratios were pooled for each treatment group to calculate statistics.

One observation to note is the difference in migratory behavior observed between murine (Sandhoff brain controls) and human (CRB/TSD samples) GM2 and GA2 species. Murine GM2 and its asialo-GA2 migrated more slowly up the silica gel TLC than did their human-derived counterparts. This behaviour may be

attributed to interspecies size variation of the ganglioside sphingosine-linked fatty acid chain, and was not considered to affect the primary observations regarding GM2 accumulation.

To confirm the identity of TLC-separated gangliosides, mass spectroscopy was performed on methanol-extracted gangliosides isolated from a silica gel TLC. Gangliosides were extracted from *hexb* -/- cerebellums, and subsequently pooled, evaporated, and resuspended in a low volume to increase total ganglioside concentration. Cerebellum-derived ganglioside samples were run in duplicate on a silica gel TLC plate. The plate was then cut in half, one half was stained and the other half was left unstained. The two halves were aligned; samples were collected from unstained plate, and extracted in 100% methanol. Extracted samples were evaporated and resuspended in 100% chloroform. MALDI-TOF mass spectroscopy was performed by the McMaster Regional Centre for Mass Spectroscopy and results were screened using the MS Search tool on the Human Metabolome Database (HMDB).

Samples scraped from putative GM2 and GA2 bands contained their predicted species. More specifically, the GM2 sample contained a peak at 1417.8379, which corresponded to a GM2 ionization M/Z in the HMBD (Figure 8B). Similarly, the GA2 mass spectra displayed a marked M/Z peak at 1243.8201 (Figure 8C). However, each sample also contained many M/Z peaks that could potentially correspond to other ganglioside species, which suggested that the samples were not pure and likely contained other gangliosides.

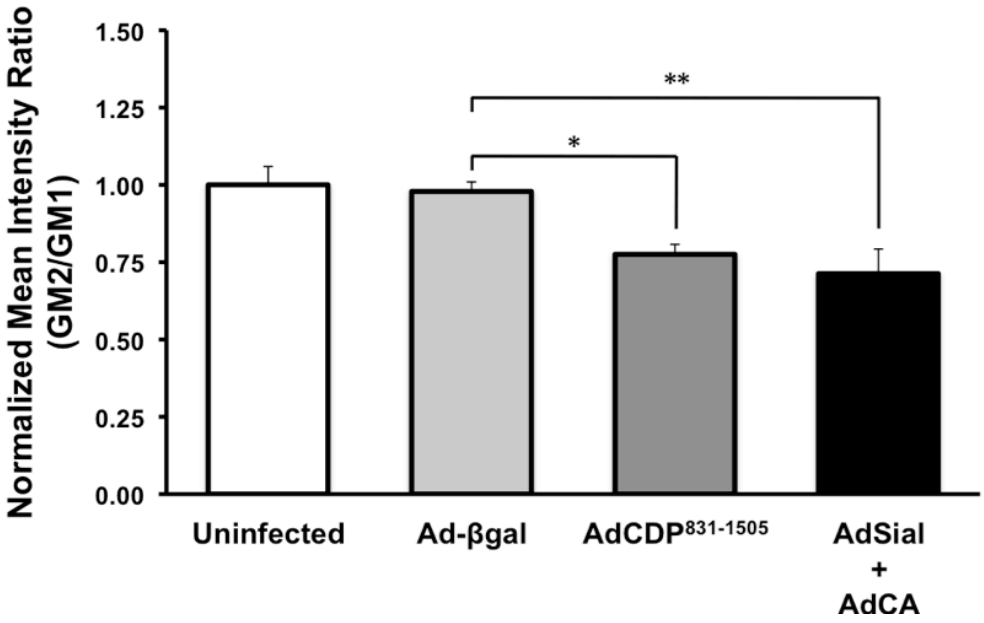

Figure 6. ***Levels of GM2 ganglioside in Tay-Sachs neuroglia following infection with AdCDP$^{831-1505}$.*** Cultured Tay-Sachs neuroglia were infected with 20MOI of adenovirus expressing β-galactosidase (β-gal), truncated CDP$^{831-1505}$ (AdCDP), or were simultaneously infected with adenoviruses containing sialidase and cathepsin A (AdSial + AdCA). Cells were harvested after 96 hours. Gangliosides isolated from harvested cell pellets were separated using silica gel thin layer chromatography and stained with resorcinol. Bands corresponding to GM2 and GM1 were quantified using ImageJ software (n=5). Tay-Sachs neuroglia treated with either AdCDP$^{831-1505}$ or AdSial + AdCA exhibited significantly reduced GM2, quantified as mean band intensity of GM2/GM1, relative to cells infected with mock (β-gal) virus (*$P < 0.05$; **$P < 0.01$).

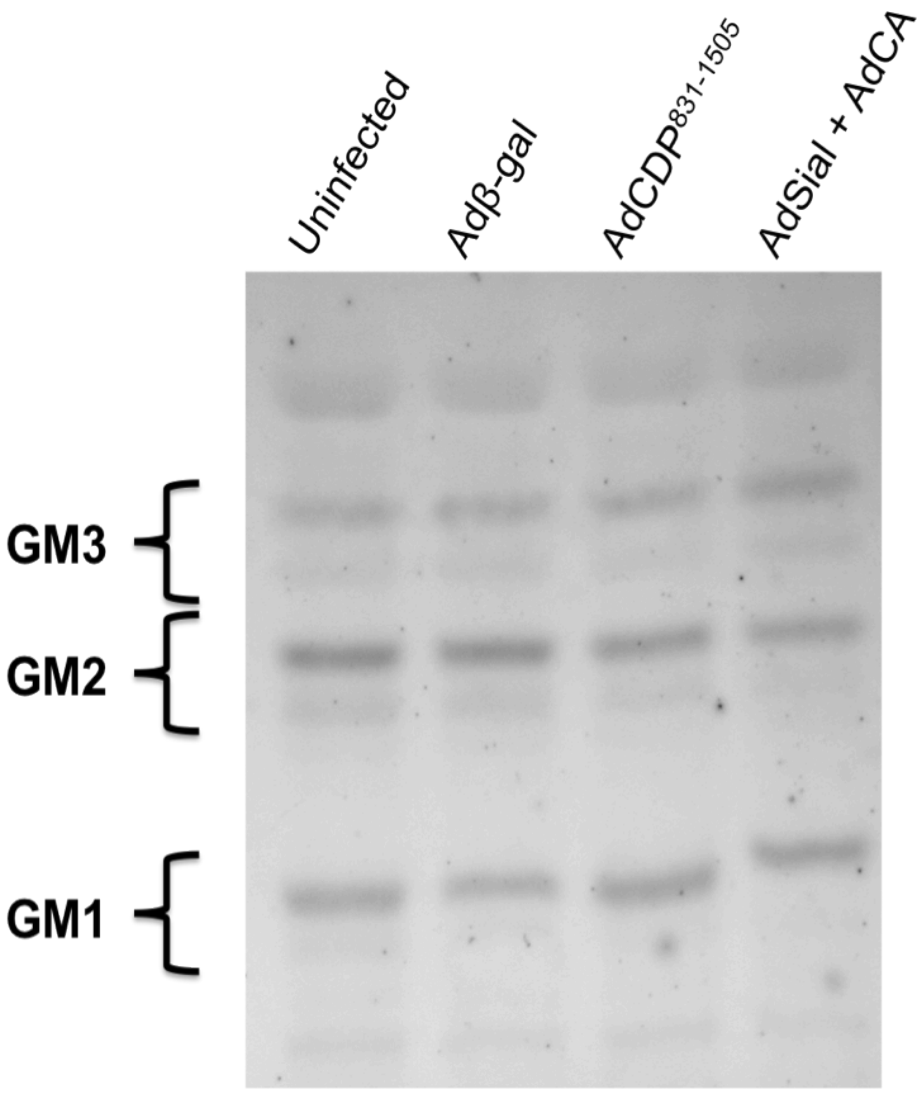

Figure 7. ***Representative silica gel thin layer chromatography plate of gangliosides isolated from Tay-Sachs neuroglia cells infected with AdCDP$^{831-1505}$.*** Cultured Tay-Sachs neuroglia were infected with 20MOI of adenovirus expressing β-galactosidase (β-gal), truncated CDP$^{831-1505}$ (AdCDP$^{831-1505}$), or were simultaneously infected with adenoviruses containing sialidase and cathepsin A (AdSial + AdCA). Cells were harvested after 96 hours. Gangliosides isolated from harvested cell pellets were separated using silica gel TLC and stained with resorcinol. Bands corresponding to GM2 and GM1 (see above) were quantified using ImageJ software. Experiment was replicated 5 times and data was pooled.

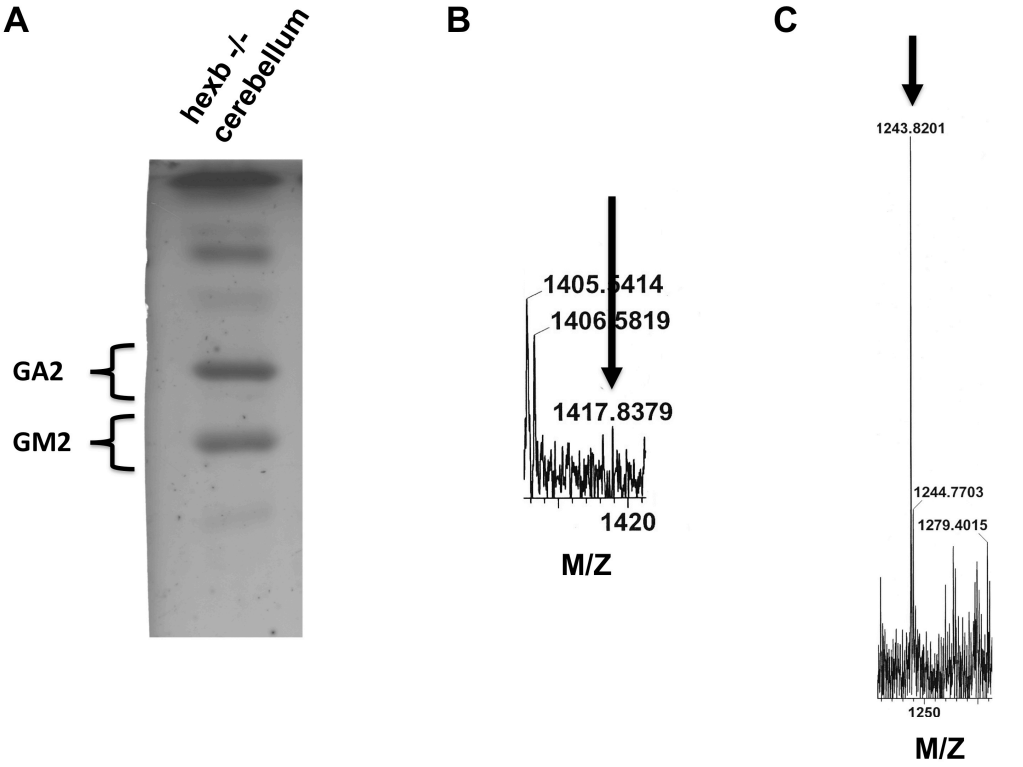

Figure 8. ***Mass spectroscopy on gangliosides separated via silica gel Thin Layer Chromatography*****.** Gangliosides were isolated from *hexb* -/- cerebellums and separated in duplicate via silica gel TLC. The TLC plate was cut in two and one half was stained with resorcinol. Both halves were aligned post-staining and the silica from the corresponding locations on the unstained half were scraped and collected. Gangliosides were extracted from the scraped silica, and were analyzed using MALDI-TOF mass spectroscopy at the McMaster Regional Centre for Mass Spectroscopy. Masses were screened using the Human Metabolome Database. (**A**) Silica gel TLC plate showing the analyzed ganglioside species. (**B**) The mass spectra from the putative GM2 sample contained a peak corresponding to GM2 (peak beneath arrow). (**C**) The mass spectra from the putative GA2 sample contained a peak corresponding to GA2 (peak beneath arrow). The species isolated from the silica gel TLC plate contained the predicted GM2 and GA2 gangliosides.

3.3 *In vitro* examination of truncated CDP$^{831-1505}$ binding to the human sialidase promoter.

Previous data has shown augmented human lysosomal sialidase promoter activity and specific sialidase activity for 4-Mu-NANA in human Tay-Sachs neuroglia when transfected with a CDP$^{831-1505}$ expressing vector. Data presented in 3.1 and 3.2 have shown increased protein expression of lysosomal sialidase as well as decreased intralysosomal GM2 ganglioside accumulation in human TSD neuroglia following infection with AdCDP$^{831-1505}$. Furthermore, analysis of the human lysosomal sialidase promoter has identified several putative domains capable of CDP-dependent regulation, including multiple CDP$^{831-1505}$ (CR3-HD) binding sites. It was therefore hypothesized that truncated CDP$^{831-1505}$, which retains the CR3-HD stable DNA binding domain (but lacks the functional repression domain), will compete with endogenous CDP for its binding site and effectively inhibit repression of sialidase expression.

To determine if CDP$^{831-1505}$ acts in *cis* on the promoter of human lysosomal sialidase, chromatin immunoprecipitation was carried out on untreated, PFG140 (mock) infected, and AdCDP$^{831-1505}$ infected TSD neuroglia. Primer sets were designed using Primer3 software to target a putative CR3-HD binding site in the lysosomal sialidase promoter (Figure 9). Each primer set generated a single product of the expected size when genomic DNA isolated from Tay-Sachs neuroglia was used as a template in a pre-ChIP PCR trial (data not shown).

Chromatin was isolated from formaldehyde-fixed neuroglia and enzymatically sheared for 10 minutes (duration was determined by prior optimization) using a random cutting shearing cocktail obtained from Active Motif. Enzymatic shearing helps to ensure consistent and easily reproducible generation of inter-nucleosome chromatin fragments within and between ChIP samples. Assessment of chromatin shearing efficiency via TBE gel electrophoresis revealed that all samples were optimally sheared with chromatin fragments of 150 - ~900bp in size (Figure 10). Sheared chromatin samples from uninfected, mock infected and AdCDP$^{831-1505}$ infected cells were then utilized in ChIP reactions using an anti-hemagglutinin (HA) antibody against truncated CDP$^{831-1505}$. Appropriate positive (RNA polymerase II) and negative (mouse IgG) control antibodies were also employed. Nine ChIP reactions were prepared as described in Table 1.

Table 1. Treatment and antibody combinations used to set up ChIP reactions to investigate binding of truncated $CDP^{831-1505}$ to the human lysosomal sialidase promoter.

Treatment	ChIP Antibody	Reaction Number
Uninfected	RNA polymerase II	1
	Mouse IgG	2
	Anti-hemagglutinin	3
$AdCDP^{831-1505}$	RNA polymerase II	4
	Mouse IgG	5
	Anti-hemagglutinin	6
PFG140 (mock)	RNA polymerase II	7
	Mouse IgG	8
	Anti-hemagglutinin	9

Enriched, post-ChIP chromatin samples were subsequently used in PCR reactions for the CR3-HD promoter fragment previously hypothesized to contain a putative CR3-HD binding site. PCR products were run on 1% TBE agarose gels. ChIP reactions using the RNA polymerase II antibody (reactions 1, 4 and 7) showed an intense PCR product of ~144bp, indicative of a successful post-ChIP sequence enrichment (Figure 11A). Reactions set up with the mouse IgG antibody (reactions 2, 5 and 8) displayed minimal-to-no post-PCR product, signifying no enrichment (Figure 11A). Conversely, only the AdCDP$^{831\text{-}1505}$ infected chromatin sample (reaction 6) displayed a PCR product following anti-HA pull down, providing evidence for *in vitro* binding of truncated CDP$^{831\text{-}1505}$ to the promoter of human lysosomal sialidase at the amplified CR3-HD site (Figure 11A). Neither the uninfected nor the mock (PFG140) infected samples demonstrated sequence enrichment following anti-HA pull down (reactions 3 and 9) (Figure 11A). Furthermore, all PCR reactions for the CR3-HD sequence produced a single band of expected size (~144bp).

Post-ChIP DNA samples were also used in PCR to amplify a region ~48kb upstream of the human *NEU1* promoter that was predicted to be devoid of CDP binding (Figure 9). Positive control (RNA polymerase II) ChIP reactions displayed positive enrichment (Figure 11B). Unexpectedly, ChIP reactions using anti-HA also showed faint, yet evident sequence enrichment. Since this region was not predicted to be a hot spot for truncated CDP binding, these results seem to be indicative of potential non-specific binding of the anti-HA antibody (Figure 11B). However, since the degree of enrichment is faint in anti-HA pulled down untreated neuroglia versus AdCDP$^{831\text{-}1505}$ infected cells, the observed positive enrichment at this intergenic site may perhaps be attributable to a novel CDP binding site as opposed to non-specific anti-HA binding.

It should be noted that PFG140 (mock virus) infected samples displayed identical results to uninfected samples.

Such data provides strong evidence to support the current hypothesis that truncated CDP$^{831\text{-}1505}$ binds to CR3-HD binding sites in the human lysosomal sialidase promoter and positively regulates promoter activity.

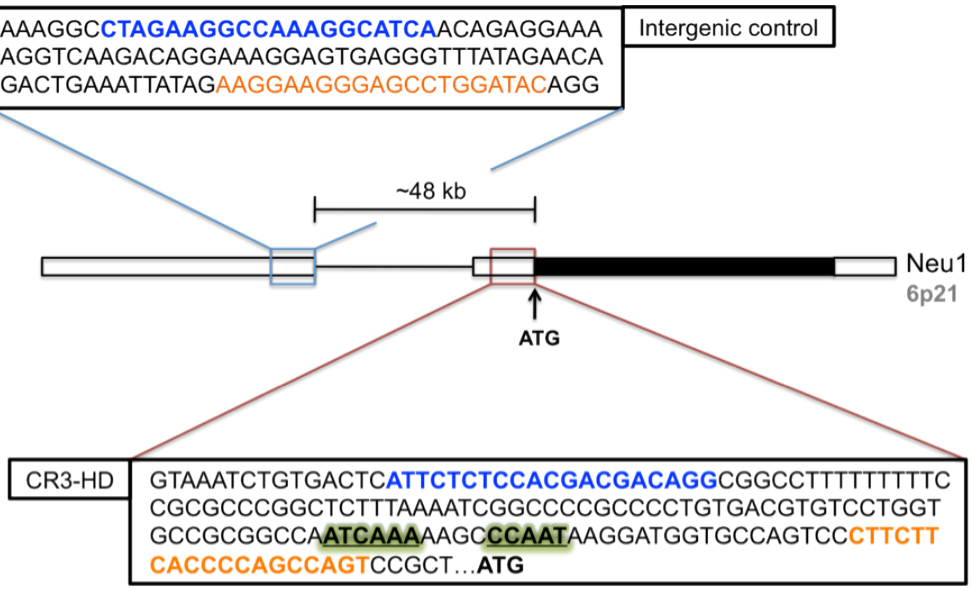

Figure 9. ***Human Neuraminidase 1 promoter and putative CCAAT Displacement Protein binding site.*** The human lysosomal sialidase (*NEU1*) promoter was manually scanned for the CCAAT Displacement Protein CR3-HD consensus binding sequence, ATCGAT, in close proximity to a CCAAT sequence. Furthermore, the promoter and other upstream intergenic regions were also scanned for regions devoid of potential CDP binding sites. Primers were designed using Primer3 software to amplify a 101bp intergenic region approximately 48kb upstream of the Neu1 translational start site. This site was utilized as a negative control site devoid of truncated CDP binding sites. A potential CD3-HD/CCAAT binding site was identified approximately 300bp upstream of the *NEU1* ATG translational start site (bolded and shaded in green). PCR primers were designed to amplify this region of the 5' UTR using Primer3 software. This primer pair yielded a 144bp product. Forward primer sequences appear bolded and in blue text; reverse primers were inversely complimentary to the bolded orange sequence.

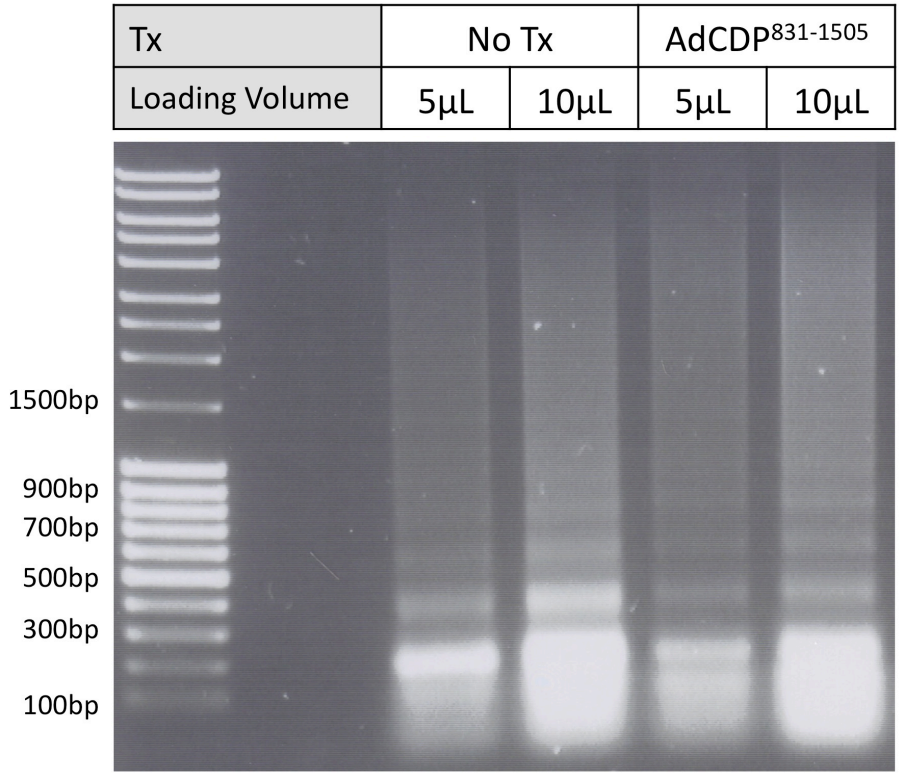

Figure 10. ***Assessment of enzymatic shearing of chromatin isolated from TSD neuroglia.*** Chromatin was isolated from formaldehyde-fixed TSD neuroglia 72 hours post-infection. Isolated chromatin was then enzymatically sheared for 10 minutes using an enzymatic shearing cocktail from Active Motif. Sheared chromatin samples were run on a 1.5% TAE agarose gel to determine the thoroughness of DNA fragmentation. All samples displayed multiple DNA bands in 150bp increments spanning from 150bp to approximately 1000bp. Such patterning was indicative of proper shearing. Tx (treatment).

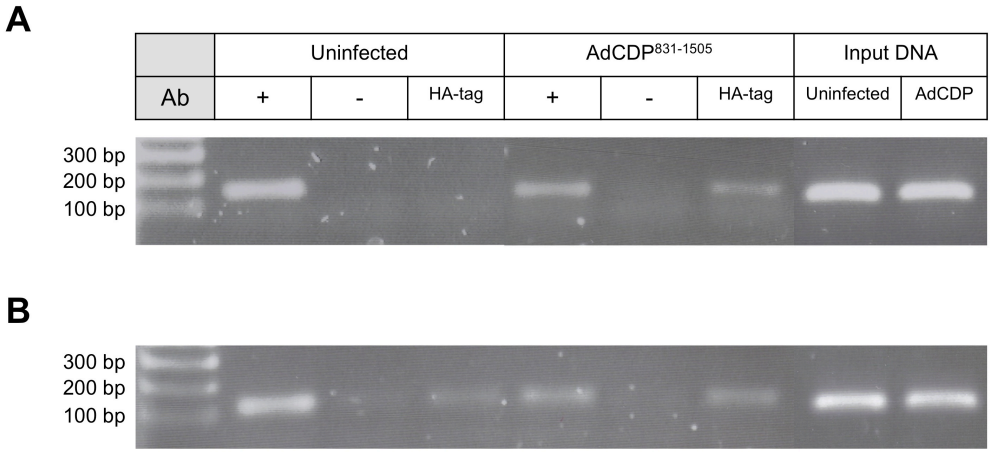

Figure 11. ***Chromatin Immunoprecipitation of truncated CDP$^{831-1505}$ in Tay-Sachs neuroglia infected with AdCDP$^{831-1505}$.*** Cultured Tay-Sachs neuroglia were left untreated or infected with 20MOI of empty adenovirus (PFG140) or adenovirus expressing truncated CDP$^{831-1505}$ (AdCDP$^{831-1505}$). Cells were harvested 72hours post-infection and subjected to chromatin immunoprecipitation (ChIP) using the ChIP-IT Express Enzymatic kit (Active Motif). ChIP reactions were set up with approximately 21µg of chromatin. Positive (RNA polymerase II; +) and negative (Mouse IgG; -) control antibodies were obtained from Active Motif. An anti-hemagglutinin (HA-tag) antibody was used to pull down truncated CDP$^{831-1505}$. (**A**) PCR for the putative truncated CDP binding site in the promoter of human *NEU1* was performed using immunoprecipitated chromatin and yielded a 144bp product. PCR product was run on 1% TBE agarose gel and stained with ethidium bromide prior to visualization. Chromatin isolated from AdCDP$^{831-1505}$ infected Tay-Sachs neuroglia and pulled down with anti-hemagglutinin (HA) exhibited positive enrichment of the CR3-HD sequence predicted to contain the truncated CDP binding site. (**B**) PCR for a region ~48kb upstream of the human *NEU1* translational start site (as depicted in Figure 8) was performed on immunoprecipitated chromatin and yielded a 101bp product. Positive control (RNA polymerase II) ChIP reactions displayed positive enrichment. Unexpectedly, ChIP reactions using anti-HA also showed enrichment, indicative of potential non-specific antibody binding or the existence of an unidentified and/or promiscuous CDP binding site. PCR product was run on 1% TBE agarose gel and stained with ethidium bromide prior to visualization. Note: PFG140 (mock virus) infected samples are not shown, as they displayed identical results to uninfected samples. Ab (antibody), HA (hemagglutinin).

SECTION II

3.4 Examination of morphological characteristics of bone marrow-derived macrophages from Tay-Sachs and Sandhoff disease mice.

Previous work has demonstrated that Tay-Sachs (*hexa* -/-) mice escape neurodegeneration and are asymptomatic until approximately 2 years of age. This differs significantly from the progression of Tay-Sachs disease in humans, as well as the mouse model of Sandhoff disease that begin to present neurodegenerative symptoms at about 3-4 months of age. The discovery of a sialidase-mediated bypass of HEXA deficiency in Tay-Sachs mice shed light on a mechanism of disease avoidance. The current hypothesis states that sialidase combined with retained HEXB activity (in *hexa* -/- mice) is responsible for keeping accumulated GM2 below a critical threshold required for widespread illness; however, it is unclear if the presence of this metabolic bypass affects other aspects of disease progression. The relationship between neuroinflammation and neurodegeneration in lysosomal storage disorders has been well established. Since CNS-resident microglia and peripherally derived, CNS-recruited macrophages are known to play critical roles in these processes, differences in Tay-Sachs and Sandhoff bone marrow-derived macrophage behaviour under conditions of stimulation were investigated. Bone marrow was collected from femurs, tibiae and humeri of wild type, *hexa* -/-, and *hexb* -/- animals, cultured, and differentiated as described in section 2.5. Differentiated macrophages were left untreated or stimulated with LPS (10μg/mL) for 24 hours. Cell size and the number of peripheral projections on untreated and LPS-stimulated macrophage cultures were quantified as measures of invasiveness and to gauge intracellular communication.

HEXB deficient cultures treated with LPS were significantly smaller in cell size (as quantified by total cellular area/nuclear area) relative to LPS treated wild type cultures. No other intergenotype differences were observed. Expectedly, cells in LPS treated cultures were significantly larger than their untreated counterparts (Figure 12A). Quantification of the number of projections around the cellular periphery of untreated versus LPS stimulated cells revealed that wild type and *hexa* -/- derived cultures possess significantly greater numbers under conditions of LPS stimulation. A similar trend was observed in *hexb* -/- cultures, but it did not reach significance (Figure 12B).

Together these results suggest that *hexa* -/- bone marrow-derived macrophages may be similar in invasiveness to those found in wild type animals and therefore, HEXA deficiency in peripherally derived macrophages does not seem to affect their migratory behaviour. Conversely, *hexb* -/- BMDMs seem to be immature by comparison or activated to a lesser extent at 24 hours post

stimulation. Furthermore, their significant reduction in quantity of projections suggests they may display lessened communicative ability and be less phagocytic relative to wild type or *hexa* -/- macrophages.

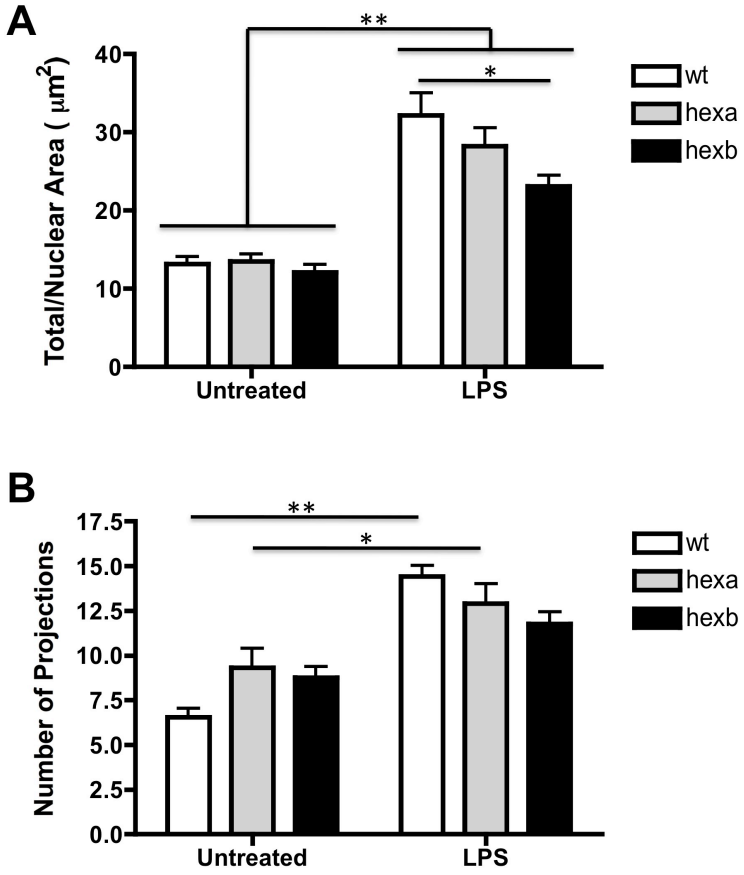

Figure 12. ***Quantification of cell size and quantity of peripheral projections in LPS stimulated hexa -/- and hexb -/- bone marrow-derived macrophages.*** Bone marrow was isolated from *hexa* -/-, *hexb* -/-, and wild type mice and differentiated in culture with M-CSF for 12 days. Following differentiation, cells were treated with LPS for 24 hours. Cultures were stained with hematoxylin, analyzed via phase contrast microscopy and parameters quantified using Axiovision software. (**A**) Total cellular area normalized to nuclear area was significantly greater in LPS treated cultures compared to their unstimulated counterpart (**P< 0.001). LPS treated cultures were round and flat as opposed to the long, thin, and polarized phenotype of unstimulated cells. Wild type cultures treated with LPS were significantly larger than *hexb* -/- under similar conditions (*P< 0.01). (**B**) Wild type and *hexa* -/- BMDMs treated with LPS possessed a significantly greater number of peripheral projections relative to their untreated counterparts (*P< 0.05; **P< 0.001). HEXB deficient cultures showed a similar trend, however, it did not reach significance. No significant differences in projection quantity were observed between wild type, *hexa* -/-, or *hexb* -/- cultures. wt (wild type).

3.5 Measurement of inflammatory mediators from *hexa* -/- and *hexb* -/- bone marrow-derived macrophages following stimulation with PAMPs.

Having observed no obvious morphological differences amongst wild type, Tay-Sachs, and Sandhoff BMDMs to suggest variation in invasiveness, alternate explanations were sought to explain the profound disparity in neurodegeneration between these genotypes. One hypothesis to explain the phenomenon of disease avoidance in *hexa* -/- mice stems from the connection between their lessened intralysosomal ganglioside accumulation, and the neuroinflammatory and neurodegenerative processes. More specifically, it was hypothesized that when exposed to similar stimuli, the immune response of bone marrow-derived macrophages from *hexb* -/- mice would be more severe compared to that of macrophage derived from Tay Sachs mice. Alternately stated, HEXA deficient BMDMs would have a dampened immune response compared to that of *hexb* -/- cultures.

To test this hypothesis, bone marrow was collected from femurs, tibiae and humeri of wild type (n=2), *hexa* -/- (n=2) and *hexb* -/- (n=2) animals and cultured as described in section 2.5. Primary cells were differentiated toward the macrophage lineage in culture for 12 days using M-CSF. Differentiated macrophages were either left untreated or subsequently stimulated with LPS (10μg/mL), Poly I:C (25μg/mL), CpG Flu 1668 (1μM) (collectively referred to as PAMPs), or GM2 ganglioside (GM2) (25μg/mL) for 24 hours. Cell culture media was sampled at 2, 4, 8, 12, and 24 hours post-stimulation and later assayed for presence/quantity of secreted cytokines. "Zero" measurements were obtained from fresh culture media.

Measurement of secreted cytokines at 24 hours post-PAMP stimulation was conducted for IL-1β, IL-10, IL-6 and MCP1. Because TNF secretion is known to peak much earlier than 24 hours post-stimulation, we chose not to measure it across all stimulants at this time point. LPS and Poly I:C treatments profoundly augmented secretion of all measured cytokines (with the exception of IL-1β) (Figure 13). Conversely, CpG Flu 1668 only minimally increased IL-6 and IL-10 secretion, while IL-1β remained below the assay's level of detection and MCP-1 did not differ significantly from its untreated baseline (Figure 13). Collectively, this data insinuates that inflammatory signaling in BMDMs is most sensitive/responsive to TLR3 and TLR4 ligands, whereas molecules acting through TLR9 show only nominal effects. Given that accumulated GM2 in Sandhoff mice is correlated with a heightened inflammatory state and that gangliosides has been shown to act as TLR4 ligands[107], it was hypothesized that GM2 would evoke similar behaviour to that observed with LPS or Poly I:C. Unexpectedly, GM2 treatment did not stimulate secretion of any measured cytokine from wild type, *hexa* -/- or *hexb* -/- BMDMs (Figure 13). In fact, GM2 appeared to have marginally suppressed MCP1 secretion across all genotypes

relative to baseline (untreated) levels (Figure 13D). Also of particular interest was that *hexb* -/- bone marrow-derived macrophages secreted significantly more IL-6 than wild type and *hexa* -/- counterparts when treated with Poly I:C. Similarly, *hexb* -/- LPS-treated macrophages secreted more IL-6 than wild type and *hexa* -/- BMDMs, however, this trend did not reach significance (Figure 13C). Additionally, *hexb* -/- macrophages receiving LPS secreted significantly less IL-10 and MCP1 in relation to similarly treated wild type and *hexa* -/- cells (Figure 13B and D).

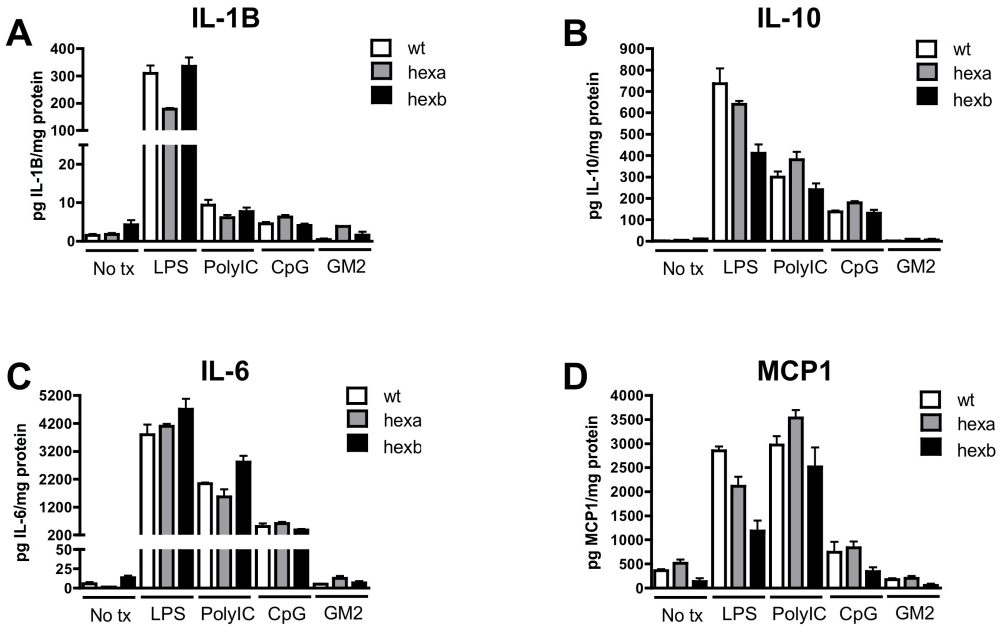

Figure 13. ***Cytokine secretion from hexa -/-, hexb -/- and wild type bone marrow-derived macrophages 24 hours after stimulation with PAMPs or GM2.*** Bone marrow was isolated from *hexa* -/-, *hexb* -/-, and wild type mice (n=2 per genotype) and differentiated in culture with M-CSF for 12 days. Following differentiation, cells were treated with LPS, Poly I:C, CpG Flu 1668 or GM2. Culture media was collected 24 hours post-treatment and assayed for secretion of IL-1β (**A**), IL-10 (**B**), IL-6 (**C**), and MCP1 (**D**). (**A**) Cells receiving treatments other than LPS as well as those receiving no treatment were below the IL-1β assay's level of detection. LPS stimulated *hexa* -/- BMDMs exhibited significantly reduced ($P< 0.001$) IL-1B secretion compared to wild type and *hexb* -/- cells. (**B**) Cells receiving no treatment or GM2 were below the detectable level of the assay. *Hexb* -/- BMDMs exposed to LPS secreted significantly less ($P< 0.001$) IL-10 than either *hexa* -/- or wild type cells, whereas *hexa* -/- secretion was not significantly different from wild type levels. *Hexb* -/- cells also secreted significantly less ($P< 0.05$) IL-10 than *hexa* -/- BMDMs when treated with Poly I:C. (**C**) Cells receiving no treatment or GM2 were below the detectable level of the assay. *Hexb* -/- BMDMs receiving Poly I:C treatment secreted significantly more ($P< 0.001$) IL-6 than their *hexa* -/- counterparts. (**D**) MCP1 secretion from *hexb* -/- BMDMs treated with LPS is significantly dampened in comparison to *hexa* -/- and wild type cells ($P< 0.05$ and $P< 0.001$, respectively). *Hexa* -/- cells receiving Poly I:C treatment secreted significantly more ($P< 0.01$) MCP1 than *hexb* -/- BMDMs exposed to the same treatment. No tx (untreated), wt (wild type).

Having observed some interesting results at 24 hours post-treatment, combined with the fact that different cytokines may be secreted at various times post-stimulation, we sought to quantify cytokine secretion temporally from 2 hours post-treatment through experiment termination (at 24 hours).

ELISA testing of cell media supernatants was performed for TNF, IL-1β, IL-6, IL-10, MCP1 and IFN-γ. Time course analysis of cytokine secretion revealed shocking intergenotype differences in LPS-stimulated secretion of MCP1 and TNF (Figure 14D and E). LPS-stimulated MCP1 secretion from *hexb* -/- macrophages was significantly reduced compared to their wild type and *hexa* -/- counterparts at all time points beyond 2 hours (Figure 14D). Conversely, LPS-stimulated TNF secretion from *hexb* -/- macrophages was significantly higher at 12 hours, peaking 4 hours later than *hexa* -/- and wild type cells. Moreover, *hexb* -/- TNF secretion levels remained significantly higher at 24 hours post treatment (Figure 14E).

Under conditions of Poly I:C stimulation, the previously observed differences in MCP1 and TNF secretion were abolished, insinuating that these differences in behaviour are PAMP-specific (Figure 15D and E). However, IL-6 secretion from *hexb* -/- BMDMs was higher than all other genotypes and reached significance at 24 hours post-treatment, providing further support for PAMP-specific genotypic differences in cytokine secretion (Figure 15C).

To elucidate whether BMDM response to GM2 treatment resulted in secretion of quick-responding TNF and our prior window of analysis was too narrow, we measured TNF secretion from GM2-receiving cultures at all sampled post-treatment time points. In agreement with initial observations, the addition of exogenous, purified GM2 does not stimulate secretion of the early responding cytokine, TNF (Figure 16).

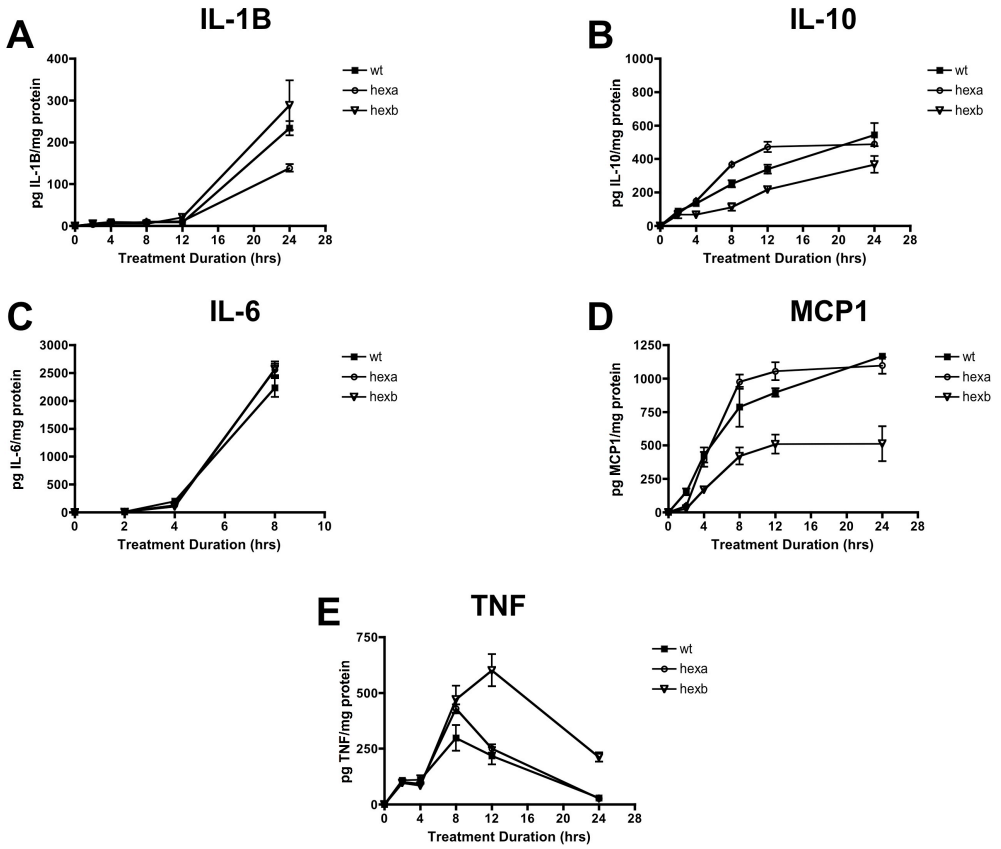

Figure 14. ***Cytokine secretion from hexa -/-, hexb -/- and wild type bone marrow-derived macrophages at multiple time points following LPS treatment.*** Bone marrow was isolated from *hexa* -/-, *hexb* -/-, and wild type mice (n=2 per genotype) and differentiated in culture with M-CSF for 12 days. Following differentiation, cells were treated with LPS and culture media was collected at 2, 4, 8, 12 and 24 hours post-treatment. Cell-free supernatants were subsequently assayed for IL-1β (**A**), IL-10 (**B**), IL-6 (**C**), MCP1 (**D**), and TNF (**E**) secretion. IL-1β secretion from *hexb* -/- BMDMs was dampened (P= 0.06) at 24 hours relative to other genotypes (**A**). IL-10 secretion from *hexb* -/- cells was significantly dampened (P< 0.05) at 8 and 12-hour time points (**B**), whereas no inter-genotype differences were observed regarding secretion of IL-6 over 8 hours (**C**). *Hexb* -/- BMDMs secreted significantly less MCP1 than cells derived from *hexa* -/- and wild type mice from 4 hours onwards (P< 0.05) (**D**). Conversely, LPS-stimulated TNF secretion from *hexb* -/- macrophages was significantly higher at 12 hours (P< 0.01), peaking 4 hours later than *hexa* -/- and wild type cells. *Hexb* -/- TNF secretion also remained at significantly higher levels up to 24 hours post treatment (P< 0.001) (**E**). wt (wild type).

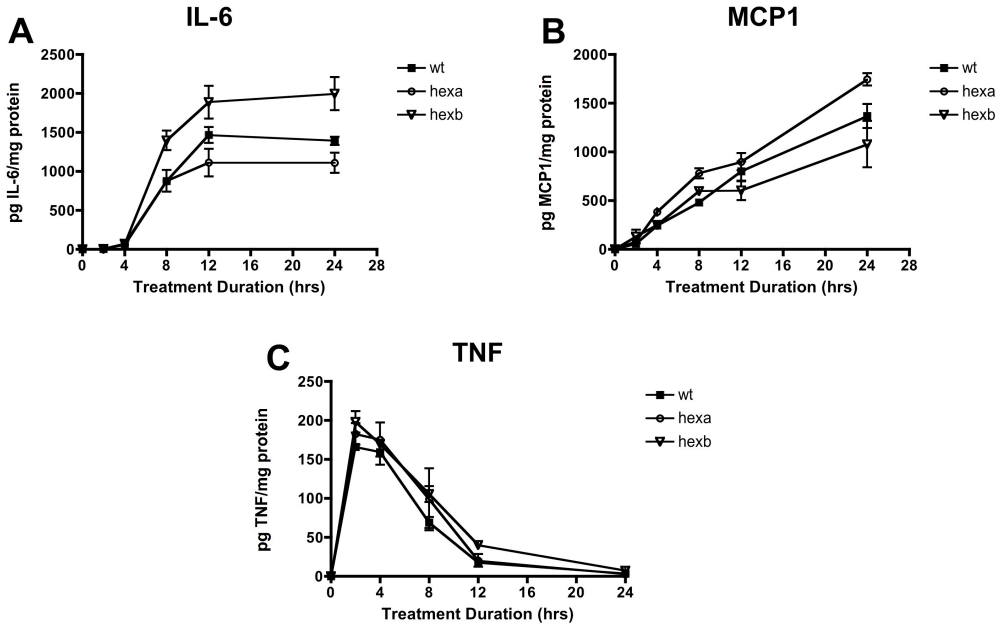

Figure 15. ***Cytokine secretion from hexa -/-, hexb -/- and wild type bone marrow-derived macrophages at multiple time points following Poly I:C treatment.*** Bone marrow was isolated from *hexa* -/-, *hexb* -/-, and wild type mice (n=2 per genotype) and differentiated in culture with M-CSF for 12 days. Following differentiation, cells were treated with Poly I:C and culture media was collected at 2, 4, 8, 12 and 24 hours post-treatment. Cell-free supernatants were subsequently assayed for IL-6 (**A**), MCP1 (**B**), and TNF (**C**) secretion. (**A**) Poly I:C-stimulated IL-6 secretion from *hexb* -/- BMDMs was significantly augmented in comparison to their *hexa* -/- counterparts ($P < 0.05$); however, the trend compared to wild type did not reach significance. Although not significant, the inverse trend was observed with regards to MCP1 secretion, where *hexa* -/- BMDMs secreted the largest quantity (**B**). (**C**) TNF secretion following Poly I:C treatment did not differ significantly between genotypes. wt (wild type).

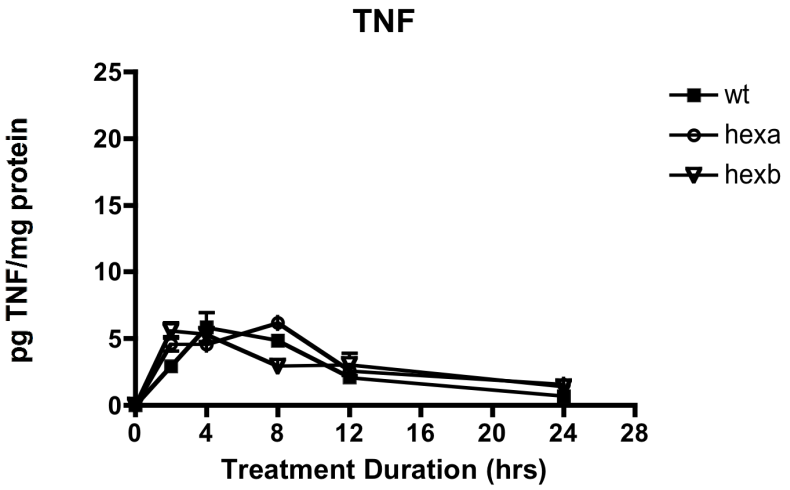

Figure 16. ***Cytokine secretion from hexa -/-, hexb -/- and wild type bone marrow derived macrophages at multiple time points following GM2 treatment.*** Bone marrow was isolated from *hexa* -/-, *hexb* -/-, and wild type mice (n=2 per genotype) and differentiated in culture with M-CSF for 12 days. Following differentiation, cells were treated with GM2 ganglioside and culture media was collected at 2, 4, 8, 12 and 24 hours post-treatment. Cell-free supernatants were subsequently assayed for TNF secretion. Treatment of cultured bone marrow macrophages with purified GM2 did not stimulate measurable secretion of TNF at any assayed time point. wt (wild type).

3.6 Investigating potential mediators of/cellular responses to differential cytokine secretion in *hexa* -/- and *hexb* -/- bone marrow-derived macrophages.

To investigate whether differences in intralysosomal accumulation of ganglioside may contribute to these differences in observed cytokine secretion and potentially immunoregulatory behaviour, *hexb* -/-, *hexb* +/- and wild type (*hexb* +/+) BMDMs were subjected to immunocytochemical analysis using SAP-A, a lysosomal marker, CD11b, a surface marker of macrophage lineage differentiation, and fluorescent Texas Red (Alexa 594) and Bodipy-F (Alexa 488) secondary antibodies.

All cells displayed marked CD11b labeling around the cell periphery, indicating that cells of all genotypes underwent M-CSF-directed macrophage lineage differentiation. More interestingly, *hexb* -/- cells possessed a trend toward larger, sharper and more distinct lysosomal SAP-A labeling, consistent with and suggestive of swollen, ganglioside packed lysosomes (Figure 17).

To further investigate whether *hexb* -/- lysosomes, which appeared swollen during the previous immunocytochemical analysis, were enlarged as a result of accumulated gangliosides, untreated or LPS (10μg/mL) stimulated bone marrow-derived macrophage cultures from wild type, *hexa* -/-, and *hexb* -/- cultures were subjected to Oil Red O and hematoxylin staining. Analysis of Oil Red O stained wild type, *hexa* -/-, and *hexb* -/- cultures by bright field/differential interference contrast microscopy revealed no clear lipid staining (Figure 18). More specifically, cells appeared completely devoid of Oil Red O lipid labeling.

Additional experimentation was also performed to reexamine ganglioside accumulation in bone marrow-derived macrophages from HEXA, HEXB, and GLB1 deficient (β-galactosidosis) mice. Gangliosides were extracted from cultures of unstimulated BMDMs from wild type, Tay-Sachs, Sandhoff, and *glb1* -/- mice and separated using silica gel thin layer chromatography as described in 2.4. Consistent with the lack of lipid accumulation observed in Oil Red O stained cultures, no accumulated GM2 or GA2 gangliosides were observed (Figure 19). Together, this data suggested that primary bone marrow cells differentiated to macrophages *in vitro* might not accumulate intralysosomal gangliosides.

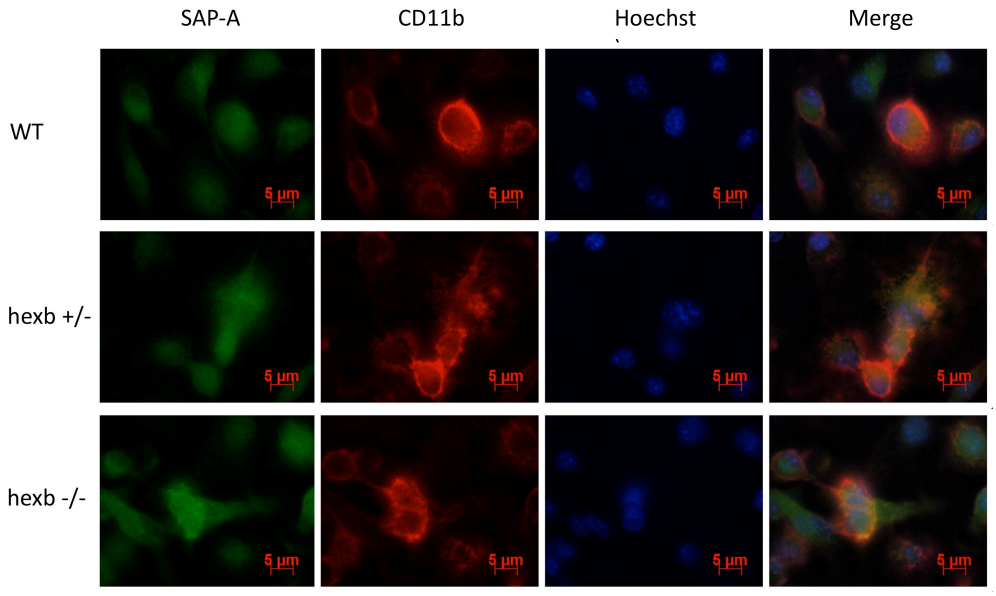

Figure 17. ***Immunocytochemical analysis of hexb -/- bone marrow-derived macrophages stained for CD11b and SAP-A.*** Macrophages were obtained from bone marrow cultured from wild type, *hexb* -/- and *hexb* +/- mice via M-CSF-driven differentiation for 12 days. Immunocytochemical analysis was performed to assess macrophage lineage differentiation using the macrophage surface marker CD11b and to evaluate lysosomal appearance using the lysosomal marker SAP-A. Extensive CD11b staining in the cell periphery of all genotypes indicated marked macrophage-like differentiation. *Hexb* KO macrophages displayed a trend towards more intense and further marked SAP-A lysosomal staining, suggestive of enlarged lysosomal compartments presumably from increased accumulation of lysosomal gangliosides. wt (wild type). Scale bar = 5µm

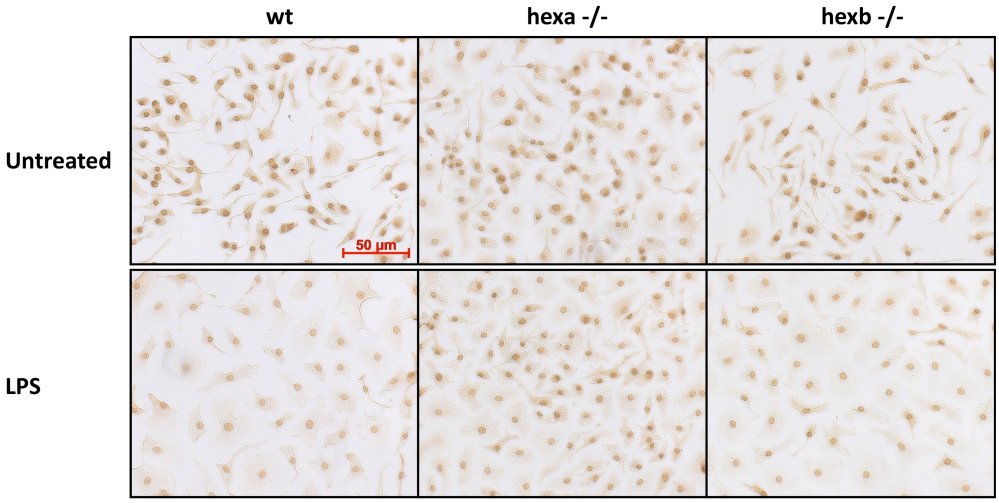

Figure 18. ***Oil Red O staining of bone marrow-derived macrophage cultures from wild type, hexa -/- and hexb -/- animals.*** Macrophages were obtained via M-CSF differentiation of cultured bone marrow. Primary cultures were differentiated for 12 days and treated with LPS for 24 hours prior to lipid staining with Oil Red O. Cells were fixed, permeabilized, and incubated with fresh Oil Red O for 1 hour prior to hematoxylin staining. No distinct Oil Red O staining was observed in either untreated or LPS stimulated cultures. wt (wild type). Scale bar = 50µm

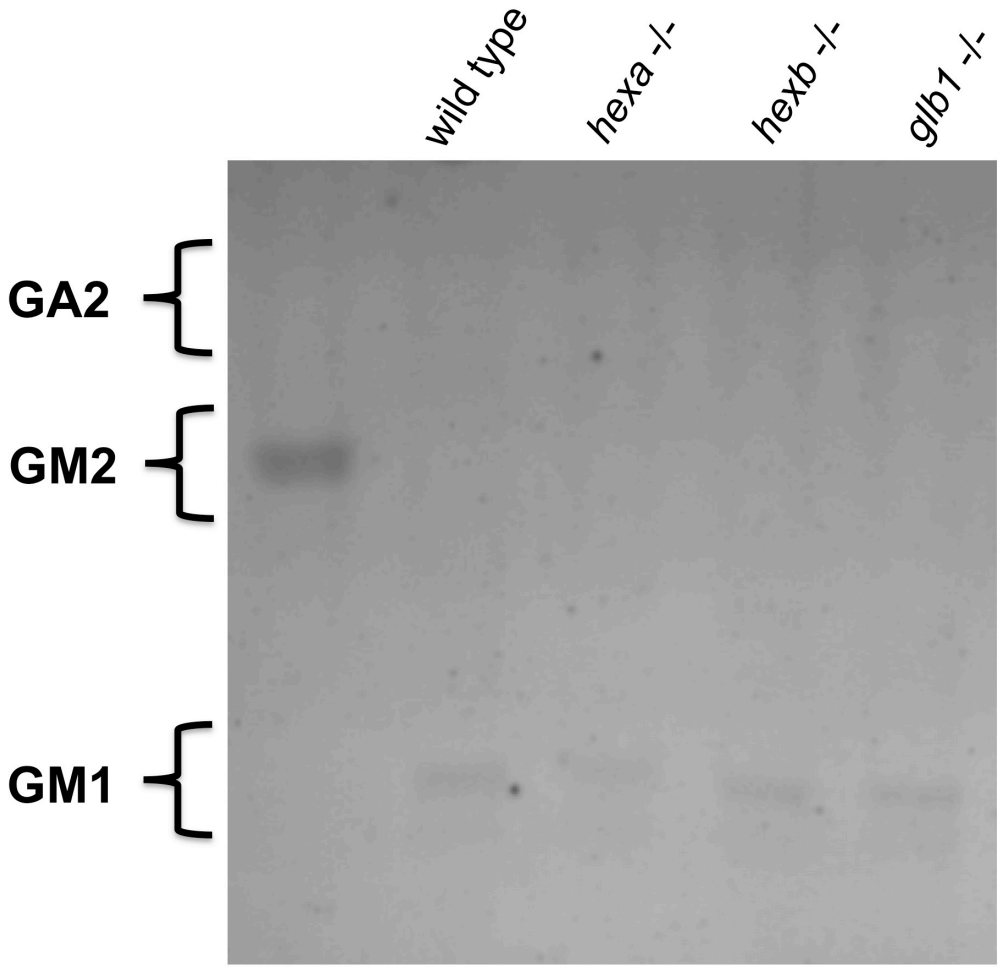

Figure 19. ***Silica gel thin layer chromatography plate of gangliosides isolated from Tay-Sachs and Sandhoff bone marrow-derived macrophages.*** Macrophages were differentiated and cultured from bone marrow of wild type, *hexa* -/-, *hexb* -/-, and *glb1* -/- mice. Gangliosides were isolated from harvested cell pellets, separated using silica gel thin layer chromatography, and stained with resorcinol. No visible accumulations were observed in any genotype, suggesting that peripheral macrophages may not accumulate a substantial quantity of ganglioside.

Intralysosomal GM2 accumulation has previously been linked to increased LAMP2 (lysosomal-associated membrane protein 2). Moreover, immunological studies have shown co-localization between GM2 and LAMP2. To further examine if intralysosomal accumulation may play a role in the altered behaviour observed in *hexb* -/- bone marrow-derived macrophage cultures, LAMP2 (~110 kDa) expression was evaluated via western blotting. BMDMs were stimulated with LPS or Poly I:C for 24 hours and subsequently subjected to SDS-PAGE. A trend towards increased LAMP2 expression was observed in untreated *glb1* -/- cultures. Similarly, LPS stimulated *hexb* -/- macrophages showed an increase in LAMP2 protein levels relative to all other genotypes; however, neither of these observations reached statistical significance (Figure 20). Of particular interest is the apparent disparity in LAMP2 protein size in *hexb* -/- and *glb1* -/- cultures. More specifically, under untreated conditions, LAMP2 protein expressed by macrophage cultures derived from *hexb* -/- and *glb1* -/- animals was smaller and larger, respectively, relative to the protein expressed by wild type and *hexa* -/- cells (Figure 20A). When treated with either LPS or Poly IC, *glb1* -/- LAMP2 protein remains up-shifted. Conversely, the shift in LAMP2 size in *hexb* -/- cultures becomes less apparent or may even disappear (Figure 20B and C). Given the role of hexosaminidase in the cleavage of terminal N-acetyl hexosamines, and the presence of these moieties on LAMP2, this data suggest that deficiency of both HEXA and HEXB (i.e. Sandhoff; *hexb* -/-) isozymes results in improper processing of lysosomal-associated glycosylated proteins such as LAMP2 in addition to intralysosomal accumulation of catabolic ganglioside intermediates. Perhaps the altered glycosylation state and/or difference in expression levels of LAMP2 contribute to cellular immunological responses.

Prior studies have demonstrated that intralysosomal ganglioside accumulation causes marked endoplasmic reticulum (ER) stress in diseased neurons[108, 109]. Such stress carried the potential to explain the altered behaviour observed in *hexb* -/- BMDMs. To examine if diseased *hexb* -/- BMDM cultures showed increased ER stress independent of clearly visible ganglioside accumulation, western blots for the ER stress marker, Grp78 (~78 kDa), were performed on LPS or Poly I:C stimulated wild type, *hexa* -/-, *hexb* -/-, and *glb1* -/- (model of GM1 gangliosidosis) bone marrow-derived macrophage cultures. If *hexb* -/- cells were experiencing accumulation-independent ER stress, one would expect levels of Grp78 protein to be significantly augmented. Grp78 protein expression was significantly reduced in untreated *hexb* -/- and *glb1* -/- BMDMs relative to wild type cultures (Figure 21A). Similar results were observed under conditions of LPS stimulation; however, *hexb* -/- and *glb1* -/- macrophages also expressed significantly less Grp78 when compared to *hexa* -/- cultures (Figure 21B). This trend was abolished when cultures were treated with Poly I:C. Poly I:C stimulation resulted in increased Grp78 expression in *glb1* -/-, a trend that reached significance relative to *hexb* -/- expression levels (Figure 21C).

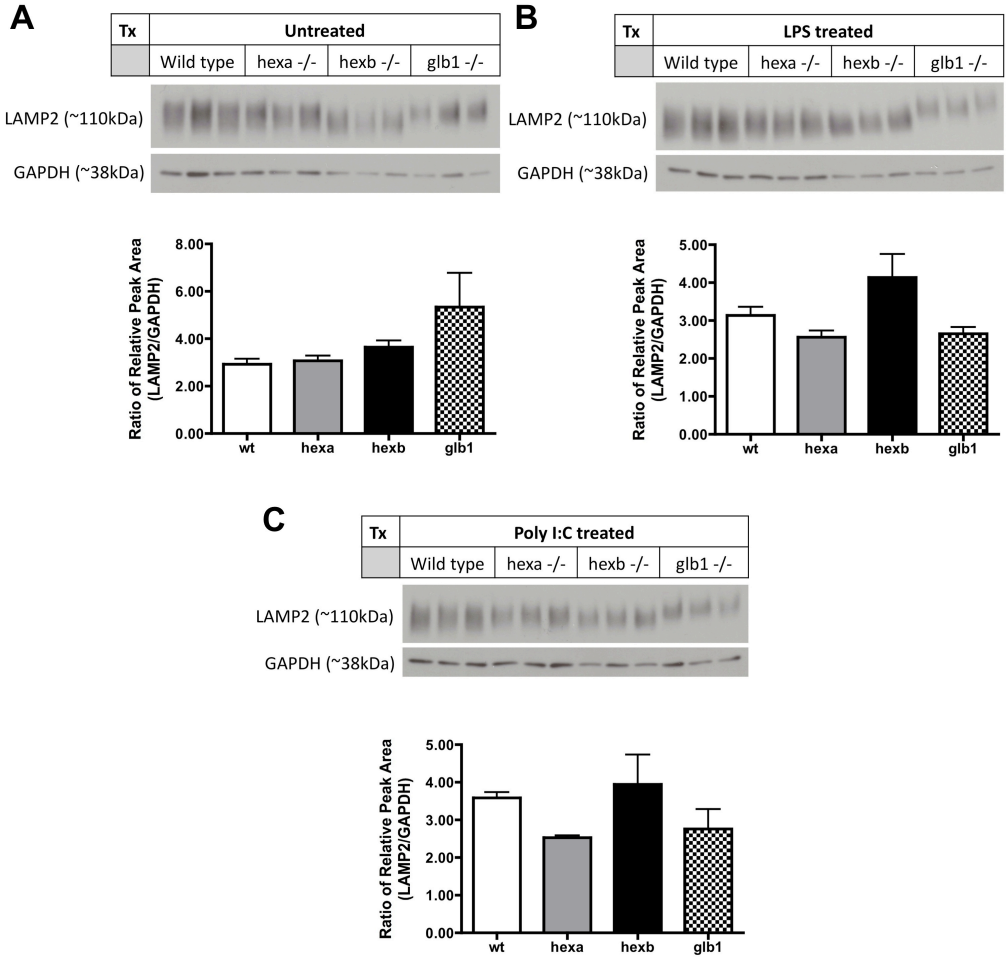

Figure 20. ***LAMP2 western blot of untreated, LPS, or Poly I:C stimulated hexa -/-, hexb -/-, and glb1 -/- bone marrow-derived macrophages.*** Bone marrow was isolated from *hexa* -/-, *hexb* -/-, *glb1* -/-, and wild type mice (n=1 per genotype) and differentiated in culture with M-CSF for 12 days. Following differentiation, cells were treated with LPS or Poly I:C and cell lysates were collected 24 hours post treatment. Cell lysates were subjected to western blotting and probed for LAMP2, a marker of the intralysosomal accumulation observed in lysosomal storage disorders. No significant intergenotype differences in LAMP2 protein levels were observed. However, untreated *glb1* -/- BMDMs and LPS stimulated *hexb* -/- both displayed a trend for increased LAMP2. Marked disparity in LAMP2 protein size was observed in untreated *hexb* -/- and *glb1* -/- macrophages, suggestive of potentially altered mature protein glycosylation. Tx (treatment), wt (wild type).

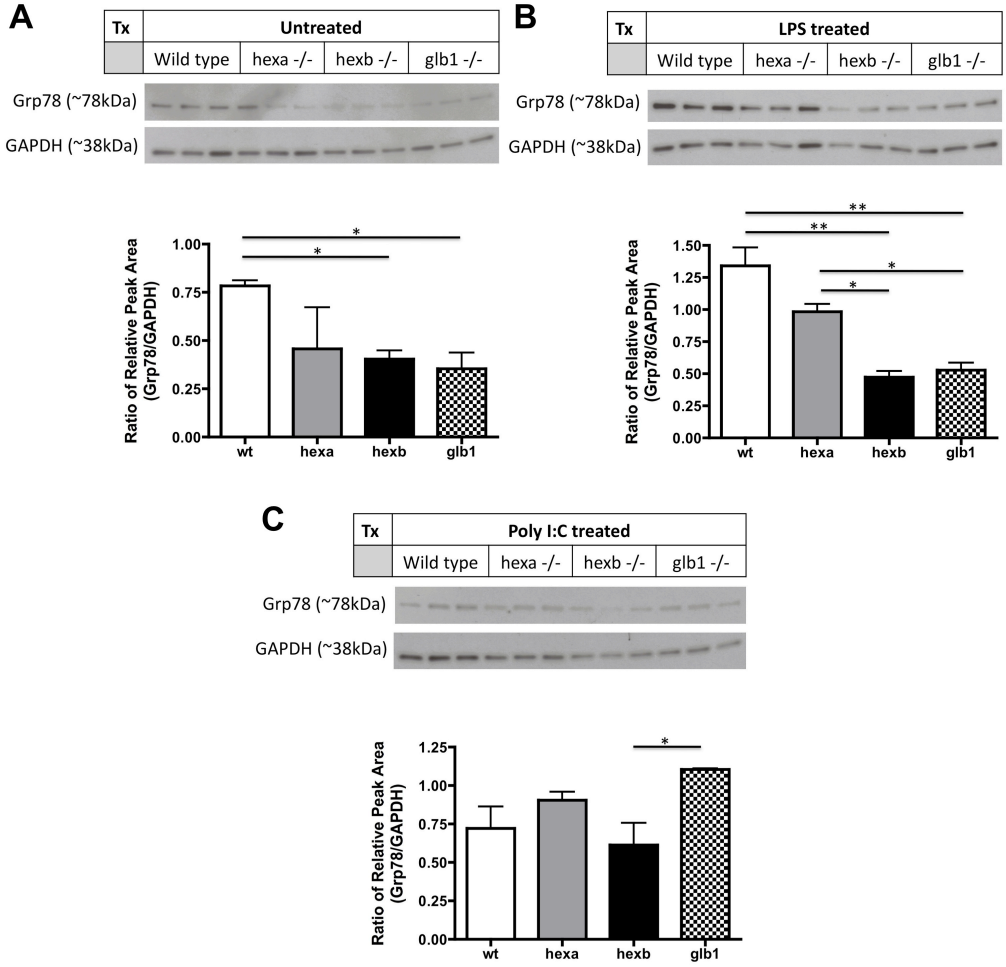

Figure 21. ***Grp78 western blot of untreated, LPS, or Poly I:C stimulated hexa -/-, hexb -/-, and glb1 -/- bone marrow-derived macrophages.*** Bone marrow was isolated from *hexa* -/-, *hexb* -/-, *glb1* -/-, and wild type mice (n=1 per genotype) and differentiated in culture with M-CSF for 12 days. Following differentiation, cells were treated with LPS or Poly I:C and cell lysates were collected 24 hours post treatment. Cell lysates were subjected to western blotting and probed for Grp78, a marker for ER stress. (**A**) Significantly reduced Grp78 expression was observed in *hexb* -/- and *glb1* -/- BMDM cultures relative to wild type macrophages (*P< 0.01). (**B**) LPS treated *hexb* -/- and *glb1* -/- BMDMs displayed significantly reduced levels of Grp78 protein relative to both wild type and *hexa* -/- cultures (*P< 0.05, **P< 0.001). (**C**) Grp78 expression in *glb1* -/- BMDMs was significantly greater than *hexb* -/- expression when stimulated with Poly I:C (*P< 0.05). Tx (treatment), wt (wild type).

Prior microarray data on brain tissue isolated from *hexb* -/- mice has shown significant transcriptional augmentation of several macrophage-associated genes, including macrophage expressed protein 1 (*Mpg1*) and glycoprotein (transmembrane) NMB (*Gpnmb*), each correlated with immune cell activation and inflammatory responses. To investigate whether these proteins are also upregulated in *hexb* -/- BMDMs and thus, potentially linked to their genotype-specific cytokine secretion profile, cell lysates from wild type, *hexa* -/- and *hexb* -/- bone marrow-derived macrophages stimulated with LPS (10μg/mL) or Poly I:C (25μg/mL) were subjected to SDS-PAGE and western blotting. Samples were loaded equally based on levels of total cellular protein and blots were probed for Mpg1 (~95 kDa) and Gpnmb (~55-60 kDa) proteins.

Mpg1 protein levels were significantly elevated in *hexb* -/- BMDMs under conditions of stimulation (LPS and Poly I:C treatments) (Figure 22B and C). Untreated wild type cultures displayed significantly increased Mpg1 expression compared to *hexa* -/- BMDMs (Figure 22C).

Gpnmb protein expression was significantly augmented in *hexb* -/- BMDMs under LPS treated conditions (Figure 23A). Conversely, no intergenotype differences in Gpnmb protein levels were observed in Poly I:C treated BMDMs (Figure 23B). Moreover, Gpnmb protein was below the level of detection in untreated cells (data not shown).

The significant increase in Mpg1 and Gpnmb expression under conditions of LPS stimulation is in agreement with the previously collected microarray data. However, one cannot ignore the marked differences in untreated Mpg1 protein expression or Poly I:C stimulated Gpnmb expression between CNS resident and peripheral cells. Such behaviour might suggest that these genetic defects have diverse cell-type-specific effects. Furthermore, the stimulation-specific difference in Gpnmb expression provides evidence for genotypic variation in response to stimuli.

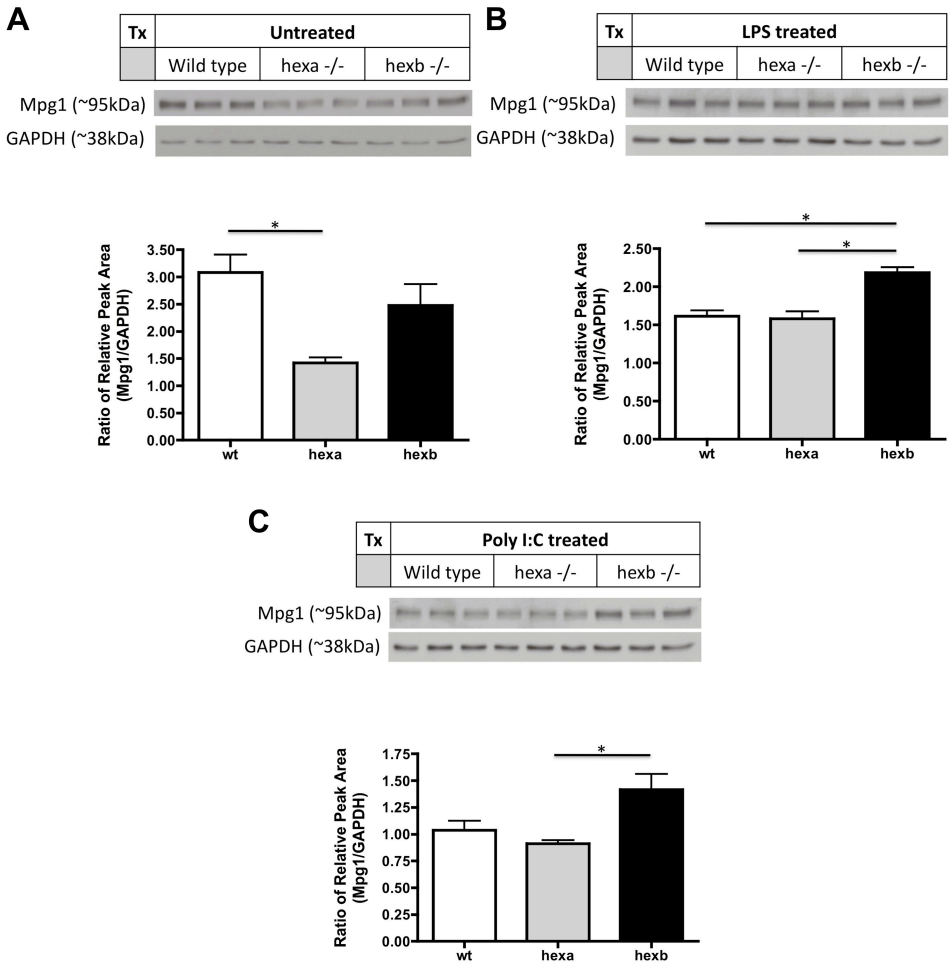

Figure 22. ***Mpg1 western blot of untreated, LPS, or Poly I:C stimulated hexa -/- and hexb -/- bone marrow-derived macrophages.*** Bone marrow was isolated from *hexa* -/-, *hexb* -/- and wild type mice (n=2 per genotype) and differentiated in culture with M-CSF for 12 days. Following differentiation, cells were treated with LPS or Poly I:C and cell lysates were collected 24 hours afterward. Cell lysates were subjected to western blotting and probed for Mpg1. (**A**) Untreated BMDMs displayed significantly elevated Mpg1 protein expression relative to *hexa* -/- BMDMs (*P< 0.05). HEXB deficient BMDMs displayed significantly augmented levels of Mpg1 in comparison to wild type and *hexa* -/- cultures under conditions of LPS stimulation (*P< 0.01)(**B**). This relationship remained significant in comparison to *hexa* -/- BMDMs when treated with Poly I:C (*P< 0.05)(**C**). Tx (treatment), wt (wild type).

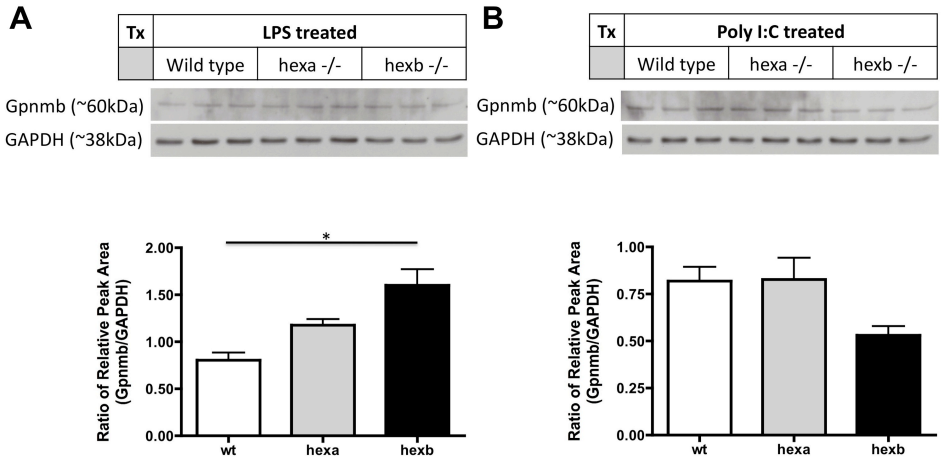

Figure 23. ***Gpnmb western blot of LPS or Poly I:C stimulated hexa -/- and hexb -/- bone marrow-derived macrophages.*** Bone marrow was isolated from *hexa* -/-, *hexb* -/- and wild type mice (n=2 per genotype) and differentiated in culture with M-CSF for 12 days. Following differentiation, cells were treated with LPS or Poly I:C and cell lysates were collected 24 hours afterward. Cell lysates were subjected to western blotting and probed for Gpnmb. Gpnmb expression was undetectable by western blotting in untreated cells. (**A**) HEXB deficient BMDMs displayed significantly augmented Gpnmb levels in comparison to wild type-derived BMDMs when treated with LPS (*P< 0.01). (**B**) Poly I:C treated cultures displayed no significant intergenotype differences. Tx (treatment), wt (wild type).

To further investigate the pattern of Grp78, Mpg1, SAP-A, and Gpnmb expression in bone marrow-derived macrophages, immunocytochemistry was performed on untreated and LPS (10μg/mL) stimulated cultures derived from wild type, *hexa* -/-, *hexb* -/-, and *glb1* -/-mice. CD11b labeling was also utilized to assess primary culture differentiation to macrophages. Bone marrow was differentiated to macrophages in culture with M-CSF for 12 days at which point culture media was replaced with fresh media containing LPS (untreated cultures received fresh media without LPS). LPS stimulation was conducted for 24 hours prior to immunocytochemical analysis.

Grp78 expression was observed almost exclusively in the nucleus amongst all genotypes. Additional perinuclear labeling was noted in selected cells. However, the pattern of Grp78 expression did not differ between genotypes (Figures 24 and 25).

Mpg-1 displayed clear perinuclear labeling. Additionally, marked Mpg-1 labeling was observed in the peripheral projections of bone marrow macrophages (Figures 24 and 25). Furthermore, untreated cells possessed fewer points of marked peripheral Mpg-1 expression than did their LPS stimulated counterparts.

Gpnmb labeling in untreated cells was marked and perinuclear (Figure 26). In LPS stimulated cultures, expression became more diffuse and increasingly homogenous throughout the nucleus and cytoplasm (Figure 27).

Labeling of untreated and LPS stimulated BMDM cultures for CD11b confirmed differentiation of primary cultures to macrophages (Figures 28 and 29). It also demonstrated culture purity and revealed little-to-no myocytic or fibroblastic culture contamination.

SAP-A expression in untreated and LPS stimulated cultures revealed a punctate pattern of labeling similar to that observed in Mpg-1 probed cultures (Figures 28 and 29). Prior immunocytochemical labeling outlined in Figure 17 suggested a trend for increased SAP-A labeling in *hexb* -/- BMDMs. Contrary to that observation, SAP-A labeling in this experiment did not appear to markedly differ between genotypes. As such, and in agreement with other data presented in this section, it is not believed that these cells possess significant intralysosomal ganglioside accumulations.

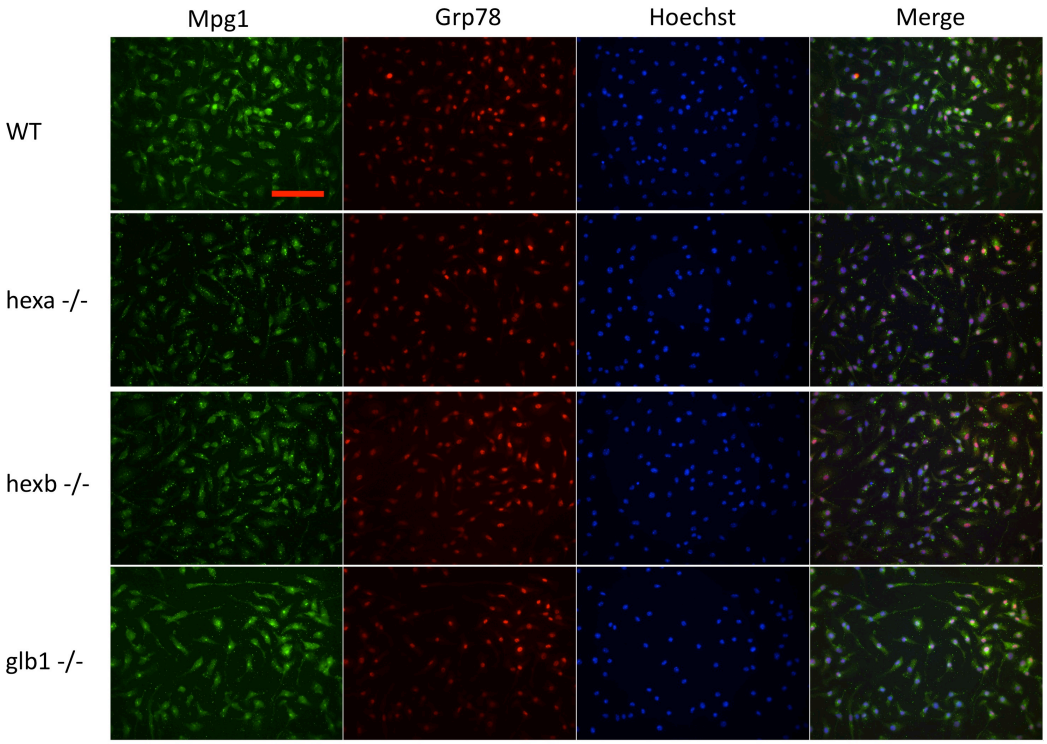

Figure 24. ***Immunocytochemical analysis of untreated bone marrow-derived macrophages labeled with Mpg1 and Grp78.*** Bone marrow was isolated from wild type, *hexa* -/-, *hexb* -/- and *glb1* -/- mice (n=1 per genotype) and differentiated in culture with M-CSF for 13 days. Immunocytochemical analysis was performed to assess expression of Mpg1 and to evaluate BiP/Grp78 staining, a marker of endoplasmic reticulum (ER) stress. Mpg-1 labeling appeared to be perinuclear with additional punctate labeling in cytoplasmic peripheral projections. Marked nuclear and perinuclear expression of Grp78 was observed. However, the pattern of Grp78 expression did not appear to differ between genotypes. Scale bar = 100μm

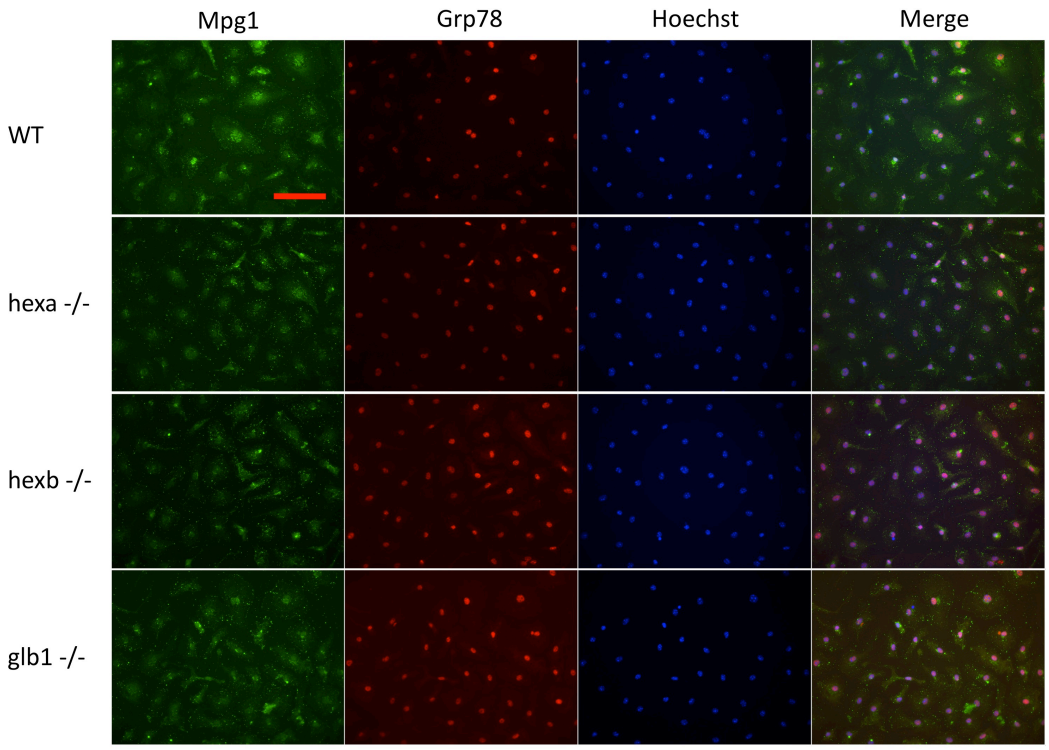

Figure 25. ***Immunocytochemical analysis of LPS stimulated bone marrow-derived macrophages labeled with Mpg1 and Grp78.*** Bone marrow was isolated from wild type, *hexa* -/-, *hexb* -/- and *glb1* -/- mice (n=1 per genotype) and differentiated in culture with M-CSF for 12 days. Following differentiation, cells were treated with LPS for 24 hours. Immunocytochemical analysis was performed to assess expression of Mpg1 and to evaluate BiP/Grp78 staining, a marker of endoplasmic reticulum (ER) stress. Mpg-1 labeling was more diffuse and cytoplasmic compared to that observed in untreated cultures. Punctate labeling in cytoplasmic peripheral projections remained and appeared more numerous in LPS stimulated cultures. Marked nuclear and perinuclear expression of Grp78 was observed. However, the pattern of Grp78 expression did not appear to differ between genotypes. Scale bar = 100μm

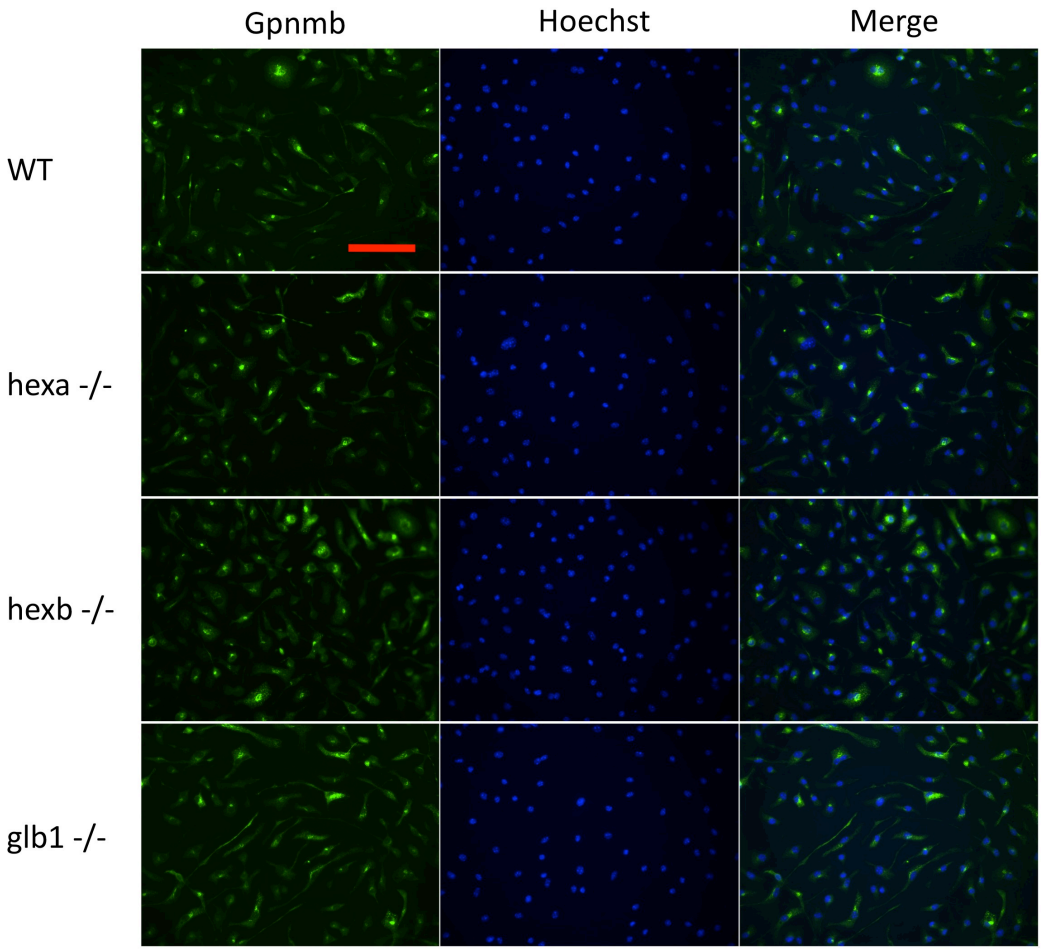

Figure 26. ***Immunocytochemical analysis of untreated bone marrow-derived macrophages labeled with Gpnmb.*** Bone marrow was isolated from wild type, *hexa* -/-, *hexb* -/- and *glb1* -/- mice (n=1 per genotype) and differentiated in culture with M-CSF for 13 days. Immunocytochemical analysis was performed to assess expression of the transmembrane glycoprotein, Gpnmb. Marked perinuclear Gpnmb labeling was observed in all genotypes. Scale bar = 100µm

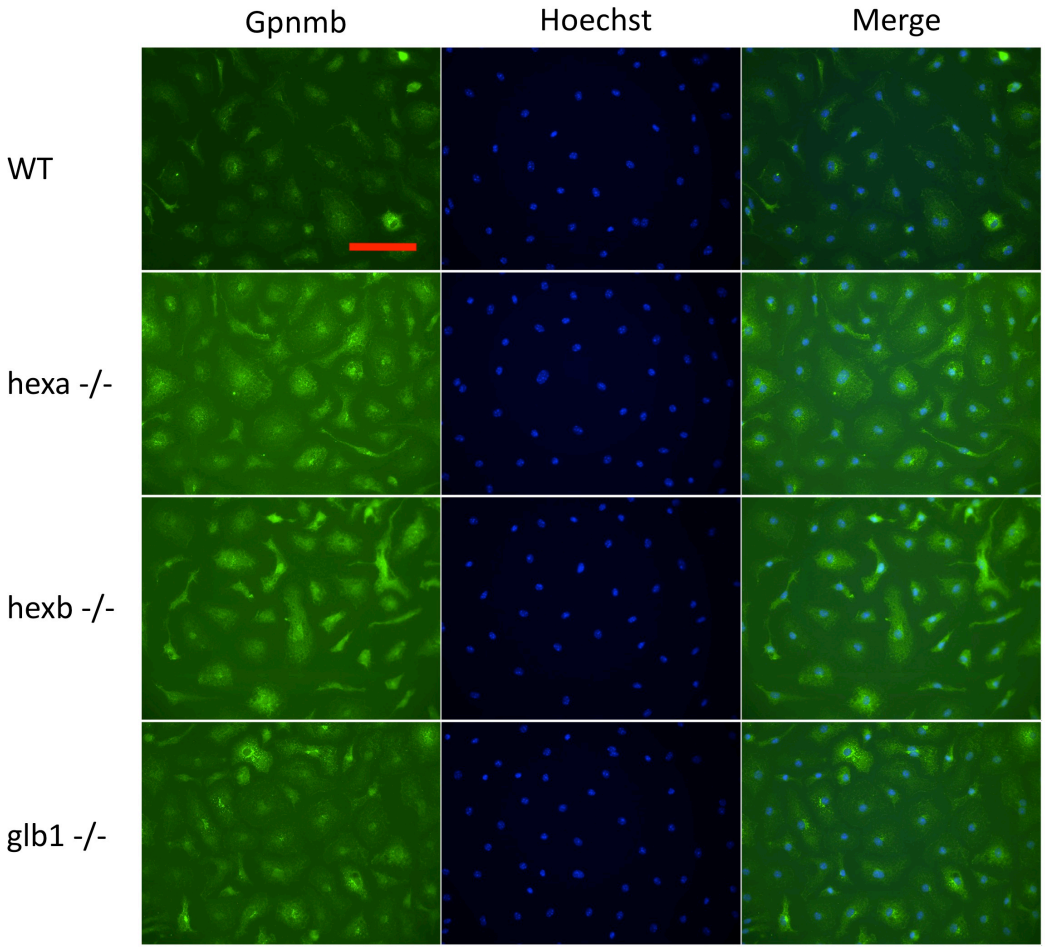

Figure 27. ***Immunocytochemical analysis of LPS stimulated bone marrow-derived macrophages labeled with Gpnmb.*** Bone marrow was isolated from wild type, *hexa* -/-, *hexb* -/- and *glb1* -/- mice (n=1 per genotype) and differentiated in culture with M-CSF for 12 days. Following differentiation, cells were treated with LPS for 24 hours. Immunocytochemical analysis was performed to assess expression of the transmembrane glycoprotein, Gpnmb. Gpnmb expression appeared to be less perinuclear than that observed in untreated BMDM cultures. Diffuse and homogenous cytoplasmic localization was observed. Scale bar = 100µm

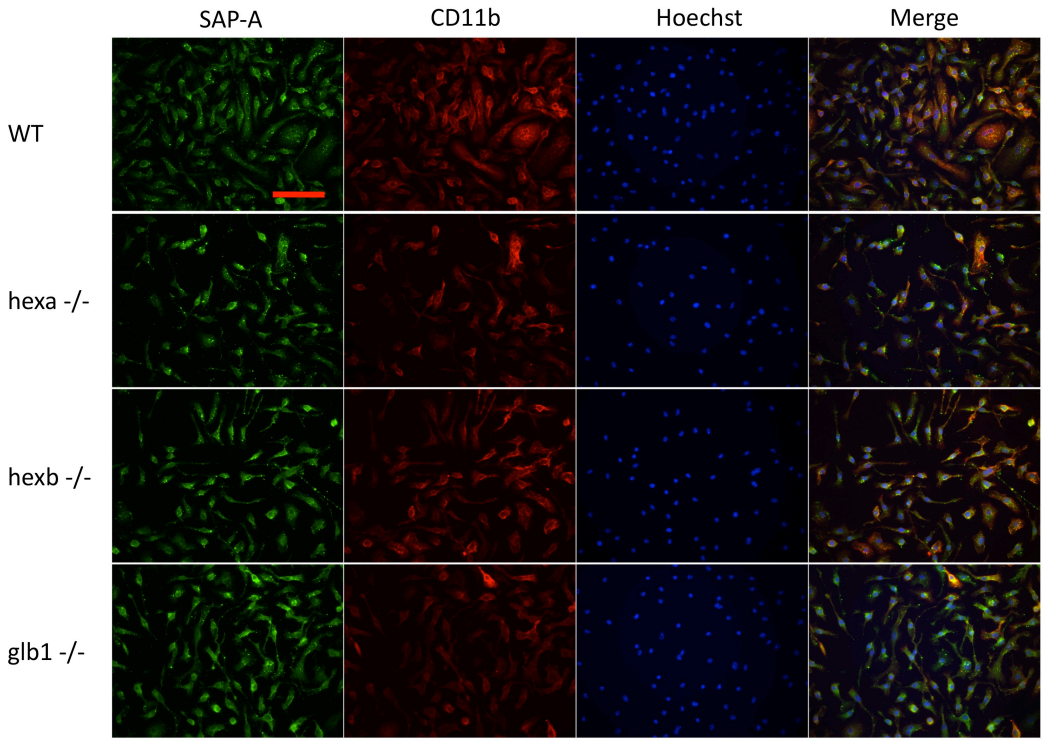

Figure 28. ***Immunocytochemical analysis of untreated bone marrow-derived macrophages labeled with SAP-A and CD11b.*** Bone marrow was isolated from wild type, *hexa* -/-, *hexb* -/- and *glb1* -/- mice (n=1 per genotype) and differentiated in culture with M-CSF for 13 days. Immunocytochemical analysis was performed to assess differentiation to macrophages and observe lysosomal SAP-A labeling. SAP-A labeling was punctate and lysosomal; however, no intergenotypic differences were observed. Marked cell surface CD11b labeling was indicative of differentiated macrophage cultures. Scale bar = 100µm

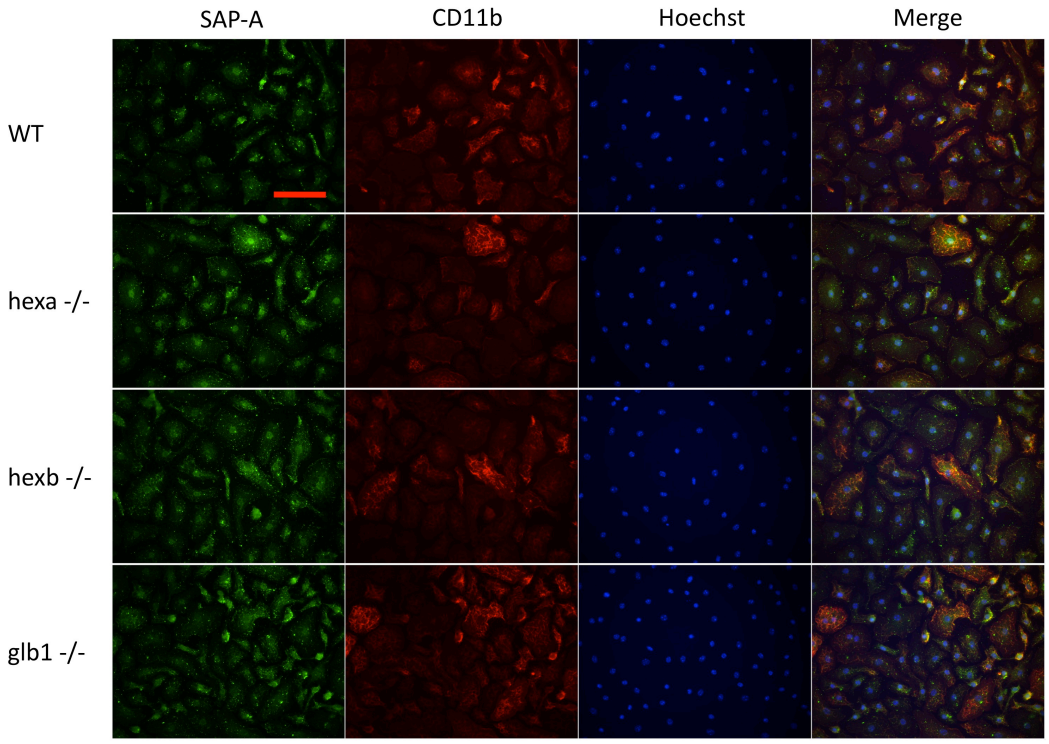

Figure 29. ***Immunocytochemical analysis of LPS stimulated bone marrow-derived macrophages labeled with SAP-A and CD11b.*** Bone marrow was isolated from wild type, *hexa* -/-, *hexb* -/- and *glb1* -/- mice (n=1 per genotype) and differentiated in culture with M-CSF for 12 days. Following differentiation, cells were treated with LPS for 24 hours. Immunocytochemical analysis was performed to assess differentiation to macrophages and observe lysosomal SAP-A labeling. SAP-A labeling was punctate and lysosomal; however, no intergenotypic differences were observed. Marked cell surface CD11b labeling was indicative of differentiated macrophage cultures. Scale bar = 100µm

Previous investigation revealed significant differences in cytokine secretion between wild type, *hexa* -/- and *hexb* -/- BMDMs. More specifically, TNF secretion from LPS stimulated *hexb* -/- macrophages was significantly augmented relative to their wild type and *hexa* -/- counterparts. Given that LPS signaling proceeds via the TLR4 receptor, we sought to measure activation of the proximal downstream signaling and feedback pathways, p38 and Stat3. Since TLR4 activation has been shown to inactivate glycogen synthase kinase 3-beta (GSK3β) as a means of regulating cytokine secretion via MyD88-dependent and MyD88-independent responses, levels of phosphorylated and total GSK3 were also assessed.

Cell lysates were generated from cultures of bone marrow-derived macrophages treated for 24 hours with either LPS (10μg/mL) or Poly I:C (25μg/mL) and were analyzed by western blot. Samples were loaded equally based on levels of total cellular protein and blots were probed for p38 (~38 kDa), Stat3 (~86 kDa), and GSK3 (~46 kDa). *Hexb* -/- BMDMs expressed significantly reduced phospho-Stat3/total Stat3 in comparison to wild type and *hexa* -/- derived BMDMs when treated with LPS (Figure 30A), an observation which was abolished when cells were treated with Poly I:C (Figure 30B). Expectedly, since untreated BMDMs do not secrete measurable amounts of IL-6, these cells did not produce quantifiable levels of phosphorylated Stat3 protein (data not shown). Phospho-p38/total p38 expression in *hexb* -/- BMDMs was significantly elevated compared to wild type BMDMs when treated with LPS (Figure 31B). Poly I:C treatment did not measurably activate the p38 signaling pathway across all tested genotypes, which may have been a result of technical issues given that untreated cells expressed detectable levels of phospho-p38 (data not shown). Untreated *hexb* -/- BMDMs produced significantly more phospho-p38/total p38 compared to *hexa* -/- cells, but this trend did not reach significance relative to wild type cultures (Figure 31A). Phosphorylated GSK3β levels were significantly elevated in both untreated and LPS stimulated *hexb* -/- BMDMs (Figure 32A and B). Although Poly I:C treatment resulted in a similar pattern of expression, the trend did not reach significance (Figure 32C).

Such cytokine secretion patterns and downstream cellular signaling behaviours, combined with a lack of observable intralysosomal ganglioside accumulation, point towards an intrinsic genetic difference in *hexb* -/- bone marrow-derived macrophages that materializes as hypersensitization to PAMPs and potentially other immune response-invoking stimuli.

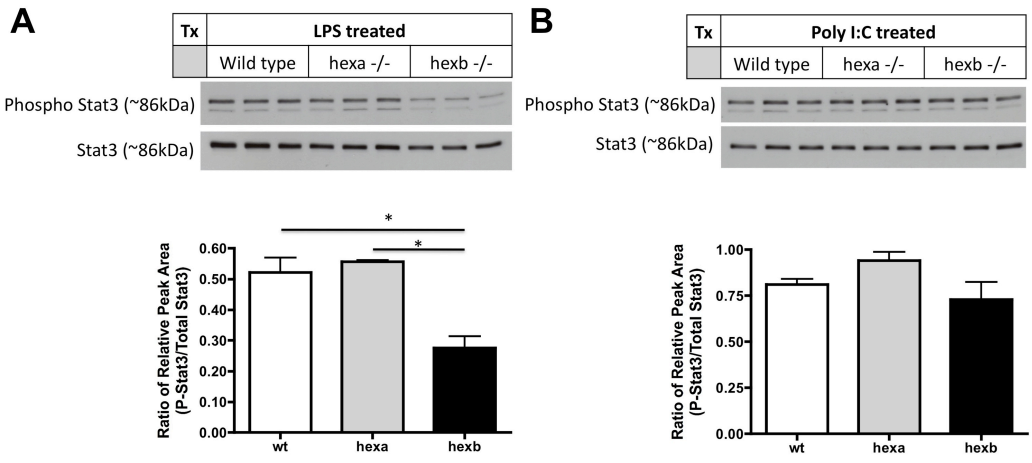

Figure 30. ***Stat3 western blot of hexa -/- and hexb -/- bone marrow-derived macrophages stimulated with LPS or Poly I:C.*** Bone marrow was isolated from *hexa* -/-, *hexb* -/- and wild type mice (n=2 per genotype) and differentiated in culture with M-CSF for 12 days. Following differentiation, cells were treated with LPS or Poly I:C and cell lysates were collected 24 hours post treatment. Cell lysates were subjected to western blotting and probed for phosphorylated and total Stat3. Untreated cells produced immeasurable quantities of phosphorylated Stat3 (data not shown). (**A**) LPS treated *hexb* -/- BMDMs displayed significantly reduced activated Stat3 in comparison to both wild type and *hexa* -/- derived cells (*P< 0.05). (**B**) No significant intergenotype differences were observed in Poly I:C treated cultures. Tx (treatment), wt (wild type).

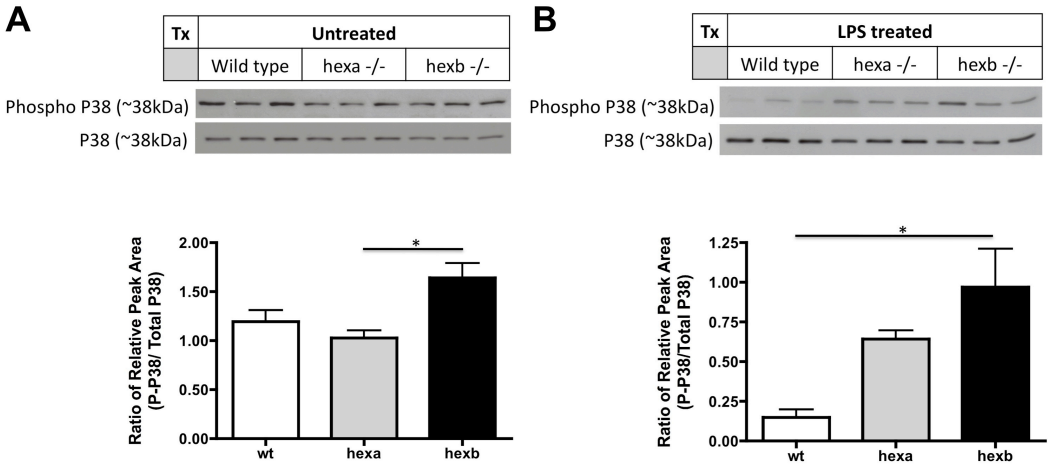

Figure 31. ***P38 western blot of untreated or LPS stimulated hexa -/- and hexb -/- bone marrow-derived macrophages.*** Bone marrow was isolated from *hexa* -/-, *hexb* -/- and wild type mice (n=2 per genotype) and differentiated in culture with M-CSF for 12 days. Following differentiation, cells were treated with LPS and cell lysates were collected 24 hours post treatment. Cell lysates were subjected to western blotting and probed for phosphorylated and total p38. Untreated (**A**) and LPS (**B**) treated *hexb* -/- BMDMs exhibited a significant increase in activated p38 when compared to wild type and *hexa* -/-, or wild type macrophages, respectively (*P< 0.05). Tx (treatment), wt (wild type).

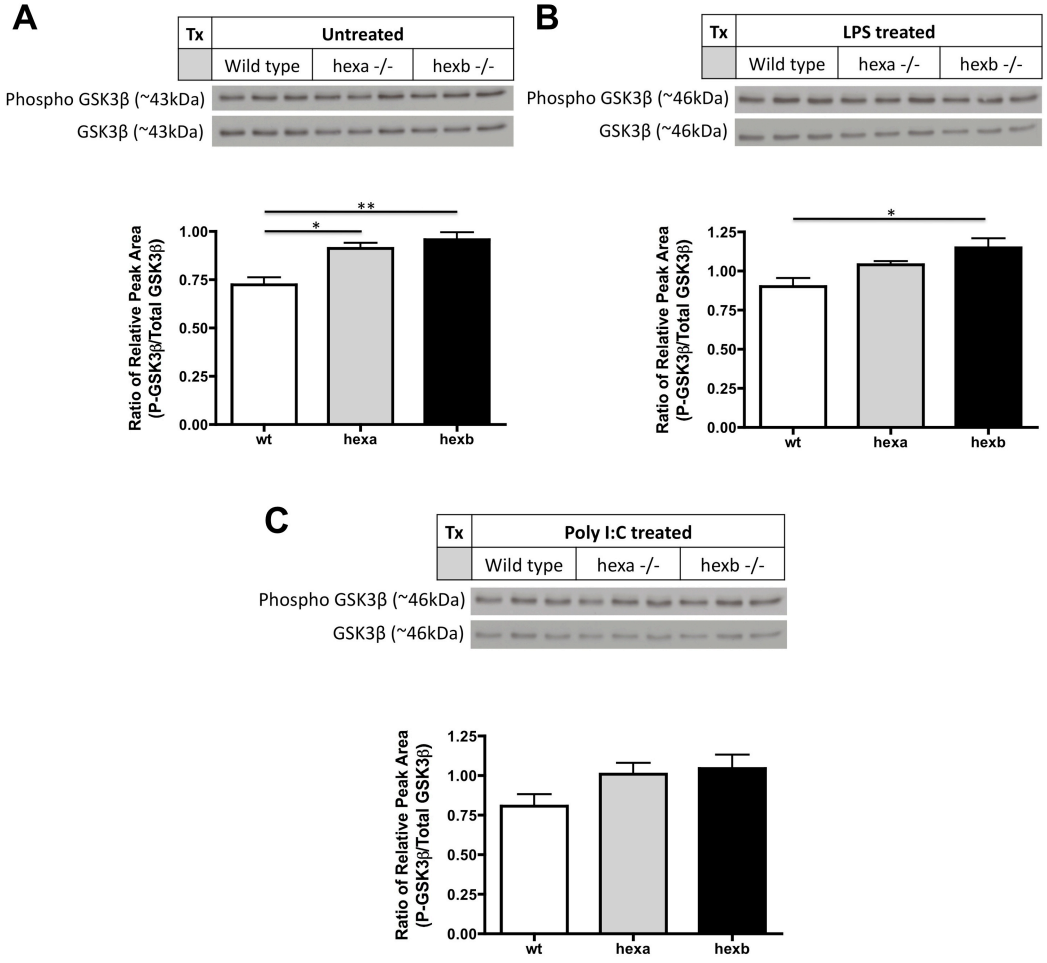

Figure 32. ***GSK3 western blot of untreated, LPS, or Poly I:C stimulated hexa -/- and hexb -/- bone marrow-derived macrophages*****.** Bone marrow was isolated from *hexa* -/-, *hexb* -/- and wild type mice (n=2 per genotype) and differentiated in culture with M-CSF for 12 days. Following differentiation, cells were treated with LPS or Poly I:C and cell lysates were collected 24 hours post treatment. Cell lysates were subjected to western blotting and probed for phosphorylated and total GSK3β. (**A**) Untreated *hexa* -/- and *hexb* -/- cultures displayed significantly elevated phosphorylated GSK3β compared to wild type cells (*P< 0.05, **P< 0.01). (**B**) Only *hexb* -/- cells exhibited a significant increase in phospho-GSK3β when treated with LPS (*P< 0.05). (**C**) No significant differences were observed amongst Poly I:C treated cultures; however, a trend for significantly elevated phospho-GSK3β existed between both *hexb* -/- and *hexa* -/-, and wild type BMDMs. Tx (treatment), wt (wild type).

Taking into consideration previously published literature that links sialidase activity with TLR4 signaling[69, 70, 110], measurement of specific sialidase activity under conditions of PAMP and GM2 treatment was performed. Differentiated BMDM cultures were treated with LPS (10μg/mL), Poly I:C (25μg/mL), CpG Flu 1668 (1μM), or GM2 (25μg/mL) for 24 hours. Cell lysates were obtained and specific sialidase activity was measured as described in 2.7.

Untreated and LPS treated wild type BMDMs showed significantly higher specific sialidase activity than *hexa* -/- cells receiving similar treatment. Wild type macrophages consistently possessed the highest sialidase activity within each treatment, with the exception of the Poly I:C treated BMDMs. BMDMs from *hexa* -/- mice showed the lowest activity across all treatments. Some treatments had dramatically opposing effects on each genotype (relative to untreated conditions), such as that of Poly I:C on *hexb* -/- BMDM specific sialidase activity (augmented) versus wild type (suppressed) and *hexa* -/- (indifferent). Poly I:C treated *hexb* -/- cells displayed significantly elevated activity compared to *hexa* -/- BMDMs exposed to the same treatment. CpG Flu 1668 and GM2 treated *hexa* -/- BMDMs displayed higher activity than their untreated counterparts. LPS did not have a stimulatory effect on the specific sialidase activity of any genotype at this time point (Figure 33).

While several intergenotype and inter-treatment differences were observed, they did not correlate with the altered pattern of TLR4-mediated cytokine secretion witnessed in *hexb* -/- BMDMs. Thus, it was hypothesized that variation in sialidase activity is not responsible for the hypersensitization of HEXB deficient macrophages.

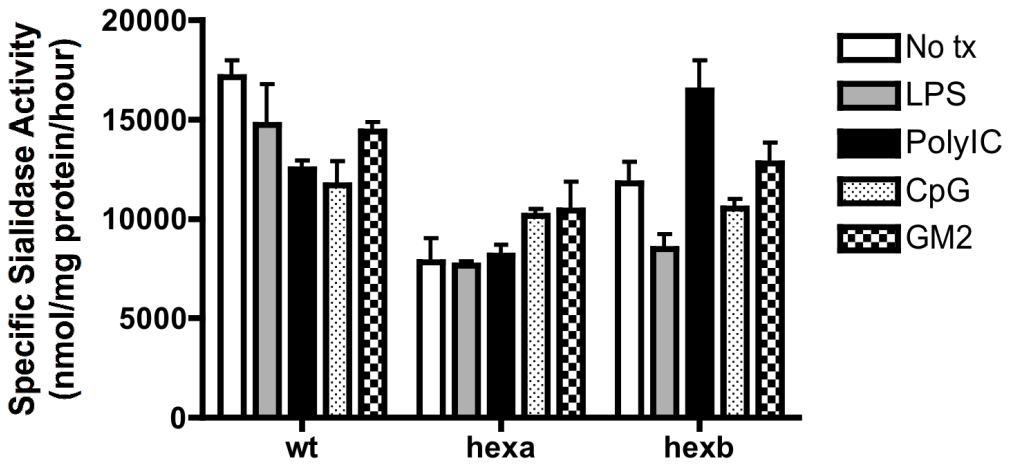

Figure 33. ***Specific sialidase activity of hexa -/-, hexb -/- and wild type bone marrow-derived macrophages following stimulation with PAMPs.*** Bone marrow was isolated from *hexa* -/-, *hexb* -/- and wild type mice (n=2 per genotype) and differentiated in culture with M-CSF for 12 days. Following differentiation, cells were treated with either LPS, Poly I:C, CpG Flu 1668 or GM2. 24 hours post-treatment, cells were harvested and whole-cell specific sialidase activity was measured. Specific sialidase activity differed significantly across treatments and between genotypes. Untreated and LPS treated wild type BMDMs showed significantly higher activity than *hexa* -/- cells receiving similar treatment. Wild type macrophages consistently possessed the highest sialidase activity within each treatment, with the exception of the Poly I:C treated BMDMs. BMDMs from *hexa* -/- mice showed the lowest activity across all treatments. Some treatments had dramatically opposing effects on each genotype such as that of Poly I:C on *hexb* -/- BMDM specific sialidase activity (augmented) versus wild type (suppressed) and *hexa* -/- (indifferent). Poly I:C treated *hexb* -/- cells displayed significantly elevated activity compared to *hexa* -/- BMDMs exposed to the same treatment. CpG Flu 1668 and GM2 treated *hexa* -/- BMDMs displayed higher activity than their untreated counterparts. LPS did not have a stimulatory effect on the specific sialidase activity of any genotype at this time point. Differences in specific sialidase activity did not correlate with the observed pattern of TLR4-mediated cytokine secretion. Tx (treatment), wt (wild type).

CHAPTER 4

DISCUSSION

4.1 CPD-mediated modulation of lysosomal sialidase as a potential candidate alternate gene therapy mechanism for the treatment of Tay-Sachs disease.

The designation GM2 gangliosidoses encompasses a group of diseases whose pathological outcomes and similar clinical phenotypes result from distinct molecular defects, all of which cause the intralysosomal accumulation of GM2 gangliosides in CNS-resident neurons. There are three inherited (autosomal recessive) disorders grouped into this class of neurodegenerative diseases: Tay-Sachs, Sandhoff and GM2 Activator deficiency[36]. Symptom severity and their age-of-onset are heavily dependent on the responsible genetic defect. Moreover, disease severity is indirectly proportional to the age-of-onset. Affected individuals may present with a variety of the following clinical manifestations: cherry red spot on the macula, mental and/or physical retardation, psychological/psychosocial disorders, motor malfunctions, seizures, blindness, ataxia, tremors, muscular atrophy and in many cases death[46].

Treatment of Tay-Sachs disease presents difficulties not typically encountered with peripherally-originating/centralized illnesses. Its intimate relationship with the central nervous system requires that peripherally-introduced therapeutic strategies/agents be able to cross the blood-brain barrier. Furthermore, and similar to other conditions involving the CNS, neuropathology accumulated prior to treatment cannot be reversed. Therefore, the pinnacle aim of therapeutic intervention in Tay-Sachs disease is lessening further degradation, and restoration of peripheral nervous system function.

Attempts to reduce the amount of stored ganglioside in the GM2 gangliosidoses have been met with limited success. Previous literature has presented several therapeutic strategies for the treatment of Tay-Sachs, including the use of pharmacological chaperones, substrate reduction, gene therapy, and enzyme replacement therapies[24, 25, 29, 31, 111]. While each of these approaches target the defective pathway directly, none have been completely successful in ameliorating disease pathology. The data presented in section I of chapter 3, which builds upon work previously conducted in the Igdoura laboratory, fortifies a novel alternate gene mechanism in human Tay-Sachs neuroglia for future therapeutic application in the treatment of Tay-Sachs disease.

Previous work utilizing the genetic Tay-Sachs murine model revealed a lack of human Tay-Sachs-associated symptoms and the maintenance of phenotypic normality (compared to wild type animals) until approximately 1 year of life[105, 106]. Further investigation uncovered the mechanism responsible for their disease avoidance - a lysosomal sialidase-mediated metabolic bypass of HEXA deficiency[64]. Murine lysosomal sialidase was able to act on accumulated GM2 and initiate its conversion to GM3 (via HEXB action) through its asialo intermediate, GA2 (Figure 4). Prior work in the Igdoura laboratory sought to investigate if this bypass pathway could be replicated in human cells.

Previous work performed a functional comparison of human and mouse lysosomal sialidase promoters in both human and mouse cell lines and revealed that an inherently more active murine promoter may be at least partially responsible for the higher levels of lysosomal sialidase and resultant sialidase-mediated bypass in *hexa* -/- mice. While these results implicated differences in basal lysosomal sialidase promoter activity as contributing to a murine-specific sialidase-mediated bypass, they did not discredit the possibility that post-translational events may also contribute, or that differences in enzymatic affinity for GM2 might exist.

In silico analysis of the human lysosomal sialidase promoter granted insight into the structure and regulatory elements of human *NEU1*. The existence of putative CDP binding sites in the human promoter, combined with previous work, which validated CDP as a modulator of murine *Neu1* promoter activity, lead to the selection of CDP as a candidate transcription factor for further analysis.

Prior evaluation of the effects of CDP and six truncations on the human lysosomal sialidase promoter demonstrated the ability for $CDP^{831\text{-}1505}$ to substantially increase (~5-fold) *NEU1* promoter function. Although these results were in contrast to full-length CDP's reputation as a transcriptional repressor, the possibility that full-length CDP may act as a potent transcriptional activator of the human *NEU1* promoter was invalidated by its minimal effect on human lysosomal sialidase promoter activity. Since $CDP^{831\text{-}1505}$ retains the CR3 and HD domains predicted to be involved in stable DNA binding, but lacks the CR1 domain that in combination with CR2 may be responsible for transient DNA binding and repression of promoter activity, it is hypothesized that truncated $CDP^{831\text{-}1505}$ has lost its repressive capacity. More specifically, $CDP^{831\text{-}1505}$ may act through a "dominant negative"-like mechanism to competitively inhibit repression of human sialidase by blocking full-length CDP from stably binding the human *NEU1* promoter for transient repression. The CR1 deficiency of $CDP^{831\text{-}1505}$ renders it incapable of CCAAT box displacement. Although contrary to this hypothesis, the possibility that $CDP^{831\text{-}1505}$ acts to directly stimulate promoter activity cannot be excluded.

Using the ATCGAT consensus sequence, multiple potential CR3-HD binding sites were discovered within the 1500bp promoter region immediately 5' of the ATG start codon of *NEU1*. However, the number of acceptable candidates was diminished due to the absence of an adjacent CCAAT binding sequence. Furthermore, many of the originally selected CDP binding sites deviated from the consensus sequence by >2 bases. As such, only the CD3-HD/CCAAT binding domain closest to the ATG codon was analyzed via ChIP for $CDP^{831\text{-}1505}$ binding. Given that CDP's DNA binding ability is known to be promiscuous, it may be beneficial to assess the previously excluded CR3-HD binding sites. ChIP conducted on Tay-Sachs neuroglia infected with adenovirus expressing $CDP^{831\text{-}1505}$ provided evidence for the association of truncated $CDP^{831\text{-}1505}$ and the human *NEU1* promoter, presumably at the putative CR3-HD/CCAAT binding site. This

finding supports the current *cis* inhibition of repression hypothesis. In support of this hypothesis is the observation that a naturally occurring 110 kDa isoform of CDP, which is comprised of the same combination of DNA-binding domains as $CDP^{831\text{-}1505}$, acts to activate transcription *in vitro*[112]. Unexpectedly, the PCR primers designed to amplify an upstream region not predicted to be a hot spot for truncated CDP binding, seemed to indicate potential non-specific binding of the anti-HA antibody (Figure 11B). However, since the degree of enrichment was faint in anti-HA pulled down untreated neuroglia versus $AdCDP^{831\text{-}1505}$ infected cells, the observed positive enrichment at this intergenic site may perhaps be attributable to a novel CDP binding site as opposed to non-specific anti-HA binding. In fact, retrospective analysis revealed a previously unrecognized potential CR3-HD binding sequence within the amplified intergenic region. If truncated CDP bound at this newly appreciated CR3-HD binding site, it could result in the type of background amplification observed in the control reactions. Thus, the ChIP data presented provides strong evidence to support the current hypothesis that truncated $CDP^{831\text{-}1505}$ interacts with CR3-HD binding sites in the human lysosomal sialidase promoter. It should be noted, however, that at this point it cannot be concluded whether $CDP^{831\text{-}1505}$ acts to inhibit promoter repression or to activate lysosomal sialidase through a currently unidentified mechanism.

Infection of Tay-Sachs neuroglia with $AdCDP^{831\text{-}1505}$ resulted in an MOI-dependent increase in intracellular levels of sialidase protein, and was previously shown to augment specific sialidase activity. The ability of CDP to influence levels of sialidase protein and functional activity in human cells is crucial for the utilization of this transcription factor or its binding site/mechanism of transcriptional activation for alternate gene therapy. However, this manipulative ability would be inadequate if it were unable to affect levels of intralysosomally accumulated GM2.

Silica gel TLC analyses of Tay-Sachs neuroglia provided evidence that modulation of sialidase via $CDP^{831\text{-}1505}$ is capable of reducing intracellular GM2 accumulation. Moreover, it provided confirmation of the decrease in GM2 using antibody independent methods (organic phase ganglioside extraction and TLC). Accumulated GM2 acted upon by sialidase in the bypass results in low-level conversion to GA2. Previously conducted FACS analysis demonstrated that GA2 was also decreased in CRB/TSD neuroglia following $AdCDP^{831\text{-}1505}$, and AdSial + AdCA infection, suggesting that when sialidase activity is upregulated newly formed GA2 is more readily accessible by HEXB for conversion to lactosylceramide (Figure 4). Thin layer chromatography does not possess the sensitivity to confirm, nor refute this previous observation. Aside from verifying the ability of $CDP^{831\text{-}1505}$ to activate a sialidase-mediated bypass capable of reducing GM2 stores in Tay-Sachs cells, these observations support pharmaceutical stimulation of the endogenous lysosomal sialidase gene as a potential treatment for HEXA deficient GM2 gangliosidoses.

Confirmation of the identity of the predicted ganglioside species run on silica gel TLC via MALDI-TOF mass spectroscopy revealed the presence of the predicted species within each corresponding sample (Figure 8). However, each sample also contained multiple other ganglioside species likely due to the fact that silica gel TLC separation may have resulted in incomplete separation of each species. The resultant minute quantities of incompletely separated (i.e. smeared) sample would not be noticeable when visualized with resorcinol staining, but the highly sensitive MALDI-TOF mass spectroscopy is capable of detecting even minuscule amounts. It is therefore only possible to claim that GM2 and GA2 gangliosides were present in each sample, but not that they were the predominant species. Nonetheless, purified, tissue culture grade bovine GM2 displayed an identical pattern of migration as the predicted GM2 band in the *hexb* -/- murine cerebellum sample (data not shown).

The precise quantity of intralysosomal GM2 clearance that is required to restore normal cell function and prevent cell death is currently unknown; however, prior reports have suggested that marginal restoration (~10%) of enzymatic activity provides sufficient aid to substantially diminish/abolish clinical symptoms[24, 113]. Presumably then, a threshold exists below which intralysosomal ganglioside accumulations become manageable and non-lethal. Although the reductions described in this work do not result in total amelioration of intracellular ganglioside accumulation, it is hypothesized that the extent that the human sialidase-mediated bypass lessens accumulations would be sufficient to show considerable improvement in clinical symptom severity.

The pursuit of effective treatments or, ideally, a cure, remains a fundamental motive for studying human disease. Discovery of the lysosomal sialidase-mediated bypass in Tay-Sachs mice demonstrated the existence of an alternate, endogenous metabolic pathway to metabolize GM2. It was subsequently hypothesized that activation of this bypass in Tay-Sachs patients, could reduce GM2 accumulation and lessen, or completely halt pathologic symptom development. Previous data, combined with the newly acquired findings presented in this thesis demonstrate that $CDP^{831\text{-}1505}$ markedly augments endogenous human *NEU1* promoter activity, resulting in elevated lysosomal sialidase protein levels and enzymatic activity in what appears a cell-type specific manner. Furthermore, elevated sialidase activity is capable of lessening pathologic ganglioside accumulations found in human Tay-Sachs cells.

The data presented in section I of chapter 3 of this thesis, for the first time establishes a completed potential mechanism utilizing endogenous lysosomal sialidase, for the treatment of Tay-Sachs disease. Moreover, it provides compelling evidence that warrants further investigation into modulation of human lysosomal sialidase as an effective alternate gene therapy technique for Tay-Sachs disease. Screening and testing candidate compounds from chemical databases is the next logical step in the progression towards clinically testable pharmaceutical modulation of sialidase. Lucrative agents would be those that have the capacity to markedly evoke lysosomal sialidase expression, and the

capability to cross the blood-brain barrier. Whether the influence of such pharmaceutical modulation is restricted to *NEU1* must also be explored, and will certainly require investigation prior to clinical trials. It is anticipated that this therapeutic approach may result in a less invasive and more cost-effective treatment option for patients suffering from Tay-Sachs. Perhaps, the use of alternate gene therapy in combination with existing, yet incompletely successful options such as those briefly mentioned above, could generate a more potent therapeutic strategy. The utilization of the aforementioned sialidase-mediated bypass pathway also supports pursuit of other circumventive mechanisms, which may be exploited to treat other lysosomal storage disorders.

4.2 Evaluation of inflammatory responses following PAMP or GM2-stimulation in bone marrow-derived macrophages from Tay-Sachs and Sandhoff mice.

Tay-Sachs and Sandhoff disease are both chronic, and often lethal, lysosomal storage disorders that result in profound neurodegeneration in progressed cases. Development and study of *hexa* -/- (Tay-Sachs) mice quickly exposed their unique mechanism of lysosomal sialidase-mediated disease avoidance. Conversely, Sandhoff mice consistently developed human-type symptoms, and fall victim to the illness at approximately 120 days of age. While this bypass of HEXA deficiency allowed Tay-Sachs mice to avoid disease via lessening of intralysosomal accumulation in CNS-resident neurons below the threshold required for widespread neuropathology, the later events through which disease was avoided in *hexa* -/- mice had yet to be explored. Given the link between neuroinflammation and neurodegeneration, as well as the recruitment of peripherally derived macrophages to the CNS in progressed illness, comparison of immunological characteristics and response to stimuli of bone marrow-derived macrophages from Tay-Sachs and Sandhoff animals was conducted.

The generation of differentiated macrophage cultures from primary cell-rich bone marrow offered several advantages. Firstly, culturing of bone marrow does not require the use of immunostimulants to increase cell yield (as is the case with thioglycolate-elicited peritoneal macrophage isolation). Furthermore, maturation characteristics can be controlled through the addition of selective differentiation compounds to *in vitro* primary cell cultures. M-CSF differentiation produces large macrophages, with mature structural features and organelles, and defined cytoplasmic projections[114]. Lastly, although *in vitro* M-CSF-differentiated macrophages do not share the same local environment as CNS-resident microglia, both are derived from bone marrow and thus, possess a similar origin[115]. Moreover, microglia and macrophages share many cell surface markers[116]; however, their unique morphological aspects and CNS residence classifies them as a distinct cell type[115]. During Tay-Sachs and Sandhoff disease

progression, pathology-related disruption of the blood-brain barrier allows immature monocytes and bone marrow-derived macrophages to be recruited to the CNS via astrocyte-produced MCP1 and blood vessel transport[115, 117, 118]. Therefore, comparison of BMDMs provided valid insight into the immunoregulatory differences between Tay-Sachs and Sandhoff mice.

PAMP stimulation of *hexa* -/- and *hexb* -/- BMDM cultures exposed several morphological differences. While cultures of all genotypes exposed to LPS possessed larger cellular size (relative to nuclear area), intergenotype comparison of LPS stimulated cultures showed that HEXB deficient cultures were significantly smaller than their wild type counterparts. Furthermore, quantification of the number of projections around the periphery of untreated versus LPS stimulated cells revealed that only wild type and *hexa* -/- derived cultures possess significantly greater numbers under conditions of LPS stimulation. Although *hexb* -/- cultures demonstrated a similar trend, it did not reach significance. Such data suggests that *hexa* -/- BMDMs may behave similarly to wild type, whereas *hexb* -/- macrophages appear either immature by comparison, or activated to a lesser extent at 24 hours post stimulation[119]. Moreover, cell size in alveolar macrophages has been linked to phagocytic capacity[120]. As such, hexb -/- macrophages may have reduced capacity for phagocytosing CNS-resident debris. Cytoplasmic projections are often used by activated macrophages for intercellular communication and are actively involved in migration and phagocytosis[121]. While no clear distinction in the interaction of neighbouring cells was observed, the possession of fewer projections in *hexb* -/- macrophages may therefore suggest the potential for compromised communication ability. Decreased phagocytic capacity in conjunction with superfluous cellular debris from dying neurons could result in amplified neuroinflammation. Further examination of the features of Tay-Sachs and Sandhoff macrophages should be conducted via electron microscopy.

Measurement of secreted IL-1β, IL-10, IL-6 and MCP1 in cell culture media via ELISA at 24 hours post stimulation did not reveal any apparent intergenotype variation in secretion in response to PAMP treatments.

Given the current hypothesis that accumulated GM2 released by dying CNS-resident neurons propagates proinflammatory behaviour, leading to further neuroinflammation and greater neurodegeneration by interaction with cell-surface TLR4[107], it was predicted that treatment of bone marrow cultures with exogenous GM2 would result in obvious augmentation in inflammatory responses. Contrary to this hypothesis, introduction of high-dose GM2 (*in vitro* dosage based on published literature) did not induce marked cytokine secretion. In fact, all measured cytokines remained below the assay's minimal level of detection. Therefore, all observed differences are due solely to variation in cellular protein, rather than accurately measured quantity of immunoregulatory molecules. Measurement of TNF in GM2 stimulated culture media at all sampled post treatment time points solidified the original finding that GM2 does not stimulate cytokine secretion. Since these macrophages clearly expressed TLR4 in

culture (as evidenced by their drastic inflammatory reaction to LPS), yet are unresponsive to GM2, this data suggests that accumulated ganglioside released from apoptotic cells in the CNS may not play a significant role in stimulating CNS-resident microglia and/or recruited macrophages. It is not possible to elucidate an alternative mechanism at this point without further investigation; however, discounting GM2 as a major contributor in progressed GM2 gangliosidoses (namely, Tay-Sachs and Sandhoff disease) automatically implies other factors and/or apoptosis-associated molecules as the major neuroinflammatory and thus, neurodegenerative stimuli. While this evidence supports a lack of GM2-mediated TLR4 activation, cultured BMDMs may still internalize the exogenously introduced GM2. In fact, current literature suggests that cells (specifically microglia and macrophages) rapidly internalize exogenous gangliosides[122, 123]. Chronic internalization (as opposed to the transient 24 hour incubation period used in experimentation) via phagocytosis or transmembrane diffusion may be required to observe GM2-mediated macrophage cell stress and resultant immunological responses. Future experimentation should monitor cytokine secretion and other markers of cell stress in GM2-treated BMDMs over a longer duration. Although the data appears convincing, one cannot rule out other non-mechanistic explanations. For example and as mentioned previously, interspecies variation in ganglioside fatty acid chain structure exists between many mammals and could possibly play a role in ligand-receptor recognition/binding. The GM2 used to treat the murine-derived BMDMs was of bovine origin and thus, may not be effectively recognized by mouse-resident cell surface toll-like receptors.

Additional examination of cytokine (TNF, IL-1β, IL-10, IL-6 and MCP1) secretion at multiple post-stimulation time points exposed marked differences in TNF, MCP1, and IL-10 production. Specifically, TNF secretion was significantly elevated in *hexb* -/- BMDMs relative to *hexa* -/- and wild type cultures at 12 and 24 hours post LPS stimulation. HEXB deficient macrophages also secreted significantly less MCP1 in comparison to their HEXA deficient and wild type counterparts beginning at 4 hours following LPS treatment. This significant reduction in MCP1 secretion was maintained at 24 hours post treatment. Furthermore, a significant reduction in IL-10 secretion was observed in *hexb* -/- BMDMs at 8 and 12 hours post LPS stimulation. Contrary to these observations, treatment of cultures with Poly I:C did not result in similar secretion patterns, suggesting that TLR3-mediated behaviour is differently affected by HEXA and HEXB deficiencies. These results therefore suggest that only selected TLR pathways (specifically TLR4) may behave abnormally, and only in response to select stimuli (e.g. LPS versus GM2 treatment). The fact that Sandhoff-derived BMDMs displayed uniquely hypersensitive behaviour to stimulation (i.e. marked differences in cytokine secretion), but did not demonstrate typical features of intralysosomal accumulations, meant that their genetically introduced HEXB deficiency must have been influencing these actions via a alternative mechanism. Although the work presented in this thesis has yet to fully elucidate a candidate

mechanism, it lends credence to an alternate hypothesis regarding the neuroinflammatory and neurodegenerative cascade in Sandhoff and potentially other ganglioside storage disorders. This hypothesis states that diseased macrophages in Sandhoff disease (and possibly other ganglioside storage illnesses) are innately hypersensitized in their responses to stimuli through an accumulation-independent mechanism, such that the magnitude (and perhaps duration) of their stress-induced inflammatory reaction is augmented relative to that observed in wild type animals. The observed augmentation in LPS-stimulated TNF secretion illuminates a potentially prominent proinflammatory mechanism via which profound neurodegeneration in *hexb* -/- animals could be mediated. In support of this, examination of *hexb tnf* double knockout animals by members of the Igdoura laboratory has demonstrated that these mice display reduced neuroinflammation, lessened CNS-resident cellular apoptosis, delayed onset of peripheral dysfunction, and a significantly prolonged lifespan. Lower levels of anti-inflammatory IL-10 secretion could also predispose HEXB deficient macrophages to secretion of prolonged, undampened cytokine storms through lessened repression of TNF secretion[124]. To ensure that the lack of a predicted increase in anti-inflammatory IL-10 secretion was not due to the relatively narrow sampling window, future secretion studies should study IL-10 secretion at 48 and 72 hours post treatment. Such prolonged intense inflammatory activity could be responsible for the profound apoptotic and neurodegenerative symptoms observed in Sandhoff disease.

Immunocytochemical labeling, Oil Red O staining, and ganglioside extraction followed by silica gel TLC separation were employed to investigate intralysosomal lipid accumulations as a possible explanation for the altered inflammatory behaviour in HEXB deficient BMDMs. Although anti-SAP-A lysosomal labeling suggested that *hexb* -/- macrophages were swollen, potentially from intralysosomal ganglioside accumulations, further investigation, which utilized methodology capable of direct ganglioside measurement, was unable to observe such accumulation. LPS stimulated BMDM cultures stained with Oil Red O appeared devoid of intracellular lipids. However, since these cultures were not lipid loaded, and Oil Red O only stains neutral lipids, it is unlikely that any accumulated ganglioside would be visible via this technique. Thus, from this data it is only possible to conclude that neither *hexa* -/-, nor *hexb* -/- BMDMs accumulate intracellular neutral lipids as a result of their metabolic deficiencies. Future investigation of ganglioside accumulation in fixed cultures should employ the borohydride-periodate acid-Schiff method, which has been proven in the literature as a robust method for ganglioside staining[125, 126, 127, 128]. Silica gel TLC separation performed on gangliosides extracted from untreated BMDMs showed no evidence of accumulation, supporting the hypothesis that *hexb* -/- macrophages possess intrinsic differences that are responsible for their aggravated behaviour. One notable requirement for the success of this protocol is the necessity for large amounts of starting material. It is therefore possible that no accumulated ganglioside was observed because of an insufficient amount of

initial material. If differences in accumulated ganglioside were definitively present in bone marrow-derived macrophages, the resultant cellular stress could be responsible for the observed differences in their *in vitro* immune response and *in vivo* pathology in Sandhoff mice. However, the absence of accumulated ganglioside is not a reason to cast doubt on experimental methodology. While it is clear from current literature that macrophages synthesize and can accumulate gangliosides (e.g. Niemann-Pick disease)[129], support for the ability of bone marrow-derived macrophages to develop substantial ganglioside accumulations during temporary *in vitro* culture is non-existent. In this aspect, BMDMs are likely dissimilar to isolated CNS-resident, mature, ganglioside-laden neurons in that they may not display accumulation of these compounds in short-term *in vitro* cultures. Further support for this hypothesis comes from additional immunocytochemical labeling performed on *hexa* -/-, *hexb* -/-, and *glb1* -/- BMDMs using SAP-A. Contrary to prior immunocytochemical data, but in agreement with findings from the Oil Red O and ganglioside extraction analyses, no intergenotype differences were observed in the pattern or intensity of SAP-A labeling. Interestingly, incubation of Tay-Sachs and Sandhoff-derived BMDMs with GM2 did not elicit a stress-induced immune response.

Analysis of LAMP2 expression in cultured BMDMs revealed only minor differences in total quantity. However, marked differences existed in the state of LAMP2 glycosylation in *hexb* -/- and *glb1* -/- derived cultures. More specifically, LAMP2 expressed by glb1 -/- BMDMs was retarded in migration, suggesting incomplete cleavage or processing of N-acetyl hexosamines. Given the genetic defects in these bone marrow cultures, it is hypothesized that the resultant enzymatic deficiencies in the β-hexosaminidase isozymes and β-galactosidase may be responsible. Previous studies have linked LAMP protein expression to cytokine secretion and immune cell responses[130, 131]. Furthermore, studies have demonstrated that LAMP expression is fundamental for the fusion of phagosomes with lysosomes[132].

Grp78 expression in cultured *hexb* -/- and *glb1* -/- BMDMs revealed reduced protein levels in comparison to wild type and *hexa* -/- macrophages. Such observations are in agreement with the observed lack of ganglioside accumulation in bone marrow macrophage cultures since accumulated intralysosomal ganglioside has been linked to ER stress in a murine model of GM1 gangliosidosis (*glb1* -/-)[108]. While this data initially appears contradictory to the ganglioside accumulation work presented in this thesis, it is important to note that Tessitore, et al. (2004) studied cultured neurons and neurospheres, as opposed to the primary cell-derived macrophage cultures[108]. It also remains possible that cells primarily targeted in gangliosidoses (neurons) may respond differently to intralysosomal accumulation than infiltrating immune cells. Furthermore, since the Sandhoff (*hexb* -/-) mouse model was generated by completely knocking out *hexb* expression[105], one does not expect this *hexb* mutation to directly influence ER stress levels as would occur if the genetic alteration (e.g. via site directed mutagenesis) generated an incorrectly folded

protein[133]. Such mutations often cause ER retention of misfolded substrates, and are associated with increased BiP/GRP78[134]. However, the lack of increase in Grp78 expression in *hexb* -/- macrophage cultures does not completely discount the existence of augmented levels of ER stress in *hexb* -/- BMDMs. Rather, reduced Grp78 expression may indicate deterioration in the ability of diseased cells to respond to cell stressors and conditions that result in ER stress. Alternatively, literature has suggested that cells are capable of secreting Grp78[135, 136]. Although this thesis presents minimal data to substantiate the following hypothesis, it may be possible that diseased-state macrophages secrete greater amounts of Grp78 than do their wild type counterparts, resulting in the observed pattern of reduced intracellular Grp78. Future experimentation should examine levels of other ER stress markers such as Chop, and secreted Grp78, as well as downstream modulators of cell death such as Jnk2 and Caspase-12. These studies are necessary to provide greater insight into disease-associated ER stress and subsequent cell death in cultured BMDMs.

Given the published involvement of sialidase in the regulation of TLR-mediated responses, the potential for altered levels of sialidase activity to play a role in the observed phenotype was investigated. However, no differences in sialidase activity that could explain the differences in cytokine secretion were observed amongst stimulated BMDMs from *hexa* -/- and *hexb* -/- mice. Therefore, present data suggests that an alternate mechanism be responsible for the intrinsic hypersensitization observed in HEXB deficient macrophages.

Using the data presented thus far, a model for ganglioside-independent *hexb* -/- hypersensitization has been developed. Autophagolysosomal-mediated breakdown of intracytoplasmic components requires LAMP2-dependent phagosomal fusion with lysosomes from the endocytic pathway[132]. Acid hydrolases contained within the mature lysosomal compartment are crucial for degradation of the autophagolysosomal contents. It is hypothesized that alterations in LAMP2 result in partial or full obstruction of this fusion process (Figure 34). Such fusion inhibition would result in autophagosomal accumulation and ultimately, altered cellular behaviour[137]. In neurons, alteration of LAMP2 glycosylation and subsequent autophagosomal abnormalities may contribute to the initiation of the neurodegenerative cascade. Alternatively, such abnormalities in immune cells may result in their hypersensitization and subsequent immunoactivation, similar to that presented in this thesis. Early onset of cytokine secretion (perhaps even prior to ganglioside-related neuronal dysfunction) could be the driving force behind the neurodegenerative cascade. Given that autophagosomes contain heat shock protein 70 (Hsp70; Hsc70) and microtubule-associated protein 1 light chain 3 (MAP1-LC3), intracytoplasmic buildup of these entities may result in a compensatory response to lessen BiP/Grp78 protein production. This hypothesis could also lend support to the reduced Grp78 protein levels previously presented and discussed in this thesis. In agreement with the observation that Gpnmb protein expression was upregulated in LPS treated *hexb* -/- macrophages, prior literature has linked Gpnmb to the phagocytic process.

More specifically, Gpnmb has been identified as a required component for the recruitment of LC3 to the phagosome, where subsequent co-localization of these proteins takes place[138]. Gpnmb aids in acidification of the early phagosome (prior to late endosomal/lysosomal fusion) and promotes crosstalk between the phagocytic and macroautophagic processes[138]. It is therefore possible that increased Gpnmb protein levels are an indication of impairment of autophagosomal fusion. However, it has yet to be determined whether this observed increase in Gpnmb is simply due to autophagosomal accumulation or alternatively, active upregulation of Gpnmb production in an attempt to rescue the defective fusion process.

Prior cytokine data demonstrated an absence of quantifiable immunological response in BMDM cultures treated with exogenous GM2. Furthermore, in the absence of measureable quantities of ganglioside accumulation in BMDM cultures, *hexb* -/- macrophages displayed a marked sensitivity to PAMP stimulation. The proposed LAMP-associated, autophagosomal-centralized model identifies a potential mechanism that is in accord with these observations (i.e. specific to the *hexb* -/- genetic deficiency and independent of ganglioside accumulation). Moreover, this hypothesis conforms to previously published work that uncovered autophagy defects and blockages in other lysosomal storage disorders[139, 140, 141]. Although current data suggests that this model may contribute to the pathological processes observed in Sandhoff and *glb1* -/- animals, it is presently unclear whether this is the primarily mechanism or whether it operates secondary to and/or in conjunction with a neuronal GM2-centralized process. Moreover, this data potentially challenges the current temporal order of neuroinflammation and neurodegeneration. Whether neuron-resident GM2 accumulation or immune cell hypersensitization initiates the pathological cascade is also a topic of debate. Simply put, these processes can thought of in the context of the "chicken or the egg" causality dilemma.

Further investigation into the signaling mechanisms that may be altered in conjunction with cytokine secretion revealed intergenotype differences in the Stat3 feedback pathway, p38 MAPK signaling and GSK3β phosphorylation. As expected, untreated BMDMs did not possess detectable levels of phosphorylated Stat3. Activated Stat3 levels in LPS stimulated *hexb* -/- BMDMs were significantly reduced compared to levels in wild type and *hexa* -/- cultures. This data is in agreement with current literature, as IL-10 expression is responsible for phosphorylation-dependent activation of Stat3, and IL-10 secretion from LPS treated HEXB deficient cultures was significantly reduced. Considering the anti-apoptotic roles of both IL-10 and Stat3, lessened levels of these vital immunoregulatory molecules may aid in a pattern of hypersensitive and exaggerated proinflammatory *hexb* -/- behaviour. The disappearance of intergenotype differences in phosphorylated Stat3 under conditions of Poly I:C treatment remains in line with the apparent lack of influence of TLR3 ligands on *hexb* -/- behaviour.

P38 MAPK phosphorylation was significantly elevated (relative to total protein levels) in *hexb* -/- BMDMs during untreated and LPS stimulated conditions. These results directly support the increase in TNF secretion, as LPS-induced NFκB-mediated TNF production is known to involve p38 MAPK phosphorylation and downstream kinase signaling[142, 143, 144]. Previous studies have reported that IL-10 receptor-mediated feedback acts to inhibit activation of the protein kinase-2 pathway by targeting p38 MAPK phosphorylation/activation. Therefore, increased phosphorylation of p38 may also be an artifact of the observed decrease in IL-10 production and subsequent feedback in HEXB deficient BMDMs[124] (Figure 35). This pro- and anti-inflammatory balance in regulatory activity is crucial for preserving immune homeostasis and minimizing collateral CNS damage during neuroinflammatory episodes. The LPS-independent increase in phosphorylated p38 levels implies that p38 activity is also being influenced by TLR-independent mechanisms. A multitude of cellular stimuli are capable of p38 regulation either via modulation of its upstream effectors, MKK3 and MKK6, or through direct action on p38 itself. More specifically, interleukins, cytokines, environmental stresses, and growth factors can influence p38 activity through their respective receptors. For example, epidermal growth factor (EGF) interaction with the EGF receptor (EGFR), or insulin or other growth factors binding to receptor tyrosine kinases are able to modulate MKKs upstream of p38[145, 146]. Furthermore, transforming growth factor-beta (TGFβ) can influence p38 directly through binding with TGFβR1[147]. G-protein coupled receptors (GPCRs) are also capable of influencing MKK and downstream p38 activity in response to environmental stressors and other GPCR agonists[148]. Given the multitude and complexity of p38 regulation, and the minimal data collected thus far, it would be difficult to hypothesize which pathways are mediating the observed responses.

Lastly, phosphorylated GSK3β (relative to total GSK3β levels) was significantly elevated in untreated and LPS treated HEXB deficient BMDMs. Although significance was not reached, a similar trend existed in Poly I:C treated cultures. Furthermore, untreated *hexa* -/- BMDMs expressed significantly more phosphorylated GSK3β than wild type cultures and was similar in expression to *hexb* -/- cells. This relationship was not maintained upon stimulation with LPS or Poly I:C. Prior evidence suggests that GSK3 helps to control early TLR4-mediated signaling[149]. More specifically, phosphorylation of GSK3 has been linked to suppression of proinflammatory cytokine secretion and augmentation of anti-inflammatory cytokines[150]. Such control has been attributed to TLR-dependent AKT-mediated phosphorylation of GSK3β through the PI3K pathway[151, 152] (Figure 35). The significant increase in phosphorylated GSK3β (relative to total) in *hexb* -/- BMDMs under all treatment conditions is potentially in agreement with the previous findings of elevated proinflammatory behaviour. Augmented GSK3β phosphorylation may be attempting to counteract the increase in TNF secretion from LPS-stimulated HEXB deficient BMDMs. Furthermore, these findings support the hypothesis that Sandhoff-derived

BMDMs are inherently more inflammatory. Such behaviour is in line with previously published work which found that TNF-induced macrophage cross-tolerance, which may be used as a mechanism to avoid stimulant-induced apoptosis, was dependent on and mediated by GSK3[153]. The lack of phosphorylated GSK3-influenced Stat3 activation and increased IL-10 anti-inflammatory immunosuppression observed in HEXB deficient BMDM cultures further supports the notion of a disconnect in the balance of immune homeostasis (Figure 35). In addition to modulating production of immunological molecules, GSK3β regulates the metabolism of β-catenin and in effect, β-catenin-dependent transcription[154]. Further investigation into β-catenin regulation in *hexb* -/- BMDMs should be conducted.

The data presented in this section demonstrates for the first time, differences in the inherent characteristics of bone marrow-derived macrophages in Sandhoff mice relative to their Tay-Sachs and wild type counterparts. Their smaller activated cell size and insignificant, yet notable decrease in the quantity of cytoplasmic projections, indicated that they may be immature compared to wild type and *hexa* -/- cultures. Their intrinsic hypersensitization to TLR4 stimulants was exemplified by a significant increase in LPS secretion when stimulated with LPS and was supported by increased levels of phosphorylated p38. Evidence for altered regulation of the IL-10/Stat3 feedback/regulatory axis was also observed. More specifically, HEXB deficient macrophages produced decreased IL-10 following LPS treatment and expressed decreased quantities of phosphorylated Stat3. Such abnormalities would encourage intense and prolonged inflammatory responses in Sandhoff mice, potentially leading to progressive neurodegeneration. Elevated levels of phosphorylated GSK3β may be indicative of a compensatory response to dampen excessive proinflammatory behaviour. Furthermore, the presence of increased phosphorylated p38 and GSK3β under unstimulated conditions suggests that TLR-independent mechanisms are also influencing immune behaviour. Although preliminary evidence has been presented to suggest that defects in autophagosomal/lysosomal fusion may be present in *hexb* -/- macrophages, a link between this process and the observed immunological and immunoregulatory differences has yet to be firmly established. Such observations, combined with a lack of response to extracellular GM2 provide evidence for augmented inflammatory behaviour in response to presently unidentified CNS-resident compounds. Alternatively, the lack of short-term incubation GM2-mediated immune activation suggests that chronic exposure to ganglioside may be required for producing marked cell stress. However, the lack of apparent ganglioside accumulation in these HEXB deficient cultures advocates for an alternate mechanism (perhaps autophagosomal accumulation) for hypersensitization to cellular stress.

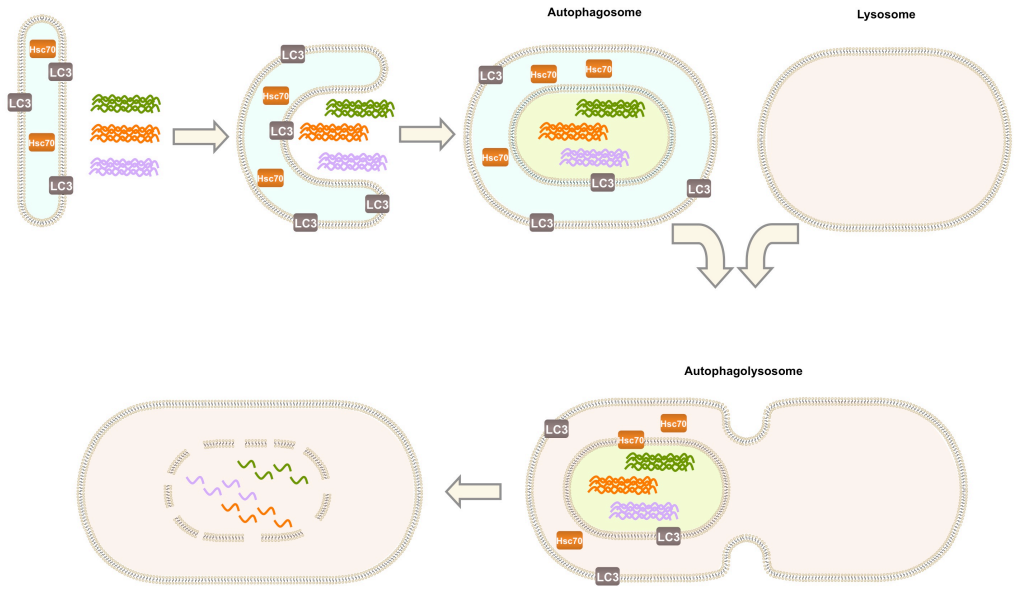

Figure 34. ***Proposed model of autophagosomal and lysosomal fusion blockage.*** Cultures of BMDMs from Tay-Sachs and Sandhoff mice revealed marked differences in their immunologic behaviour in response to extracellular toll-like receptor stimuli. Furthermore, such disturbances in *hexb* -/- bone marrow-derived macrophage behaviour appear to occur independently of intralysosomal ganglioside accumulations. It is hypothesized that the enzymatic deficiency may lead to defects in the fusion between autophagosomes and mature lysosomes from the endocytic pathway. Such blockage would prevent the formation of autophagolysosomes, consequently leading to autophagosomal accumulation, retention of catabolic substrates, and a residual buildup of HSP70 and Grp78. This buildup may result in a compensatory reduction of Grp78 levels, while pushing the cell into an aggravated state. Figure adapted from VisiScience Science Slides 2011 (VisiScience, Chapel Hill, North Carolina). Hsc70 (Hsp70; Heat shock protein 70), LC3 (MAP1LC3; Microtubule-associated protein 1 light chain 3).

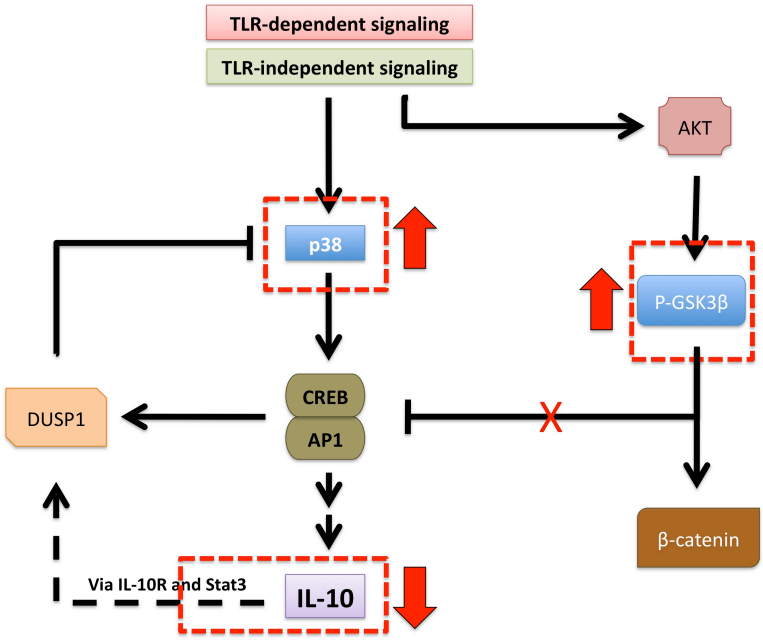

Figure 35. ***Summary of aberrant signaling observed in hexb -/- bone marrow-derived macrophages.*** Cultures of bone marrow-derived macrophages exhibited profound differences in cytokine secretion and other immunohomeostatic processes. Alterations in phospho-p38, phospho-GSK3β, phospho-Stat3, and IL-10 were observed in HEXB deficient cultures. TLR4-dependent increase in LPS secretion was correlated with augmented phosphorylated p38 and GSK3β. Conversely, decreased levels of phosphorylated Stat3 protein and IL-10 secretion were observed under the same conditions. Downstream TLR4 signaling influences PI3K, and subsequent AKT phosphorylation. Negative regulation of GSK3β activity via AKT-mediated phosphorylation remains a putative compensatory control mechanism for augmented proinflammatory *hexb* -/- behaviour. GSK3β influences c-Jun phosphorylation and thus, its transcriptional influence on AP1-mediated inflammatory cytokine production. However, the influence of GSK3β on the anti-inflammatory axis appears to be disconnected (reduced rather than increased Stat3/IL-10 feedback), suggesting a major immunosuppressive defect in *hexb* -/- cultures. Although not shown in this figure, AKT and GSK3β also influence levels of nuclear NFκB. Additionally, GSK3β activity influences nuclear translocation of β-catenin and β-catenin-dependent transcription. Given that phosphorylated p38 and GSK3β were both elevated in untreated *hexb* -/- macrophages, a TLR4-independent pathway must also exist; however, whether these findings are linked to defects in autophagosomal/lysosomal fusion is presently unclear. AKT (PKB; protein kinase B), AP1 (activator protein 1), CREB (cAMP response element-binding), DUSP1 (dual specificity protein phosphatase 1), IL-10 (interleukin-10), P-GSK3β (phosphorylated glycogen synthase kinase 3 beta), Stat3 (signal transducer and activator of transcription 3).

References

1. Fishman PH, Brady RO. Biosynthesis and function of gangliosides. Science 1976;194(4268):906-15.

2. Todeschini RA, Hakomori SI. Functional role of glycosphingolipids and gangliosides in control of cell adhesion, motility, and growth, through glycosynaptic microdomains. Biochim Biophys Acta 2008;1780(3):421-33.

3. Lopez PH, Schnaar RL. Gangliosides in cell recognition and membrane protein regulation. Curr Opin Struct Biol 2009;19(5):549-57.

4. Sonnino S, Mauri L, Chigorno V, Prinetti A. Gangliosides as components of lipid membrane domains. Glycobiology 2007;17(1):1-13.

5. Kolter T, Proia RL, Sandhoff K. Combinatorial ganglioside biosynthesis. JBC 2002;277:25859-62.

6. McJarrow P, Schnell N, Jumpsen J, Clandinin T. Influence of dietary gangliosides on neonatal brain development. Nutr Rev 2009;67(8):451-63.

7. Yu RK, Nakatani Y, Yanagisawa M. The role of glycosphingolipid metabolism in the developing brain. J Lipid Res 2009;50:440-5.

8. Fishman PH, Moss J, Vaughan M. Uptake and metabolism of gangliosides in transformed mouse fibroblasts. Relationship of ganglioside structure to choleragen response. JBC 1976;251:4490-4.

9. Zeigler M, Bach G. Internalization of exogenous gangliosides in cultured skin fibroblasts for the diagnosis of mucolipidosis IV. Clin Chim Acta 1986;157(2):183-9.

10. Kolter T, Sandhoff K. Sphingolipid metabolism diseases. Biochim Biophys Acta 2006;1758(12):2057-79.

11. van Echten G, Sandhoff K. Ganglioside metabolism. enzymology, topology, and regulation. J Biol Chem 1993;268:5341-4.

12. Vellodi A. Lysosomal storage disorders. Br J Haematol 2004(128):413-31.

13. Beutler E. Lysosomal storage diseases: Natural history and ethical and economic aspects. Mol Genet Metab 2006(88):208-15.

14. Meikle PJ, Hopwood JJ, Clague AE, Carey WF. Prevalence of lysosomal storage disorders. JAMA 1999;281(3):249-54.

15. Neufeld EF. Lysosomal storage diseases. Annu Rev Biochem 1991;60:257-80.

16. Bruni S, Loschi L, Incerti C, Gabrielli O, Coppa G. Update on treatment of lysosomal storage diseases. Acta Myol 2007;26:87-92.

17. Kolter T, Sandhoff K. Recent advances in the biochemistry of sphingolipidoses. Brain Pathol 1998;8(1):79-100.

18. McDowell GA, Mules EH, Fabacher P, Shapira E, Blitzer MG. The presence of two different infantile tay-sachs disease mutations in a cajun population. . Am J Hum Genet 1992;51(5):1071-7.

19. Paw BH, Tieu PT, Kaback MM, Lim J, Neufeld EF. Frequency of three hex A mutant alleles among jewish and non-jewish carriers identified in a tay-sachs screening program. Am J Hum Genet 1990;47(4):698-705.

20. Mahuran DJ. Beta-hexosaminidase: Biosynthesis and processing of the normal enzyme, and identification of mutations causing jewish tay-sachs disease. Clin Biochem 1995;28(2):101-6.

21. Malatack JJ, Consolini DM, Bayever E. The status of hematopoietic stem cell transplantation in lysosomal storage disease. Pediatr Neurol 2003;29(5):391-403.

22. Sawkar AR, D'Haeze W, Kelly JW. Therapeutic strategies to ameliorate lysosomal storage disorders. Cell Mol Life Sci 2006;63(10):1179-92.

23. Brady RO. Enzyme replacement for lysosomal diseases. Annu Rev 2006;57:283-96.

24. Beck M. New therapeutic options for lysosomal storage disorders: Enzyme replacement, small molecules and gene therapy. Hum Genet 2007;121(1):1-22.

25. Ioannou YA, Enriquez A, Benjamin C. Gene therapy for lysosomal storage disorders. Expert Opin Biol Ther 2003;3(5):789-801.

26. Platt FM, Neises GR, Dwek RA, Butters TD. N-butyldeoxynojirimycin is a novel inhibitor of glycolipid biosynthesis. JBC 1994;269:8362-5.

27. Jeyakumar M, Dwek RA, Butters TD, Platt FM. Storage solutions: Treating lysosomal disorders of the brain. Nat Rev Neurosci 2005;6:713-25.

28. Cox TM, Aerts JM, Andria G, Beck M, Belmatoug N, Bembi B, Chertkoff R, Vom Dahl S, Elstein D, Erikson A, et al. The role of the iminosugar N-butyldeoxynojirimycin (miglustat) in the management of type I (non-neuronopathic) gaucher disease: A position statement. J Inherit Metab Dis 2006;26(6):513-26.

29. Aerts JM, Hollak CE, Boot RG, Groener JE, Maas M. Substrate reduction therapy of glycosphingolipid storage disorders. J Inherit Metab Dis 2006;29(2-3):449-56.

30. Asano N, Ishii S, Kizu H, Ikeda K, Yasuda K, Kato A, Martin OR, Fan JQ. In vitro inhibition and intracellular enhancement of lysosomal alpha-galactosidase A activity in fabry lymphoblasts by 1-deoxygalactonojirimycin and its derivatives. Eur J Biochem 2000;267(13):4179-86.

31. Matsuda J, Suzuki O, Oshima A, Yamamoto Y, Noguchi A, Takimoto K, Itoh M, Matsuzaki Y, Yasuda Y, Ogawa S, et al. Chemical chaperone therapy for brain pathology in G_{M1}-gangliosidosis. Proc Natl Acad Sci USA 2003;100(26):15912-7.

32. Sawkar AR, Adamski-Werner SL, Cheng WC, Wong CH, Beutler E, Zimmer KP, Kelly JW. Gaucher disease-associated glucocerebrosidases show mutation-dependent chemical chaperoning profiles. Chem Biol 2005;12(11):1235-44.

33. Yam G, Bosshard N, Zuber C, Steinmann B, Roth J. Pharmacological chaperone corrects lysosomal storage in fabry disease caused by trafficking-incompetent variants Am J Physiol Cell Physiol 2005(290):1076-82.

34. Yamashita T, Wada R, Sasaki T, Deng C, Bierfreund U, Sandhoff K, Proia RL. A vital role for glycosphingolipid synthesis during development and differentiation. PNAS 1999;96(16):9142-7.

35. Koybasi S, Senkal CE, Sundararaj K, Spassieva S, Bielawski J, Osta W, Day TA, Jiang JC, Jazwinski SM, Hannun YA, et al. Defects in cell growth regulation by C18:0-ceramide and longevity assurance gene 1 in human head and neck squamous cell carcinomas. J Biol Chem 2004(279):44311-9.

36. Charria-Ortiz GA. The GM2 gangliosidoses in: Lysosomal storage diseases. Springer US; 2007.

37. Kiselyov K, Jennigs Jr JJ, Rbaibi Y, Chu CT. Autophagy, mitochondria and cell death in lysosomal storage diseases. Autophagy 2007;3(3):259-62.

38. Futerman AH, van Meer G. The cell biology of lysosomal storage disorders. Nat Rev Mol Cell Biol 2004;5:554-65.

39. Walkley S. Secondary accumulation of gangliosides in lysosomal storage disorders. Semin Cell Dev Biol 2004;15(4):433-44.

40. Schrödera M, Kaufman RJ. ER stress and the unfolded protein response. Mutat Res 2005;569(1-2):29-63.

41. Lindholm D, Wootz H, Korhonen L. ER stress and neurodegenerative diseases. Cell Death Differ 2006;13:385-92.

42. Wei H, Kim S, Zhang Z, Tsai P, Wisniewski KE, Mukherjee AB. ER and oxidative stresses are common mediators of apoptosis in both neurodegenerative and non-neurodegenerative lysosomal storage disorders and are alleviated by chemical chaperones. Hum Mol Genet 2008;17(4):469-77.

43. Neufeld EF. Natural history and inherited disorders of a lysosomal enzyme, beta-hexosaminidase. J Biol Chem 1989;264(19):10927-30.

44. Gilbert F, Kucherlapati R, Creagan RP, Murnane MJ, Darlington GJ, Ruddle FH. Tay-sachs' and sandhoff's diseases: The assignment of genes for hexosaminidase A and B to individual human chromosomes. Proc Nat Acad Sci 1975;72(1):263-7.

45. Sango K, McDonald MP, Crawley JN, Mack ML, Tifft CJ, Skop E, Starr CM, Hoffmann A, Sandhoff K, Suzuki K, et al. Mice lacking both subunits of lysosomal −hexosaminidase display gangliosidosis and mucopolysaccharidosis. Nat Genet 1996;14:348-52.

46. Filho JA, Shapiro BE. Tay-sachs disease. Arch Neurol 2004;61:1466-8.

47. Myerowitz R. Tay-sachs disease-causing mutations and neutral polymorphisms in the hex A gene. Hum Mutat 1999;9(3):195-208.

48. Myerowitz R, Hogikyan ND. A deletion involving alu sequences in the beta-hexosaminidase alpha-chain gene of french canadians with tay-sachs disease. J Biol Chem 1987;262:15396-9.

49. Pampiglione G, Privett G, Harden A. Tay-sachs disease: Neurophysiological studies in 20 children. Develop Med Child Neurol 1974;16(2):201-8.

50. Rucker JC, Shapiro BE, Han YH, Kumar AN, Garbutt S, Keller EL, Leigh RJ. Neuro-ophthalmology of late-onset Tay–Sachs disease (LOTS). Neurology 2004;63(10):1918-26.

51. Neudorfer O, Kolodny EH. Late-onset tay-sachs disease. IMAJ 2004;6:107-11.

52. MacQueen GM, Rosebush PI, Mazurek MF. Neuropsychiatric aspects of the adult variant of tay-sachs disease. J Neuropsychiatry Clin Neurosci 1998;10:10-9.

53. Rosebush PI, MacQueen GM, Clarke JT, Callahan JW, Strasberg PM, Mazurek MF. Late-onset tay-sachs disease presenting as catatonic schizophrenia: Diagnostic and treatment issues. J Clin Psychiatry 1995;56(8):347-53.

54. Gulinelloa M, Chenb F, Dobrenis K. Early deficits in motor coordination and cognitive dysfunction in a mouse model of the neurodegenerative lysosomal storage disorder, sandhoff disease. Behav Brain Res 2008;193(2):315-9.

55. Cross AS, Wright DG. Mobilization of sialidase from intracellular stores to the surface of human neutrophils and its role in stimulated adhesion responses of these cells. J Clin Invest 1991;88(6):2067-2076.

56. Carrillo MB, Milner CM, Ball ST, Snoek M, Campbell RD. Cloning and characterization of a sialidase from the murine histocompatibility-2 complex: Low levels of mRNA and a single amino acid mutation are responsible for reduced sialidase activity in mice carrying the Neu1(a) allele. Glycobiology 1997;7(7):975-986.

57. Monti E, Bassi MT, Papini N, Riboni M, Manzoni M, Venerando B, Croci G, Preti A, Ballabio A, Tettamanti G, et al. Identification and expression of NEU3, a novel human sialidase associated to the plasma membrane. Biochem J 2000;349(1):343-351.

58. Gadhoum SZ, Sackstein R. CD15 expression in human myeloid cell differentiation is regulated by sialidase activity. Nat Chem Biol 2008;4(12):751-7.

59. Pattison S, Pankarican M, Rupar CA, Graham FL, Igdoura SA. Five novel mutations in the lysosomal sialidase gene (NEU1) in type II sialidosis patients and assessment of their impact on enzyme activity and intracellular targeting using adenovirus-mediated expression. Hum Mutat 2004;23(1):32-9.

60. van der Spoel A, Bonten E, d'Azzo A. Transport of human lysosomal neuraminidase to mature lysosomes requires protective protein cathepsin A. EMBO J 1998;17(6):1588-1597.

61. Igdoura SA, Gafuik C, Mertineit C, Saberi F, Pshezhetsky AV, Potier M, Trasler JM, Gravel RA. Cloning of the cDNA and gene encoding mouse lysosomal sialidase and correction of sialidase deficiency in human sialidosis and mouse SM/J fibroblasts. Human Molecular Genetics 1998;7(1):115-120.

62. Champigny MJ, Johnson M, Igdoura SA. Characterization of the mouse lysosomal sialidase promoter. Gene 2003;319:177-87.

63. Nepveu A. Role of the multifunctional CDP/Cut/Cux homeodomain transcription factor in regulating differentiation, cell growth and development. Gene 2001;270(1-2):1-15.

64. Igdoura SA, Mertineit C, Trasler JM, Gravel RA. Sialidase-mediated depletion of GM2 ganglioside in tay-sachs neuroglia cells. Hum Mol Genet 1999;8(6):1111-6.

65. Pshezhetsky AV, Richard C, Michaud L, Igdoura S, Wang S, Elsliger M, Qu J, Leclerc D, Gravel R, Dallaire L, et al. Cloning, expression and chromosomal mapping of human lysosomal sialidase and characterization of mutations in sialidosis. Nat Genet 1997;15:316-20.

66. Bonten EJ, Arts WF, Beck M, Covanis A, Donati MA, Parini R, Zammarchi E, d'Azzo A. Novel mutations in lysosomal neuraminidase identify functional domains and determine clinical severity in sialidosis. Hum Mol Genet 2000;9(18):2715-25.

67. Federicoa A, Battistinia S, Ciaccia G, de Stefanoa N, Gattib R, Durandb P, Guazzia GC. Cherry-red spot myoclonus syndrome (type I sialidosis). Dev Neurosci 1991;13(4-5):320-6.

68. Palmeria S, Villanovaa M, Malandrinia A, van Diggelend OP, Huijmansd JG, Ceutericke C, Rufab A, DeFalcoc D, Ciaccia G, Martine JJ, et al. Type I sialidosis: A clinical, biochemical and neuroradiological study. Eur Neurol 2000;43(2):88-94.

69. Amith SR, Jayanth P, Franchuk S, Finlay T, Seyrantepe V, Beyaert R, Pshezhetsky AV, Szewczuk MR. Neu1 desialylation of sialyl α-2,3-linked β-galactosyl residues of TOLL-like receptor 4 is essential for receptor activation and cellular signaling. Cell Signal 2009;22(2):314-24.

70. Amith SR, Jayanth P, Franchuk S, Siddiqui S, Seyrantepe V, Gee K, Sameh Basta S, Beyaert R, Pshezhetsky AV, Szewczuk MR. Dependence of pathogen molecule-induced toll-like receptor activation and cell function on Neu1 sialidase. Glycoconj J 2009;26(9):1197-212.

71. Stollg G, Jander S. The role of microglia and macrophages in the pathophysiology of the CNS. Prog Neurobiol 1999;58(3):233-47.

72. DeLegge MH. Neurodegeneration and inflammation. Nutr Clin Pract 2008;23(1):35-41.

73. Wyss-Coray T, Mucke L. Inflammation in neurodegenerative disease--a double-edged sword. Neuron 2002;35(3):419-32.

74. Akiyamaa H, Bargera S, Barnuma S, Bradta B, Bauera J, Colea GM, Cooperа NR, Eikelenbooma P, Emmerlinga M, Fiebicha BL, et al. Inflammation and Alzheimer's disease. Neurobiol Aging 2000;21(3):383-421.

75. McGeer PL, McGeer EG. Inflammatory processes in amyotrophic lateral sclerosis. Muscle Nerve 2002;26(4):459-70.

76. Graves M, Fiala M, Dinglasan LA, Liu N, Sayre J, Chiappelli F, van Kooten C, Vinters H. Inflammation in amyotrophic lateral sclerosis spinal cord and brain is mediated by activated macrophages, mast cells and T cells. Amyotroph Lateral Scler 2004;5(4):213-9.

77. Wada R, Tifft CJ, Proia RL. Microglial activation precedes acute neurodegeneration in sandhoff disease and is suppressed by bone marrow transplantation. PNAS 2000;97(20):10954-9.

78. Olson JK, Miller SD. Microglia initiate central nervous system innate and adaptive immune responses through multiple TLRs. J Immunol 2004;173:3916-24.

79. Henkel JS, Engelhardt JI, Siklós L, Simpson EP, Kim SH, Pan T, Goodman JC, Siddique T, Beers DR, Appel SH. Presence of dendritic cells, MCP-1, and activated microglia/macrophages in amyotrophic lateral sclerosis spinal cord tissue. Ann Neurol 2003;55(2):221-35.

80. Becher B, Fedorowicz V, Antel JP. Regulation of CD14 expression on human adult central nervous system-derived microglia. J Neurosci Res 1996;45(4):375-81.

81. Nelson PT, Soma LA, Lavi E. Microglia in diseases of the central nervous system. Ann Med 2002;34(7):491-500.

82. Tracy Fischer-Smith,* Sidney Croul,*† Aderonke Adeniyi,* Katarzyna Rybicka,* Susan Morgello,‡ Kamel Khalili,* and Jay Rappaport*. Macrophage/Microglial accumulation and proliferating cell nuclear antigen expression in the central nervous system in human immunodeficiency virus encephalopathy. Am J Path 2004;164(6):2089-99.

83. Bate C, Veerhuis R, Eikelenboom P, Williams A. Microglia kill amyloid-[beta]1-42 damaged neurons by a CD14-dependent process. Neuroreport 2004;15(9):1427-30.

84. Hanisch UK. Microglia as a source and target of cytokines. Glia 2002;40(2):140-55.

85. Qin L, Li G, Qian X, Liu Y, Wu X, Liu B, Hong J, Block ML. Interactive role of the toll-like receptor 4 and reactive oxygen species in LPS-induced microglia activation. Glia 2005;52(1):78-84.

86. Min KJ, Yang MS, Jou I, Joe EH. Protein kinase A mediates microglial activation induced by plasminogen and gangliosides. Exp Mol Med 2004;36(5):461-7.

87. Goodwina JL, Uemura E, Cunnick JE. Microglial release of nitric oxide by the synergistic action of β-amyloid and IFN-γ. Brain Res 1995;692(1-2):207-14.

88. Pei Z, Pang H, Qian L, Yang S, Wang T, Zhang W, Wu X, Dallas S, Wilson B, Reece JM, et al. MAC1 mediates LPS-induced production of superoxide by microglia: The role of pattern recognition receptors in dopaminergic neurotoxicity. Glia 2007;55(13):1362-73.

89. Roy A, Fung YK, Liu X, Pahan K. Up-regulation of microglial CD11b expression by nitric oxide. JBC 2006;281:14971-80.

90. Hendriks JJA, Teunissen CE, de Vries HE, Dijkstra CD. Macrophages and neurodegeneration. Brain Res Rev 2005;48(2):185-95.

91. Perry VH, Andersson PB, Gordon S. Macrophages and inflammation in the central nervous system. Trends Neurosci 1993;16(7):268-73.

92. Wu Y, Proia RL. Deletion of macrophage-inflammatory protein 1α retards neurodegeneration in sandhoff disease mice. PNAS 2004;101(22):8425-30.

93. de Vries HE, Kuiper J, de Boer AG, Van Berkel TJ, Breimer DD. The blood-brain barrier in neuroinflammatory diseases. Pharmacol Rev 1997;49(2):143-56.

94. Kawai T, Akira S. TLR signaling. Cell Death Differ 2006;13:816-25.

95. Bsibsi M, Ravid R, Gveric D, Van Noort J. Broad expression of toll-like receptors in the human central nervous system. J Neuropathol Exp Neurol 2002;61(11):1013-21.

96. Yamamoto M, Sato S, Hemmi H, Uematsu S, Hoshino K, Kaisho T, Takeuchi O, Takeda K, Akira S. TRAM is specifically involved in the toll-like receptor 4−mediated MyD88-independent signaling pathway. Nat Immunol 2003;4:1144-50.

97. Choe J, Kelker MS, Wilson IA. Crystal structure of human toll-like receptor 3 (TLR3) ectodomain . Science 2005;309(5734):581-5.

98. Lehnardt S, Massillon L, Follett P, Jensen FE, Ratan R, Rosenberg PA, Volpe JJ, Vartanian T. Activation of innate immunity in the CNS triggers neurodegeneration through a toll-like receptor 4-dependent pathway. Proc Natl Acad Sci U S A 2003;100(14):8514-9.

99. Fernandez-Lizarbe S, Pascual M, Guerri C. Critical role of TLR4 response in the activation of microglia induced by ethanol. J Immunol 2009;183:4733-44.

100. Jung DY, Lee H, Jung B, Ock J, Lee M, Lee W, Suk K. TLR4, but not TLR2, signals autoregulatory apoptosis of cultured microglia: A critical role of IFN- as a decision maker. J Immunol 2005;174:6467-76.

101. Wang T, Town T, Alexopoulou L, Anderson JF, Fikrig E, Flavell RA. Toll-like receptor 3 mediates west nile virus entry into the brain causing lethal encephalitis. Nat Med 2004;10(12):1366-73.

102. Min K, Pyo H, Yang M, Ji K, Jou I, Joe E. Gangliosides activate microglia via protein kinase C and NADPH oxidase. Glia 2004;48(3):197-206.

103. Kim OS, Park EJ, Joe EH, Jou I. JAK-STAT signaling mediates gangliosides-induced inflammatory responses in brain microglial cells. JBC 2002;277:40594-601.

104. Town T, Jeng D, Alexopoulou L, Tan J, Flavell RA. Microglia recognize double-stranded RNA via TLR3. J Immunol 2006;176:3804-12.

105. Sango K, Yamanaka S, Hoffmann A, Okuda Y, Grinberg A, Westphal H, McDonald MP, Crawley JN, Sandhoff K, Suzuki K, et al. Mouse models of tay-sachs and sandhoff diseases differ in neurologic phenotype and ganglioside metabolism. Nat Genet 1995;11(2):170-6.

106. Phaneuf D, Wakamatsu N, Huang JQ, Borowski A, Peterson AC, Fortunato SR, Ritter G, Igdoura SA, Morales CR, Benoit G, et al. Dramatically different phenotypes in mouse models of human tay-sachs and sandhoff diseases. Hum Mol Genet 1996;5(1):1-14.

107. Jou I, Lee JH, Park SY, Yoon HJ, Joe E, Park EJ. Gangliosides trigger inflammatory responses via TLR4 in brain glia. Am J Pathol 2006;168(5):1619-30.

108. Tessitore A, del P Martin M, Sano R, Ma Y, Mann L, Ingrassia A, Laywell ED, Steindler DA, Hendershot LM, d'Azzo A. GM1-ganglioside-mediated activation of the unfolded protein response causes neuronal death in a neurodegenerative gangliosidosis. Mol Cell 2004;15(5):753-66.

109. d'Azzo A, Tessitore A, Sano R. Gangliosides as apoptotic signals in ER stress response. Cell Death Differ 2006;13(3):404-14.

110. Abdulkhalek S, Amith SR, Franchuk SL, Jayanth P, Guo M, Finlay T, Gilmour A, Guzzo C, Gee K, Beyaert R, et al. Neu1 sialidase and matrix metalloproteinase-9 cross-talk is essential for toll-like receptor activation and cellular signaling. J Biol Chem 2011;286(42):36532-49.

111. Weinreb NJ, Charrow J, Andersson HC, Kaplan P, Kolodny EH, Mistry P, Pastores G, Rosenbloom BE, Scott CR, Wappner RS, et al. Effectiveness of enzyme replacement therapy in 1028 patients with type 1 gaucher disease after 2 to 5 years of treatment: A report from the gaucher registry. Am J Med 2002;113(2):112-9.

112. Moon NS, Premdas P, Truscott M, Leduy L, Bérubé G, Nepveu A. S phase-specific proteolytic cleavage is required to activate stable DNA binding by the CDP/Cut homeodomain protein. Mol Cell Biol 2001;21(18):6332-45.

113. Tropak MB, Reid SP, Guiral M, Withers SG, Mahuran D. Pharmacological enhancement of beta-hexosaminidase activity in fibroblasts from adult tay-sachs and sandhoff patients. J Biol Chem 2004;279(14):13478-87.

114. Morioka Y, Naito M, Sato T, Takahashi K. Immunophenotypic and ultrastructural heterogeneity of macrophage differentiation in bone marrow and fetal hematopoiesis of mouse in vitro and in vivo. J Leukoc Biol 1994;55(5):642-51.

115. Guillemin GJ, Brew BJ. Microglia, macrophages, perivascular macrophages, and pericytes: A review of function and identification. J Leukoc Biol 2004;75(3):388-97.

116. Giulian D, Li J, Bartel S, Broker J, Li X, Kirkpatrick JB. Cell surface morphology identifies microglia as a distinct class of mononuclear phagocyte. J Neurosci 1995;15(11):7712-26.

117. Fuentes ME, Durham SK, Swerdel MR, Lewin AC, Barton DS, Megill JR, Bravo R, Lira SA. Controlled recruitment of monocytes and macrophages to specific organs through transgenic expression of monocyte chemoattractant protein-1. J Immunol 1995;155(12):5769-76.

118. Glabinski AR, Balasingam V, Tani M, Kunkel SL, Strieter RM, Yong VW, Ransohoff RM. Chemokine monocyte chemoattractant protein-1 is expressed by astrocytes after mechanical injury to the brain. J Immunol 1996;156(11):4363-8.

119. Papadimitriou JM, Ashman RB. Macrophages: current views on their differentiation, structure, and function. Ultrastruct Pathol 1989;13(4):343-72.

120. Oberdörster G, Ferin J, Morrow PE. Volumetric loading of alveolar macrophages (AM): a possible basis for diminished AM-mediated particle clearance. Exp Lung Res 1992;18(1):87-104.

121. Morioka Y, Naito M, Sato T, Takahashi K. Immunophenotypic and ultrastructural heterogeneity of macrophage differentiation in bone marrow and fetal hematopoiesis of mouse in vitro and in vivo. JLB 1994;55(5):642-51.

122. Zeigler M, Bach G. Internalization of exogenous gangliosides in cultured skin fibroblasts for the diagnosis of mucolipidosis IV. Clin Chem Acta 1986;157(2):183-9.

123. Nakamura M, Tsunoda A, Furukawa Y, Sakai T, Saito M. Rapid internalization of exogenous ganglioside GM3 and its metabolism to ceramide in human myelogenous leukemia HL-60 cells compared with control ganglioside GM1. FEBS Lett 1997;400(3):350-4.

124. Kontoyiannis D, Kotlyarov A, Carballo E, Alexopoulou L, Blackshear PJ, Gaestel M, Davis R, Flavell R, Kollias G. Interleukin-10 targets p38 MAPK to modulate ARE-dependent TNF mRNA translation and limit intestinal pathology. EMBO J 2001;20(14):3760-70.

125. Buk SJA, Filipe MI. Histochemical staining of sulphated and non-sulphated sialomucin in intestinal epithelium: Practical difficulties associated with the KOH—AB 1.0—PAPS method. Histochem J 1986;18(10):576-8.

126. Hahn CN, del Pilar Martin M, Schröder M, Vanier MT, Hara Y, Suzuki K, Suzuki K, d'Azzo A. Generalized CNS disease and massive GM1-ganglioside accumulation in mice defective in lysosomal acid beta-galactosidase. Hum Mol Genet 1997;6(2):205-11.

127. Alaedini A, Latov N. Transglutaminase-independent binding of gliadin to intestinal brush border membrane and GM1 ganglioside. J Neuroimmunol 2006;177(1-2):167-72.

128. Kasperzyk JL, d'Azzo A, Platt FM, Alroy J, Seyfried TN. Substrate reduction reduces gangliosides in postnatal cerebrum-brainstem and cerebellum in GM1 gangliosidosis mice. J Lipid Res 2005;46(4):744-51.

129. Reid PC, Sakashita N, Sugii S, Ohno-Iwashita Y, Shimada Y, Hickey WF, Chang TY. A novel cholesterol stain reveals early neuronal cholesterol accumulation in the niemann-pick type C1 mouse brain. J Lipid Res 2004;45(3):582-91.

130. Alter G, Malenfant JM, Altfeld M. CD107a as a functional marker for the identification of natural killer cell activity. J Immunol Methods 2004;294(1-2):15-22.

131. Aktas E, Kucuksezer UC, Bilgic S, Erten G, Deniz G. Relationship between CD107a expression and cytotoxic activity. Cell Immunol 2009;254(2):149-54.

132. Huynh KK, Eskelinen EL, Scott CC, Malevanets A, Saftig P, Grinstein S. LAMP proteins are required for fusion of lysosomes with phagosomes. EMBO J 2007;26(2):313-24.

133. Weitz G, Proia RL. Analysis of the glycosylation and phosphorylation of the α-subunit of the lysosomal enzyme, β-hexosaminidase A, by site-directed mutagenesis. JBC 1992;267(14):10039-44.

134. Zokaeem G, Bayleran J, Kaplan P, Hechtman P, Neufeld EF. A shortened beta-hexosaminidase alpha-chain in an italian patient with infantile tay-sachs disease. Am J Hum Genet 1987;40(6):537-47.

135. Marín-Briggiler CI, González-Echeverría MF, Munuce MJ, Ghersevich S, Caille AM, Hellman U, Corrigall VM, Vazquez-Levin MH. Glucose-regulated protein 78 (Grp78/BiP) is secreted by human oviduct epithelial cells and the recombinant protein modulates sperm-zona pellucida binding. Fertil Steril 2010;93(5):1574-84.

136. Kern J, Untergasser G, Zenzmaier C, Sarg B, Gastl G, Gunsilius E, Steurer M. GRP-78 secreted by tumor cells blocks the antiangiogenic activity of bortezomib. Blood 2009;114(18):3960-7.

137. Fortunato F, Bürgers H, Bergmann F, Rieger P, Büchler MW, Kroemer G, Werner J. Impaired autolysosome formation correlates with lamp-2 depletion: Role of apoptosis, autophagy, and necrosis in pancreatitis. Gastroenterology 2009;137(1):350-60.

138. Li B, Castano AP, Hudson TE, Nowlin BT, Lin SL, Bonventre JV, Swanson KD, Duffield JS. The melanoma-associated transmembrane glycoprotein Gpnmb controls trafficking of cellular debris for degradation and is essential for tissue repair. FASEB J 2010;24(12):4767-81.

139. Tessitore A, Pirozzi M, Auricchio A. Abnormal autophagy, ubiquitination, inflammation and apoptosis are dependent upon lysosomal storage and are useful biomarkers of mucopolysaccharidosis VI. Pathogenetics 2009;2(1):4.

140. Settembre C, Fraldi A, Jahreiss L, Spampanato C, Venturi C, Medina D, de Pablo R, Tacchetti C, Rubinsztein DC, Ballabio A. A block of autophagy in lysosomal storage disorders. Hum Mol Genet 2008;17(1):119-29.

141. Koike M, Shibata M, Waguri S, Yoshimura K, Tanida I, Kominami E, Gotow T, Peters C, von Figura K, Mizushima N, et al. Participation of autophagy in storage of lysosomes in neurons from mouse models of neuronal ceroid-lipofuscinoses (batten disease). Am J Pathol 2005;167(6):1713-28.

142. Raingeaud J, Gupta S, Rogers JS, Dickens M, Han J, Ulevitch RJ, Davis RJ. Pro-inflammatory cytokines and environmental stress cause p38 mitogen-activated protein kinase activation by dual phosphorylation on tyrosine and threonine. J Biol Chem 1995;270(13):7420-6.

143. Jiang Y, Liu A, Zhang L. The role of activation of p38 MAPK induced by LPS in TNF-alpha gene expression. Zhonghua Yi Xue Za Zhi 1999;79(5):360-4.

144. Lee JC, Young PR. Role of CSB/p38/RK stress response kinase in LPS and cytokine signaling mechanisms. J Leukoc Biol 1996;59(2):152-7.

145. Jiang H, Grenley MO, Bravo MJ, Blumhagen RZ, Edgar BA. EGFR/Ras/MAPK Signaling Mediates Adult Midgut Epithelial Homeostasis and Regeneration in Drosophila. Cell Stem Cell 2010;8(1):84-95.

146. Sundaram MV. RTK/Ras/MAPK signaling. Wormbook. 2006:1-19.

147. Yu L, Hebert MC, Zhang YE. TGF-β receptor-activated p38 MAP kinase mediates Smad-independent TGF-β responses. EMBO J 2002;21(14):3749-59.

148. Clerk A, Michael A, Sugden PH. Stimulation of the p38 mitogen-activated protein kinase pathway in neonatal rat ventricular myocytes by the G protein-coupled receptor agonists, endothelin-1 and phenylephrine: a role in cardiac myocyte hypertrophy. J Cell Biol 1998;142(2):523-35.

149. Foley JF. GSK-3β masters TLR4 responses. Sci Signal 2008;1(45):ec385.

150. Wang H, Garcia CA, Rehani K, Cekic C, Alard P, Kinane DF, Mitchell T, Martin M. IFN-β production by TLR4-stimulated innate immune cells is negatively regulated by GSK3-β. J Immunol 2008;181:6797-802.

151. Hazeki K, Nigorikawa K, Hazeki O. Role of Phosphoinositide 3-Kinase in Innate Immunity. Biol Pharm Bull 2007;30:1617-23.

152. Ha T, Hua F, Liu X, Ma J, McMullen JR, Shioi T, Izumo S, Kelley J, Gao X, Browder W, et al. Lipopolysaccharide-induced myocardial protection against ischaemia/reperfusion injury is mediated through a PI3K/Akt-dependent mechanism. Cardiovasc Res 2008;78(3):546-53.

153. Park SH, Park-Min K, Chen J, Hu X, Ivashkiv LB. Tumor necrosis factor induces GSK3 kinase–mediated cross-tolerance to endotoxin in macrophages. Nat Immunol 2011;12:607-15.

154. Monick MM, Carter AB, Robeff PK, Flaherty DM, Peterson MW, Hunninghake GW. Lipopolysaccharide activates Akt in human alveolar macrophages resulting in nuclear accumulation and transcriptional activity of beta-catenin. J Immunol 2001;166(7):4713-20.